

Electronic Thesis and Dissertation Repository

10-4-2022 2:00 PM

The Effect of OATP2B1-Mediated Statin Transport on Beta Cell Dysfunction

Jihoon Kwon, *The University of Western Ontario*

Supervisor: Schwarz, Ute I., *The University of Western Ontario*

A thesis submitted in partial fulfillment of the requirements for the Master of Science degree in Physiology and Pharmacology

© Jihoon Kwon 2022

Follow this and additional works at: <https://ir.lib.uwo.ca/etd>



Part of the [Pharmacology Commons](#), and the [Physiology Commons](#)

Recommended Citation

Kwon, Jihoon, "The Effect of OATP2B1-Mediated Statin Transport on Beta Cell Dysfunction" (2022).
Electronic Thesis and Dissertation Repository. 8896.
<https://ir.lib.uwo.ca/etd/8896>

This Dissertation/Thesis is brought to you for free and open access by Scholarship@Western. It has been accepted for inclusion in Electronic Thesis and Dissertation Repository by an authorized administrator of Scholarship@Western. For more information, please contact wlsadmin@uwo.ca.

Abstract

Statins are a class of cholesterol-lowering drugs which work by inhibiting the mevalonate pathway. Statin treatment has been linked to an increase in the risk of new-onset diabetes mellitus, and previous studies have suggested impairment in insulin secretion following statin treatment. Recent work from our laboratory confirmed the expression of organic anion transporting polypeptide 2B1 (OATP2B1), an important statin uptake transporter, in human pancreatic beta cells. Our study examined the role of OATP2B1 in statin-associated beta cell toxicity using INS-1 cells as a beta cell model. We showed that OATP2B1 augments cellular accumulation of rosuvastatin and atorvastatin, but not pravastatin. While rosuvastatin and atorvastatin led to a dose-dependent reduction in insulin secretion, OATP2B1 had no effect. However, OATP2B1 was found to facilitate statin-induced mitochondrial toxicity, apoptosis and ATP level reduction. In conclusion, our findings support an important role of OATP2B1-mediated statin uptake on beta cell toxicity but not insulin secretion.

Keywords

Organic anion transporting polypeptide, statins, P-glycoprotein, breast cancer resistance protein, mitochondrial function, mass spectrometry, pancreatic beta cells, insulin secretion

Summary for Lay Audience

Statins are commonly prescribed cholesterol-lowering drugs. These statins work by reducing the amount of cholesterol synthesized in the liver. Recently, statin therapy has been linked to an increased risk of diabetes mellitus. Organic anion transporting polypeptide (OATP)2B1 is an important transport protein residing on the surface of many cell types, including insulin-secreting pancreatic beta cells, and helps bring many substances, including statins, into the cell. We sought to study the effect of OATP2B1 on the accumulation of statins inside cells, and possible toxicities caused by statins using a cell model, INS-1. We created INS-1 cells that express large amounts of OATP2B1, and we found that these cells had a higher accumulation of rosuvastatin and atorvastatin within the cells. While insulin secretion was impaired after treatment of INS-1 cells with increasing rosuvastatin and atorvastatin concentrations, OATP2B1 had no effect on insulin secretion. After treating the INS-1 cells with different statins at high concentrations, OATP2B1 enhanced known adverse effects of statins, including function of the mitochondria, the main site of energy or ATP production in cells, as well as increased markers of programmed cell death (apoptosis). In summary, our study highlighted a possible connection between the transport protein OATP2B1 and harmful effects on pancreatic beta cells caused by statins at very high doses.

Acknowledgments

First, I would like to express my sincere gratitude to my supervisor, Dr. Ute Schwarz. You have been my inspiration and the source of motivation in navigating through my project. It has been a long and challenging at times, especially with the pandemic, but in the end, you made this project possible for me. Being able to simply chat with you whenever I needed and through our weekly meetings, was a great resource for constant feedback and new information. Thank you for being such an excellent mentor and a colleague.

To my advisory committee members, Dr. Rommel Tirona, Dr. Rennian Wang and my graduate studies committee representative, Dr. Rithwik Ramachandran, the bi-annual advisory meetings with you have been an excellent chance for me to receive constructive feedback and a fountain of new ideas and suggestions.

To my current and former colleagues at the personalized medicine laboratory, Dr. Samantha Medwid, Dr. Richard Kim, Dr. Aze Wilson, Cameron Ross, Jaymie Mailloux, Heidi Liao, Daniel Taylor, Valerie Swanston, Hanshin Lee, Sherry Wang, Claire Adams, John Choi, thank you for making the days at the lab more fun, lively and enjoyable.

To my loving parents, thank you for your constant support and love. None of this would have been possible without you.

Table of Contents

Abstract.....	ii
Summary for Lay Audience.....	iii
Acknowledgments.....	iv
Table of Contents.....	v
List of Tables.....	viii
List of Figures.....	ix
List of Abbreviations.....	xi
Chapter 1.....	1
1 Introduction.....	1
1.1 Organic Anion Transporting Polypeptides.....	1
1.2 ABC Efflux Transporters.....	4
1.3 Endocrine Pancreas and Diabetes Mellitus.....	7
1.4 Statins and Their Mechanisms of Action.....	9
1.5 Statin-Induced New Onset Diabetes Mellitus (NODM).....	15
1.6 Rationale, Aims and Hypothesis.....	19
Chapter 2.....	21
2 Materials and Methods.....	21
2.1 Immunofluorescent Staining of Human Pancreas Sections for Statin Efflux Transporters.....	21
2.2 Cell Culture, Subculturing and Maintenance.....	22
2.3 Adenoviral Transduction as an Overexpression Model for Human OATP2B1 ...	23
2.4 Western Blot of OATP2B1 and OXPHOS Complex.....	24

2.5	Statin Transporter Gene Expression Analysis	25
2.6	Statin Uptake and Quantification in INS-1 cells using LC-MS/MS.....	27
2.7	Glucose-Stimulated Insulin Secretion following 24-hour Statin Treatment.....	31
2.8	MTT Assay	32
2.9	ATP Assay	33
2.10	Caspase 3/7 and Caspase 9 Assay.....	34
2.11	Graphing and Statistical Analyses	34
Chapter 3.....		35
3	Results	35
3.1	Characterization of the Endogenous Expression of Statin Transporters in the Human Pancreas.....	35
3.2	Characterization of the Endogenous Expression of Statin Transporters in INS-1 Cells	49
3.3	OATP2B1 overexpression model in INS-1 cells	51
3.4	The Effect of OATP2B1 and Inhibition of Statin Efflux Transporters on Cellular Statin Accumulation.....	53
3.5	Role of OATP2B1 in Statin-Induced Impairment of Glucose-Stimulated Insulin Secretion and the Involvement of the Mevalonate Pathway.....	59
3.6	Role of OATP2B1 in Statin-Mediated Effect on Mitochondrial Function.....	69
3.7	Role of OATP2B1 in Statin-Mediated Effect on Cellular ATP Concentration....	73
3.8	Role of OATP2B1 in Statin-Mediated Effects on Caspase 3/7 and 9 Activity	76
Chapter 4.....		79
4	Discussion and Conclusion	79
4.1	Summary of Key Findings	79
4.2	Contribution to Existing Literature.....	84
4.3	Limitations of study and future directions	89
4.4	Conclusion	92

References 93

Appendix A: Exploratory Evaluation of Mrp Expression in INS-1 Cells Compared to
Rat Liver and Attempted CRISPR-Mediated Downregulation of P-gp, Mrp1 and
Mrp3 109

Curriculum Vitae 115

List of Tables

Table 1.1. Overview of human OATPs, their tissue expression and substrates.....	2
Table 1.2. Physicochemical characteristics and pharmacokinetic parameters of rosuvastatin, atorvastatin and pravastatin following 40-mg oral dose.....	12
Table 2.1. Paraffin-embedded normal pancreatic tissue sections used for immunofluorescence staining of P-gp and BCRP.....	21
Table 2.2. Forward and reverse sequences of RT-qPCR primers for statin uptake and efflux transporters in INS-1 cells.....	27
Supplementary Table 1. MRP expression and substrate specificities in humans... 	109
Supplementary Table 2. Forward and reverse sequences of RT-qPCR primers for rat Mrps in INS-1 cells.....	110
Supplementary Table 3. CRISPR-Cas9 gRNA sequences used for CRISPR knockout in INS-1 cells.....	111

List of Figures

Figure 1.1. A schematic representation of a beta cell and the steps involved in insulin secretion following glucose stimulation.....	8
Figure 1.2. Schematic summarizing key mechanisms underlying statin-induced beta cell dysfunction.....	18
Figure 2.1. Sample standard curves for rosuvastatin, atorvastatin and pravastatin (0-100 ng/mL).....	30
Figure 3.1. Representative images of P-glycoprotein (P-gp) co-localization with insulin-producing beta cells in normal adult human pancreas.....	36
Figure 3.2. Representative images of breast cancer resistance protein (BCRP) co-localization with insulin-producing beta cells in normal adult human pancreas.....	39
Figure 3.3. Representative images of P-glycoprotein (P-gp) co-localization with glucagon-producing alpha cells in normal adult human pancreas.....	42
Figure 3.4. Representative images of breast cancer resistance protein (BCRP) co-localization with glucagon-producing alpha cells in normal adult human pancreas.....	45
Figure 3.5. Quantitative co-localization analysis of P-glycoprotein (P-gp) and breast cancer resistance protein (BCRP).....	48
Figure 3.6. Statin efflux transporter expression in INS-1 cells.....	50
Figure 3.7. Characterization of OATP2B1 overexpression in INS-1 cells using immunofluorescent staining (A, B) and western blot (C).....	52
Figure 3.8. Statin uptake in Ad-OATP2B1 INS-1 cells compared to Ad-LacZ.....	54

Figure 3.9. Effect of statin concentration and time on rosuvastatin uptake with or without inhibitors of statin efflux transporters in Ad-OATP2B1 INS-1 cells compared to Ad-LacZ.....	57
Figure 3.10. Insulin concentration following low-glucose stimulation (A, B), high-glucose stimulation (C, D), stimulation index (E, F) and normalized stimulation index (%DMSO) (G, H) after 24-hour rosuvastatin treatment.....	62
Figure 3.11. Insulin concentration following low-glucose stimulation (A, B), high-glucose stimulation (C, D), stimulation index (E, F) and normalized stimulation index (%DMSO) (G, H) after 24-hour atorvastatin treatment.....	64
Figure 3.12. Insulin concentration following low-glucose stimulation (A, B), high-glucose stimulation (C, D), stimulation index (E, F) and normalized stimulation index (%DMSO) (G, H) after 24-hour pravastatin treatment.....	66
Figure 3.13. Dose-response curves for formazan formation following 24-hour treatment with increasing statin concentrations in Ad-OATP2B1 or Ad-LacZ INS-1 cells.....	69
Figure 3.14. Representative western blot (A) and quantification of band intensity (B) for mitochondrial complexes I-V following atorvastatin treatment in Ad-OATP2B1 or Ad-LacZ INS-1 cells.....	71
Figure 3.15. ATP level (represented as % DMSO) following 24-hour statin treatment in Ad-LacZ control, OATP2B1-overexpressing and non-transduced INS-1 cells.....	74
Figure 3.16. Caspase 3/7 (A) or 9 (B) activity in OATP2B1-overexpressing versus Ad-LacZ INS-1 cells following 24-hour statin/substrate treatment.....	77
Figure 4.1. A summary of key findings.....	82
Supplementary Figure 1. Mrp expression in INS-1 cells.....	112

List of Abbreviations

ABC	ATP-binding cassette transporter
Ad-LacZ	adenovirus for LacZ
Ad-OATP2B1	adenovirus for OATP2B1
ADP	adenosine diphosphate
ANOVA	analysis of variance
ATP	adenosine triphosphate
BCA	bicinchoninic acid
BCRP	breast cancer resistance protein
Bax	Bcl-2 associated X protein
cDNA	complementary DNA
CO₂	carbon dioxide
CRISPR	clustered regularly interspaced short palindromic repeat
CYP	cytochrome P450
Ca²⁺	calcium ion
Ct	threshold cycle
DNA	deoxyribonucleic acid
DMSO	dimethylsulfoxide
eIC₅₀	estimated half-maximal inhibitory concentration

ELISA	enzyme-linked immunosorbent assay
eNOS	endothelial nitric oxide synthase
ER	endoplasmic reticulum
FBS	fetal bovine serum
FPP	farnesyl pyrophosphate
GAPDH	glyceraldehyde-3-phosphate dehydrogenase
GGPP	geranylgeranyl pyrophosphate
GLUT	glucose transporter
GSIS	glucose-stimulated insulin secretion
GTP	guanosine triphosphate
HEPES	4-(2-hydroxyethyl)-1-piperazineethanesulfonic acid
HMG-CoA	3-hydroxy-3-methylglutaryl coenzyme A
HRP	horseradish peroxidase
hs-CRP	high-sensitivity C-reactive protein
IC50	half-maximal inhibitory concentration
KRHB	Kresb-Ringer HEPES buffer
K_m	Michaelis constant
LC-MS/MS	liquid chromatography-tandem mass spectrometry
LDL	low-density lipoprotein
MDR	multidrug resistance protein

MOI	multiplicity of infection
MRP	multidrug resistance-associated protein
MTT	3-(4,5-dimethylthiazol-2-yl)-2,5-diphenyltetrazolium bromide
NO	nitric oxide
NODM	new-onset diabetes mellitus
Na⁺	sodium ion
OATP	organic anion transporting polypeptide
PGC-1α	peroxisome proliferator-activated receptor gamma coactivator-1 alpha
P-gp	P-glycoprotein
PI3K	phosphatidylinositol 3-kinase
PPARγ	peroxisome proliferator-activated receptor gamma
PVDF	polyvinylidene fluoride
RNA	ribonucleic acid
ROS	reactive oxygen species
RPMI	Roswell Park Memorial Institute
RT-qPCR	reverse transcription-quantitative polymerase chain reaction
RhoA	Ras homology gene family member A
SI	stimulation index
SLCO	solute carrier superfamily

SREBP sterol regulatory element-binding protein

Tmax time for maximal systemic concentration

Chapter 1

1 Introduction

1.1 Organic Anion Transporting Polypeptides

Membrane transporters are increasingly being recognized as important determinants of cellular drug entry and consequently drug concentration at target sites. Of these, organic anion transporting polypeptides (humans: OATP, gene: solute carrier protein [*SLCO*], rodents: *Oatp*, gene: *Slco*) are a family of membrane-bound transport proteins that play a crucial role in the cellular uptake of many endogenous substrates and drugs. While substrates of OATPs are largely amphipathic organic anions, neutral and positively charged substrates have also been reported (Hagenbuch & Stieger, 2013). OATPs are multi-specific transporters, and various forms of OATPs are expressed in the epithelial cells of virtually every internal organ in the body (Roth et al., 2012). To date, 11 OATPs have been identified in humans, which includes OATP1A2, OATP1B1, OATP1B3, OATP1C1, OATP2A1, OATP2B1, OATP3A1, OATP4A1, OATP5A1 and OATP6A1, differing in their substrate specificity and tissue distribution (Glaeser et al., 2010; Schulte & Ho, 2019). These human OATPs are comprised of 643-848 amino acids and are predicted to contain 12 transmembrane domains with intracellular N- and C-termini (Roth et al., 2012). It is also important to note that many human OATPs do not exactly correspond to rodent orthologues; for example, in humans, OATP1A2 is the only member of the OATP1A subfamily identified, whereas the rat *Oatp1a* subfamily consists of *Oatp1a1*, *Oatp1a3*, *Oatp1a4*, *Oatp1a5* and *Oatp1a6*, sharing between 66 to 77% amino acid sequence identity with the human counterpart (Hagenbuch & Meier, 2003, 2004). In contrast, OATP2B1 in humans have only one corresponding rodent orthologue, *Oatp2b1*.

1.1.1. Overview OATP subfamilies, expression and substrate specificity

In humans, there are 6 families of OATPs (OATP1-6) with several members in each family with different substrate specificity and expression pattern. A summary of the various OATPs, as well as their substrate specificity is summarized below in Table 1.1.

Table 1.1. Overview of human OATPs, their tissue expression and substrates.

Adapted from Hagenbuch & Stieger, 2013; Kim, 2017; Piazzagalli et al., 2002.

OATP	Tissue Expression	Substrate examples
OATP1A2	Brain, kidney, liver, lung, prostate, placenta	Bile salt, steroid hormones, fexofenadine, rocuronium
OATP1B1	Liver	Bilirubin, bile salts, thyroid hormones, statins
OATP1B3	Liver, pancreas	Bilirubin, bile salts, thyroid hormones, statins
OATP1C1	Brain	Thyroid hormones, folate, methotrexate
OATP2A1	Kidney, heart, skeletal muscle, placenta	Prostaglandins
OATP2B1	Liver, brain, lung, small intestine, pancreas	Estrone-3-sulfate, glyburide, statins
OATP3A1	Ubiquitous	Bile salts, cyclosporine
OATP4A1	Ubiquitous	Thyroid hormones, steroid conjugates
OATP4C1	Kidneys	Thyroid hormones, methotrexate
OATP5A1	N/A	Unknown
OATP6A1	Testes	Unknown

OATP, organic anion transporting polypeptide

Specifically, OATP1B1, OATP1B3 and OATP2B1 are thought to be the three OATPs that mediate the hepatic uptake of statins (Deng et al., 2021). Specifically, OATP1B1 is known to transport atorvastatin, cerivastatin, fluvastatin, pravastatin, pitavastatin and rosuvastatin (Ho et al., 2006; Kalliokoski & Niemi, 2009). OATP1B3 is known to transport fluvastatin, pitavastatin, pravastatin and rosuvastatin (Ho et al., 2006; Kalliokoski & Niemi, 2009). Lastly, OATP2B1 is known to transport atorvastatin, fluvastatin, rosuvastatin and pravastatin (Ho et al., 2006; Kalliokoski & Niemi, 2009). Interestingly, while the OATP1B subfamily is generally considered liver-specific under physiological conditions, our lab recently reported expression of OATP1B3 within the human pancreatic islets, with predominant localization to glucagon-secreting alpha cells (Kim et al., 2017). Furthermore, expression of OATP2B1, abundant in liver and many other tissues, was also found in insulin-secreting beta cells of the pancreas, suggesting a possible role of OATP1B3 and OATP2B1 in not only the hepatic uptake of statins, but also in the human pancreatic islets (Kim et al., 2017).

1.1.2. Mechanisms of OATP transport

OATPs are thought to mediate a bidirectional transport of substrates, enabling the influx of endogenous or exogenous substrates with the exchange for intracellular substrates such as glutathione or bicarbonate (Leuthold et al., 2012). It is known that OATP-mediated transport occurs independent of ATP or Na⁺ gradient; however, the chemical driving force behind OATP transport remains unclear (Roth et al., 2012).

With respect to the exact transport mechanism, a rocker-switch mechanism, where substrates are translocated through a central, positive core, has been suggested as a common mechanism for all OATP isoforms, while there may be some OATP-specific differences in the transport mechanism. (Meier-Abt et al., 2004). OATPs express multiple binding sites with varying affinities for a wide range of substrates and modulators. For example, in OATP2B1, site-directed mutagenesis studies demonstrate a reduced pravastatin and rosuvastatin uptake with mutations to histidine residues in positions 579 and 618, suggesting that these may be important residues for mediating OATP2B1-mediated uptake of statins (Hoshino et al., 2016).

The importance of OATPs in human health is highlighted by diseases owing to alterations in OATP function or variability in drug efficacy and toxicological outcomes resulting from *SLCO* mutations or polymorphisms. For example, Rotor Syndrome, a rare congenital form of hyperbilirubinemia, occurs due to mutations in OATP1B1 and OATP1B3, which leads to transport deficiencies with reduced uptake of bilirubin into the liver and thus reduced bilirubin clearance from the body, resulting in the inability to uptake (van de Steeg et al., 2012). On the other hand, increased expression of OATP1B3 has been implicated in pancreatic ductal adenocarcinoma (Thakkar et al., 2013). Furthermore, polymorphisms in various OATPs isoforms have been found to lead to altered response to drugs that are substrates of OATPs, including statins. A retrospective study in Japan found that the patient cohort carrying the impaired function 521T->C polymorphism in *SLCO1B1* experienced a decreased cholesterol-lowering effect compared to patients homozygous for the T wild type allele (Tachibana-Iimori et al., 2004). Such *SLCO* polymorphisms may therefore be used as a possible predictor for statin exposure, efficacy, and consequently, statin-induced muscle toxicity ((DeGorter et al., 2013; Tachibana-Iimori et al., 2004; Xiang et al., 2018). In addition, polymorphisms of *SLCO2B1*, such as 332G>A, 601G>A, 935G>A and 1457C>T were found to significantly decrease the OATP2B1-mediated cellular accumulation of rosuvastatin, one of its known substrates, relative to wild-type (Medwid et al., 2021).

1.2 ABC Efflux Transporters

ATP-binding cassette (ABC) family of proteins are efflux transporters with an important role in the pharmacokinetics of most drugs used today through active transport (Schinkel & Jonker, 2012). While the ABC family of transporters is highly diverse in mammals, carriers that are particularly important for drug transport include ABCB1 (also known as P-glycoprotein or P-gp- human gene: *MDR1*, rodent genes: *Mdr1a*, *Mdr1b*), ABCG2 (also known as breast cancer resistance protein or BCRP- human gene: *ABCG2*, rodent

gene: *Abcg2*) and members of the ABCC subfamily (formerly known as multidrug resistance-related proteins or MRPs, human gene: *ABCC*, rodent gene: *Abcc*). These transporters are typically expressed on the plasma membrane and mediate the cellular export of target pharmacological compounds in an active, ATP-dependent, manner against their concentration gradients (Schinkel & Jonker, 2012). We will focus herein on P-gp and BCRP because of their known role in statin pharmacokinetics and their expression in human pancreatic islets (see below).

1.2.1. P-glycoprotein structure, transport mechanism and expression

First to be discovered among the ABC transporters, P-gp consists of 12 transmembrane domains and two intracellular nucleotide binding domains (Schinkel & Jonker, 2012). These nucleotide binding domains bind and catalyze the hydrolysis of ATP, thereby enabling the ATP hydrolysis to be coupled with active transport of target compounds against their concentration gradient (Higgins et al., 1997). An important characteristic of P-gp is its substrate promiscuity, with hundreds of known substrates ranging from 330 to 4000 Daltons (Aller et al., 2009). Importantly, P-gp is known to transport atorvastatin, fluvastatin, pitavastatin and rosuvastatin (Deng et al., 2021).

Recent X-ray structural data of mouse P-gp, which share ~90% sequence identity to human P-gp, provided key insights into its transport mechanism. Nucleotide-free P-gp adapts an inward-facing conformation with a dimeric structure consisting of two nearly symmetrical halves formed from six transmembrane helical domains each, forming a large internal cavity open to the inner leaflet and the cytoplasmic side (Aller et al., 2009). The drug binding pocket has an upper half that predominantly contains hydrophobic and aromatic residues allowing for the binding of lipophilic compounds, as well as a region of polar and charged residues for hydrophilic compounds (Aller et al., 2009). Experimental evidence suggest that P-gp binds a variety of substrates through an induced-fit mechanism, where each substrate causes a specific shift in the packing of the transmembrane segments (Choudhuri & Klaassen, 2006).

In humans, P-gp is expressed in the apical membrane of hepatocytes, enterocytes of the small intestines, kidney proximal tubules, and endothelial cells, among other tissues

(Fromm, 2002). P-gp is also expressed in blood-tissue barriers, including the blood-brain, blood-placenta and blood-testis barrier, where it serves as a barrier or protective role in the active removal of many drugs, including chemotherapeutic agents (Cordoncardo et al., 1989; Hartz et al., 2016). Interestingly, P-gp expression has been reported in many types of cancer, including leukemia and breast cancer, where it confers drug resistance in tumors through the active efflux of chemotherapeutic drugs, hence its alternate name, multidrug resistance transporter or MDR1 (Faneyte et al., 2001; Fromm, 2002). Note that rodents have two genes encoding for P-gp- *Mdr1a* and *Mdr1b*- however, *Mdr1a* seems to share about 80% homology with human P-gp and is the main rodent isoform of interest (Sauna et al., 2001).

1.2.2. BCRP structure, transport mechanism and expression

Unlike P-gp, BCRP only contains one intracellular nucleotide binding domain and one membrane-spanning domain consisting of 6 transmembrane helices (Mao & Unadkat, 2015). Recent structural studies suggest that BCRP is able to form homodimers or homooligomers through protein-protein interactions; however, the functional role of dimerization/oligomerization and how ATP hydrolysis is coupled to drug transport at the molecular level are still poorly understood (Mao & Unadkat, 2015; Ni et al., 2010).

Like other members of the ABC family of transporters, BCRP shows a broad substrate specificity, including chemotherapeutic agents such as methotrexate, topotecan and imatinib, and other drugs such as glyburide, cimetidine and statins (Ni et al., 2010). Specifically, fluvastatin, pitavastatin, rosuvastatin and atorvastatin are known substrates of BCRP, and polymorphisms of the ABCG2 gene, such as 421C>A, was shown to be a predictor of rosuvastatin exposure in humans (Deng et al., 2021; DeGorter et al., 2013). BCRP is expressed in the apical membrane of hepatocytes and small intestine, kidneys, blood-brain barrier and placenta. Interestingly, BCRP is also highly expressed in primitive stem cells, where it serves a protective role against xenobiotics during development and in breast cancer and leukemia, where it confers drug resistance to common chemotherapeutic agents (Ni et al., 2010; Robey et al., 2007).

1.3 Endocrine Pancreas and Diabetes Mellitus

The pancreas is a unique organ with both exocrine and endocrine functions. The endocrine portion of the pancreas is comprised of the Islets of Langerhans, or simply islets, which consist of five major cell types- alpha cells which secrete glucagon, beta cells which secrete insulin, delta cells which secrete somatostatin, PP cells which secrete pancreatic polypeptide and epsilon cells which secrete ghrelin (Ballian & Brunicardi, 2007; Sakata et al., 2019). Somatostatin acts to inhibit insulin and glucagon release, pancreatic polypeptide acts to inhibit the exocrine secretion from the pancreas and ghrelin acts to increase appetite. Glucagon and insulin are the primary hormones responsible for glucose homeostasis, serving reciprocal roles of increasing and decreasing blood glucose levels, respectively (Hoang et al., 2014). Interestingly, the architecture of pancreatic islets shows some inter-species differences; rodent islets are thought to primarily consist of a core of beta cells, up to 90%, with alpha cells surrounding the periphery of the islets (Hoang et al., 2014). In humans, islets appear to have a mixed morphology, with alpha cells being relatively more numerous and beta cells interspersed throughout the entire islet (Hoang et al., 2014).

1.3.1. Beta cell and insulin secretion

In beta cells, insulin is initially produced as pre-proinsulin, which undergoes conformational maturation at the endoplasmic reticulum to proinsulin, which is then translocated to the Golgi apparatus and packaged into secretory vesicles and cleaved into functional insulin and C-peptide (Fu et al., 2013). In humans, the glucose transporter GLUT1 is thought to facilitate the uptake of glucose into the beta cells, while in rodents, Glut2 seems to be the main glucose transporter in beta cells (Berger & Zdzieblo, 2020). Once inside the cell, glucose undergoes glycolysis to yield pyruvate, which is then oxidized in the mitochondria, the site of electron transport chain, which results in an accumulation of ATP (Berger & Zdzieblo, 2020). This increase in the intracellular ATP/ADP ratio is sensed by the K^+ -ATP channels on the plasma membrane of the beta cell and leads to their closure, resulting in beta cell depolarization. This depolarization is sensed by and triggers the opening of voltage-dependent Ca^{2+} channels, leading to

calcium ion influx, which primes the insulin granules to fuse with the plasma membrane, resulting in insulin exocytosis (Fu et al., 2013). A schematic representation of a beta cell with major steps involved in glucose-stimulated insulin secretion, is shown in the schematic below (**Figure 1.1**).

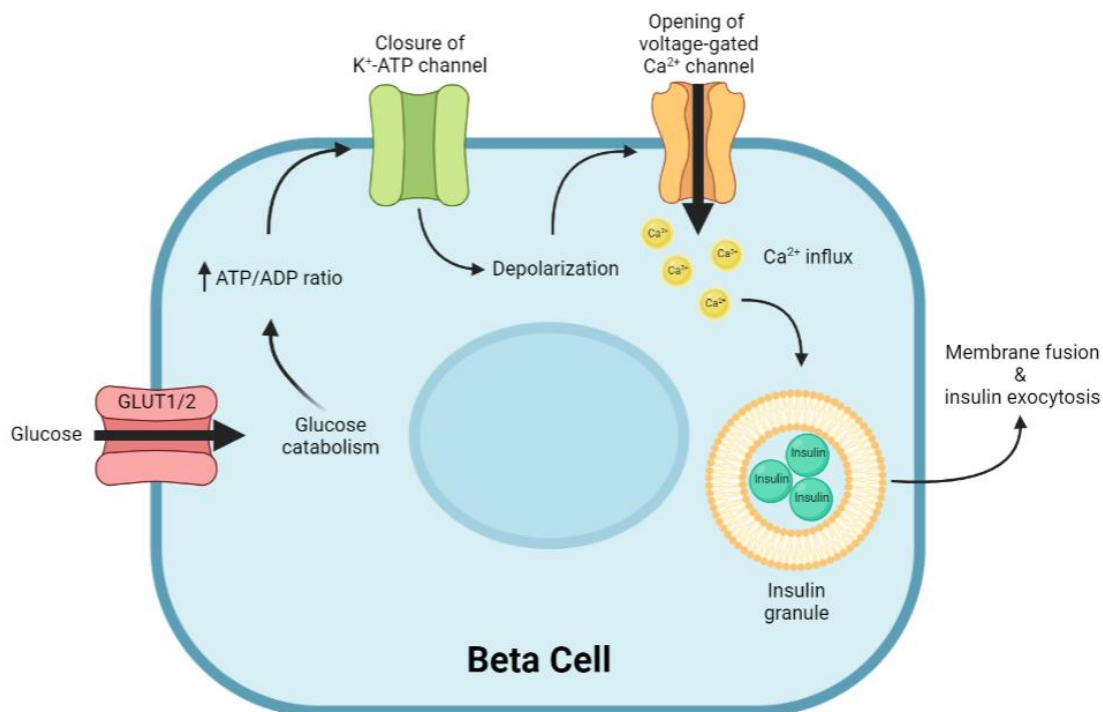


Figure 1.1. A schematic representation of a beta cell and the steps involved in insulin secretion following glucose stimulation. Figure was created using BioRender with information adapted from Fu et al., 2013; Galicia-Garcia et al., 2020.

1.3.2. Type 1 and type 2 diabetes mellitus

Insulin is a crucial hormone involved in the pathogenesis of diabetes mellitus, as it is the primary hormone that drives blood glucose down and promotes glucose utilization post-prandially. Diabetes mellitus refers to a group of metabolic diseases caused by chronic hyperglycemia as a result of impaired insulin secretion, insulin action/sensitivity or a

combination of both (Kharroubi, 2015). Type 1 diabetes constitutes less than 10% of diagnosed cases and is mostly attributed to the autoimmune destruction of beta cells, resulting in the lack of endogenous insulin secretion required for glucose control (Daneman, 2006; Kharroubi, 2015). Type 2 diabetes is responsible for between 90~95% of cases, and the majority of diagnosed patients are adults (Kharroubi, 2015). The major pathophysiological characteristic of type 2 diabetes is insulin resistance in the peripheral tissues, as well as the resulting increased demand for insulin and gradual beta cell dysfunction (Druet et al., 2006). Specifically, beta cell dysfunction and later cell death lead to reduced insulin secretion, which impairs the body's ability to maintain a physiological blood glucose level, whereas insulin resistance leads to decreased glucose uptake in the muscle and adipose tissue and promotes gluconeogenesis in the liver (Galicia-Garcia et al., 2020). Insulin normally acts to promote carbohydrate and lipid metabolism in the peripheral tissues, stimulate glycogen synthesis and inhibit glycogen breakdown. However, with insulin resistance, such insulinogenic actions are impaired, contributing to diabetes. While it was traditionally thought that beta cell dysfunction is mediated mostly through simple beta cell death, emerging evidence suggest a complex network of molecular pathways that likely contributes to beta cell dysfunction, including local islet inflammation, oxidative damage and mitochondrial dysfunction (Galicia-Garcia et al., 2020).

1.4 Statins and Their Mechanisms of Action

1.4.1. Clinical benefits of statins

Statins are a common class of drugs prescribed for the treatment of hypercholesterolemia and to reduce the risk of cardiovascular events such as coronary heart disease. Currently, about 3 million Canadians are taking statins, making them one of the most prescribed class of drugs (Hennessy et al., 2016). Therapeutic benefits of statins, including reduction in plasma low-density lipoprotein (LDL), reduced risk of myocardial infarction and for

the treatment of hypercholesterolemia has been well documented in a number of randomized clinical trials (Ridker et al., 2008; Shepherd et al., 2004).

1.4.2. Mechanisms of action of statins

Statins act as competitive inhibitors of 3-hydroxy-3-methylglutaryl coenzyme A (HMG-CoA) reductase, the rate-limiting enzyme in the mevalonate pathway. Inhibition of this enzyme therefore reduces the amount of cholesterol synthesized in the liver. In addition to direct enzymatic inhibition, statins are thought to induce conformational changes in the HMG-CoA reductase, preventing it from adopting a functional structure (Stancu & Sima, 2001). Furthermore, statin-mediated inhibition of HMG-CoA reductase is thought to induce protease activation which cleaves the sterol regulatory element binding proteins (SREBPs) (Stancu & Sima, 2001). The SREBPs are normally membrane-bound proteins on the endoplasmic reticulum (ER), but the protease-mediated cleavage of the SREBPs in response to the inhibition of the HMG-CoA reductase allows a soluble moiety to translocate to the nucleus, consequently inducing the transcription of LDL receptors (Goldstein & Brown, 2009). The resulting increase in the number of LDL receptors on the hepatocyte membrane allows for a greater uptake of circulating LDL into the liver and consequently mediate its removal, effectively lowering serum LDL levels. Although statins do induce a compensatory increase in the expression of HMG-CoA reductase through the SREBPs, causing a net increase in the pool of HMG-CoA reductase, it does not increase net cholesterol synthesis due to the effective and specific inhibition of the enzyme by the statins (Goldstein & Brown, 2009).

Besides this primary mechanism of action of mevalonate pathway inhibition, a number of pleiotropic effects exist which may explain some of the clinical benefits of statins. First, statin treatment has been shown to increase myocardial perfusion and improve endothelial function (Davignon, 2004). Specifically, statins are thought to prevent the downregulation of endothelial nitric oxide synthase (eNOS) and directly enhance its enzymatic activity, resulting in increased bioavailability of nitric oxide (NO) (Martínez-gonzález et al., 2001), an important signaling molecule for endothelium-mediated hemodynamic homeostasis and regulation of vascular smooth muscle cells. Furthermore,

statins have been shown to significantly reduce plasma high-sensitivity C-reactive protein (hs-CRP) levels, suggesting a direct anti-inflammatory effects of statins and consequently its therapeutic benefits in the prevention of cardiovascular events (Jialal et al., 2001).

1.4.3. Pharmacokinetic parameters of common statins

Statin agents differ in their pharmacokinetic parameters and thus their absorption, distribution, metabolism and excretion. In patients receiving therapeutic doses of statins (5-80 mg daily), plasma concentrations between 1-10 ng/mL, equivalent to about 2~20 nmol/L, have been observed (DeGorter et al., 2013). Statins can be broadly classified into lipophilic or hydrophilic statins based on the log value of the partition coefficient (log P) or according to their potency to inhibit the HMG-CoA reductase using the IC_{50} , the half-maximal inhibitory concentration. **Table 1.2.** summarizes relevant characteristics for rosuvastatin, atorvastatin and pravastatin, the three commonly prescribed statins that are of interest to our research project, as differences in their physiochemical properties and a shared affinity for OATPs may relate to potential differences in statin-mediated toxicities in the endocrine pancreas (further discussed below). For example, atorvastatin is a lipophilic statin and can more readily enter the cells through diffusion and is also extensively metabolized before being excreted (Lennernäs, 2003). On the other hand, rosuvastatin and pravastatin are hydrophilic statins and therefore are primarily dependent on facilitated transport to cross the plasma membrane. The majority of rosuvastatin and pravastatin are also excreted as the parent drug, with only a fraction of the dose undergoing metabolism by cytochrome P450 (CYP) and other phase II drug-metabolizing enzymes (Hatanaka, 2000; Martin et al., 2003).

Table 1.2. Physicochemical characteristics and pharmacokinetic parameters of rosuvastatin, atorvastatin and pravastatin following 40-mg oral dose. IC₅₀ values were obtained from purified human HMG-CoA. Adapted from Bellosta et al., 2004; Chapman & Mctaggart, 2002; Deng et al., 2021; Ho et al., 2006.

Parameter	Rosuvastatin	Atorvastatin	Pravastatin
Lipophilic/hydrophilic	Hydrophilic	Lipophilic	Hydrophilic
T_{max} (hr)	3	2-3	0.9-1.6
Bioavailability (%)	20	12	18
Protein binding (%)	88	80-90	43-55
Phase I and II Metabolism	CYP2C9 (major) CYP2C19 (minor)	CYP3A4	sulfation
Uptake Transport	OATP1A2, OATP1B1, OATP1B3, OATP2B1	OATP1B1, OATP1B3, OATP2B1	OATP1B1, OATP1B3, OATP2B1
Efflux Transport	P-gp, BCRP	P-gp, BCRP	N/A
IC₅₀	5.4	8.2	44.1

BCRP, breast cancer resistance protein; CYP, cytochrome P450; IC₅₀, half-maximal inhibitory concentration; OATP, organic anion transporting polypeptide; P-gp, P-glycoprotein; T_{max}, time for maximal systemic concentration.

1.4.4. Statin-induced myopathy

Even though statins are considered one of the most effective pharmacological treatment options in reducing the risk of cardiovascular diseases such as myocardial infarction and stroke, their side effect profile, most notably statin-induced myopathy, represents an important clinical barrier (Antons et al., 2006; Sathasivam, 2012). In randomized clinical trials, the incidence of statin-induced myopathy has been reported to be between 1.5-5% (Bitzur et al., 2013). One retrospective observational study showed that the patient group taking statins experienced an approximate doubling of myopathic event, mostly in the form of myalgia or muscle pain and mild myositis, an inflammation of the skeletal muscles, as measured through varying criteria for clinical markers such as an increase in serum creatine kinase levels, compared to patient group not undergoing statin treatment (Nichols & Koro, 2007). In particular, increased reports of rhabdomyolysis, a rare but potentially life-threatening form of myopathy caused by statins, has been the cause for the withdrawal of cerivastatin from the market in 2001 (Pasternak et al., 2002). Studies have suggested several risk factors for the increased risk of statin-induced myopathy, including existing kidney or liver disease, exercise, Asian race and co-treatment with other medications such as fibrates (Antons et al., 2006).

Although the exact mechanisms of statin-induced myotoxicity have not been fully elucidated, several candidate mechanisms have been proposed, including mevalonate pathway-mediated effects, cellular pathways, genetic factors and altered statin uptake or metabolism, the latter leading to increased systemic statin exposure (Ward et al., 2019). *In vitro* experiments showed that statins may induce a concentration-dependent increase in apoptosis, or programmed cell death, within skeletal myoblasts, myotubes and in differentiated human skeletal muscle cells (Dirks & Jones, 2006). Studies suggest that statin-induced apoptosis of skeletal muscle cells may at least in part be mediated by the mitochondria. One study showed that statins induce the activation of calpain, a family of non-lysosomal cysteine proteases, in human skeletal muscle cells (Sacher et al., 2005). Calpain activation leads to the translocation of Bcl-2 associated X protein (Bax) and activates mitochondrial apoptotic pathway through the release of cytochrome c and the consequent activation of caspase-9 and caspase-3 (Sacher et al., 2005). Furthermore, co-

treatment of statins with mevalonate led to a partial reversal of caspase-9 and caspase-3 activation, suggesting the importance of the mevalonate pathway in mediating mitochondrial caspase activation (Sacher et al., 2005).

Besides reducing cholesterol biosynthesis through a competitive inhibition of the mevalonate pathway, statins also reduce the pool of isoprenoid by-products along the mevalonate pathway, most notably farnesyl pyrophosphate (FPP) and geranylgeranyl pyrophosphate (GGPP)(Dirks & Jones, 2006). These isoprenoids contribute to the post-translational modification of a number of target proteins through prenylation (du Souich et al., 2017). For example, Ras homology gene family member A (RhoA) is a major target protein that is prenylated and activated by GGPP (du Souich et al., 2017). This leads to the phosphorylation of phosphatidylinositol 3-kinase (PI3K) and ultimately activates the transcription factor peroxisome proliferator-activated receptor gamma coactivator-1 alpha (PGC-1 α), leading to the recruitment of peroxisome proliferator-activated receptor gamma (PPAR γ), an important regulator of mitochondrial function and proliferation (Rodrigue-Way et al., 2014). In addition, statin-associated impairments in mitochondrial calcium signaling and depletion in sarcolemmal membrane cholesterol have been suggested (Sathasivam, 2012; Sirvent et al., 2008).

While these *in vitro* studies highlight a number of possible mechanisms of statin-induced myotoxicity, it is unclear how well such findings extend *in vivo* (Dirks & Jones, 2006). Previous *in vivo* studies using animal models showed statin-associated myotoxicity as measured by membrane damage, abnormalities in electromyography readings and changes in ultrastructural morphology (Taha et al., 2014). Overall, statin-induced myotoxicity is a commonly reported phenomenon and is likely multifactorial and statin-dependent, but a major contribution seems to stem from mitochondrial dysregulation and apoptosis (Sirvent et al., 2008).

1.5 Statin-Induced New Onset Diabetes Mellitus (NODM)

1.5.1. Clinical evidence of statin-induced NODM

While myopathy is the most common and relatively well studied side effect of statins, recent evidence suggests that statin treatment is linked to increased risk of developing new-onset diabetes mellitus (NODM). A meta-analysis of randomized clinical trials reported a relative risk increase of about 10-12%, which is likely dose- and statin-dependent, with a higher dose generally correlated with a greater risk increase and rosuvastatin being associated with the greatest risk increase compared to pravastatin (Betteridge & Carmena, 2016; Navarese et al., 2013; Ridker et al., 2008). Specifically, the largest randomized clinical trial with rosuvastatin to date with over 17800 subjects, suggested that treatment with 20 mg rosuvastatin daily led to a 25% increased relative risk of NODM diagnosis (3% incidence) compared to placebo (2.4% incidence) at study endpoint (median 1.9 years) (Ridker et al., 2008). On the other hand, a randomized clinical trial involving pravastatin with over 4100 subjects showed that 40 mg pravastatin daily was associated with ~30% reduction in NODM incidence compared to placebo (Ames et al., 1995; Freeman et al., 2001). While the exact reasons are not known, it is suspected that this protective effect may be a result of the very low potency of pravastatin, combined with its pleiotropic effects such as anti-inflammatory effects and improved endothelial function which act to decrease the risk of developing NODM (Freeman et al., 2001).

1.5.2. Mechanisms of statin-induced beta cell dysfunction

The mechanisms by which statins contribute to diabetogenesis are thought to be multifactorial. Consistent with the pathology of type 2 diabetes, statins have been shown to lead to insulin resistance in the peripheral tissues such as skeletal muscle and adipocytes and also at the level of beta cells by impairing insulin secretion (Betteridge & Carmena, 2016). A follow-up study of more than 8700 non-diabetic patients receiving statins found a dose-dependent increase in the diagnosis of type 2 diabetes, as well as impairment in insulin sensitivity as measured by the Matsuda Index, which considers the

insulin and glucose concentrations at fasted and post-glucose state (Cederberg et al., 2015). Using primary mouse islets, one study reported that the impairment in insulin secretion following atorvastatin treatment may be both dose- (0, 1.5 to 15 μM) and time-dependent (24 hours to 7 days), with a 24-hour treatment with 15 μM atorvastatin treatment resulting in about 30% reduction in insulin secretion (Hoffmeister et al., 2020). Another study using a beta cell model have found a similar result, showing a dose-dependent reduction in insulin secretion following 48-hour rosuvastatin treatment, with a ~30% reduction in insulin secretion at 20 μM (Salunkhe et al., 2016). Moreover, the statin-induced impairment in insulin secretion was supported in an animal study, where a high-fat diet-induced increase in insulin secretion was further impaired in mice receiving rosuvastatin (Salunkhe et al., 2016).

By inhibiting the mevalonate pathway, statins reduce the pool of coenzyme Q10, an important intermediate in mitochondrial electron transport chain. Although findings are mixed regarding whether supplementation of coenzyme Q10 reduces statin-induced toxicities in humans, coenzyme Q10 likely plays a key role in statin-induced mitochondrial dysfunction by impairing ATP production (Deichmann et al., 2010). Besides its role as the primary cellular energy source, ATP is an important mediator required for insulin secretion by controlling the K^+ -ATP channel, which subsequently activates L-type, voltage-gated Ca^{2+} channels for insulin secretion (Betteridge & Carmena, 2016). Patch-clamp techniques have supported that some statins reversibly inhibit L-type calcium channel activity in beta cells and inhibit the rise in cytosolic calcium, which is required for insulin granule exocytosis (Yada et al., 2009). In addition to impaired ATP production, statins are known to increase reactive oxygen species (ROS) level, production of amyloid beta proteins and activation of intrinsic apoptosis through the activation of Bax (Mollazadeh et al., 2021). Similar to mechanisms of statin-induced myopathy, as discussed previously, statin-induced calpain activation is thought to enable the translocation of Bax to the outer mitochondrial membrane and causing the release of cytochrome c (Mollazadeh et al., 2021). This release of which in turn initiates the apoptotic cascade through the activation of caspase 9, a mitochondrial caspase, which in turn activates downstream effector caspases 3 and 7, leading to beta cell death (Mollazadeh et al., 2021; Shaw & Kirshenbaum, 2006). Furthermore, several small

GTPases serve a crucial role in normal beta cell function through cytoskeletal dynamics and vesicle trafficking (Veluthakal & Thurmond, 2021). These GTPases undergo farnesylation, a type of post-translational modification, by FPP and GGPP, two key intermediates in the mevalonate pathway which is inhibited by statins as described above (Veluthakal & Thurmond, 2021). Consequently, impaired farnesylation of these small GTPases by FPP and GGPP may impair insulin secretion through cytoskeletal remodeling and defects in the trafficking of insulin granules. A schematic detailing the proposed mechanisms of statin-induced beta cell toxicity, highlighting key intermediates involved in the mevalonate pathway, is shown in **Figure 1.2**.

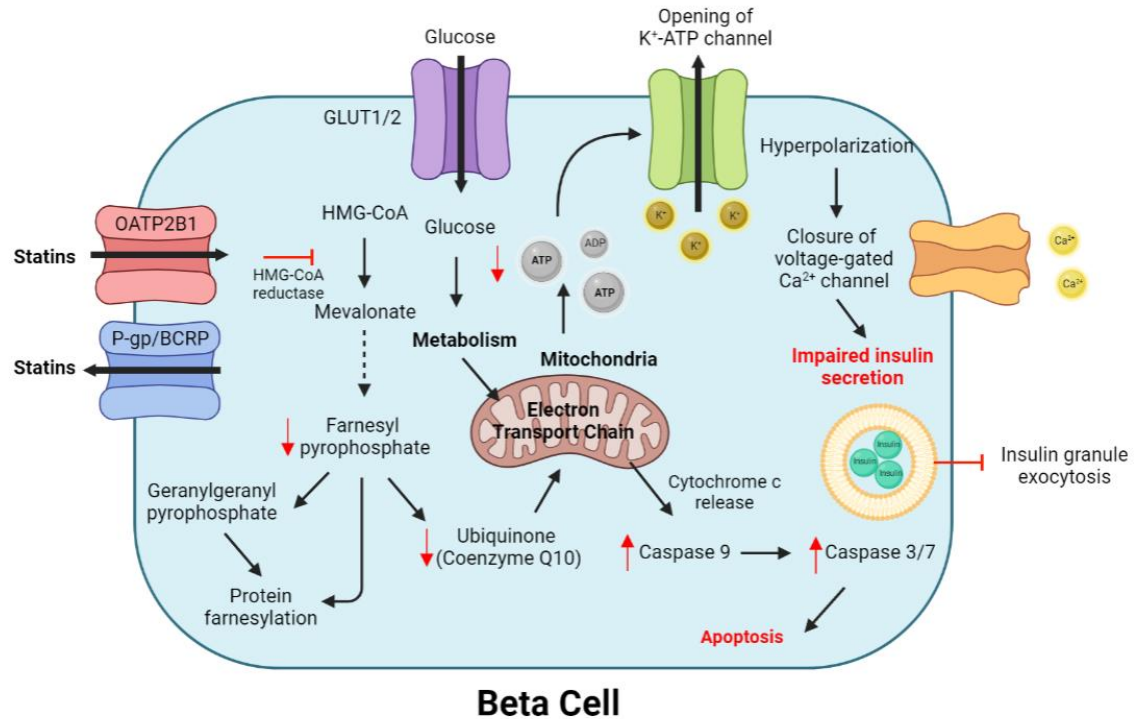


Figure 1.2. Schematic summarizing key mechanisms underlying statin-induced beta cell dysfunction. Figure was created using BioRender with information adapted from various sources (Betteridge & Carmena, 2016; Deichmann et al., 2010; Mollazadeh et al., 2021; Yada et al., 1999).

ADP, adenosine diphosphate; ATP, adenosine triphosphate; BCRP, breast cancer resistance protein; GLUT, glucose transporter; HMG-CoA, 3-hydroxy-3-methylglutaryl coenzyme A; OATP, organic anion transporting polypeptide; P-gp, P-glycoprotein.

1.6 Rationale, Aims and Hypothesis

1.6.1. Rationale

Statins are cholesterol-lowering drugs that work by inhibiting the mevalonate pathway. Recently, statin treatment has been linked to an increase in the risk of new-onset diabetes mellitus in patients, likely associated with increased statin dose and potency (Betteridge & Carmena, 2016; Navarese et al., 2013; Ridker et al., 2008). Previous cell-based and animal studies suggest statin-induced impairment in beta cell function, including reduced insulin secretion, apoptosis and mitochondrial dysfunction (Betteridge & Carmena, 2016; Deichmann et al., 2010; Mollazadeh et al., 2021).

An important family of transporters involved in hepatic uptake of statins are organic anion transporting polypeptides (OATPs), including OATP2B1, of which rosuvastatin, atorvastatin and pravastatin are known substrates (Ho et al., 2006; Kalliokoski & Niemi, 2009). Our lab has recently reported expression of OATP2B1 in normal adult pancreatic islets, with preferential distribution to the beta cell (Kim et al., 2017). Moreover, we also observed gene expression of the efflux transporters P-gp and BCRP in normal human islets (Kim, 2017), which are known statin carriers. While mRNA expression analysis suggests the presence of P-gp and BCRP in human beta cells (Kutlu et al., 2009), their cellular localization within the islet has yet to be fully characterized.

While several mechanisms underlying statin-induced beta cell dysfunction have been proposed, the link between OATP2B1-mediated statin transport and its effect on beta cell function via the mevalonate pathway, including insulin secretion, ATP level, apoptosis activation and mitochondrial function has not been studied. Initial data have been previously obtained by a former Master's student in our lab (Kim, 2017).

Accordingly, this project aimed to study the role of OATP2B1 on the cellular accumulation of statins and its association with beta cell dysfunction and underlying mechanisms of statin toxicity using INS-1 cells. INS-1 cells are a commonly used beta cell line which is derived from X-ray-induced rat insulinoma; specifically, our project used INS-1 832/13 cells, a subclone of INS-1 cells that were generated through a stable

transfection with human proinsulin gene and are more resistant to apoptosis than the parental INS-1 cells (Safety Data Sheet, Millipore-Sigma). Similar to beta cells *in vivo*, the physiological response of robust insulin secretion following glucose stimulation makes the INS-1 cells an appropriate model to study beta cell function and insulin secretion (Hohmeier et al., 2000).

1.6.2. Hypothesis

- 1) We hypothesized that, like OATP2B1, the statin efflux transporters P-gp and BCRP localize to the human beta cell.
- 2) We hypothesized that human OATP2B1 facilitates the cellular statin accumulation in a rat beta cell model (INS-1) overexpressing OATP2B1, which is further augmented by the inhibition of statin efflux transporters P-gp and Bcrp.
- 3) We hypothesized that OATP2B1 augments statin-induced impairment in beta cell function such as insulin secretion, cellular ATP level, mitochondrial function and apoptosis activation via inhibition of HMG-CoA reductase, and that supplementation with mevalonate pathway intermediates, FPP and GGPP, will rescue these effects in a rat beta cell model (INS-1) overexpressing OATP2B1.

1.6.3. Specific aims

- 1) To characterize the endogenous expression of statin uptake and efflux transporters in human pancreatic islets and INS-1 cells.
- 2) To establish a transient OATP2B1-overexpression model in INS-1 cells and characterize the role of OATP2B1 on cellular statin accumulation with or without known pharmacological inhibitors of statin efflux transporters expressed in INS-1 cells.
- 3) To elucidate the role of OATP2B1 in statin-induced impairment of beta cell function using INS-1 cells by assessing insulin secretion, cellular ATP level, mitochondrial function and apoptosis activation.

Chapter 2

2 Materials and Methods

2.1 Immunofluorescent Staining of Human Pancreas Sections for Statin Efflux Transporters

To investigate the expression of statin efflux transporters P-gp and BCRP in the human pancreas, we conducted immunostaining on paraffin-embedded normal adult human pancreas sections (Biochain, Catalog #: T2234188, Newark, California, USA). The sample ID, along with the subject's sex and age are summarized in **Table 2.1**.

Table 2.1. Paraffin-embedded normal pancreatic tissue sections used for immunofluorescence staining of P-gp and BCRP. All sections were obtained from BioChain (Newark, California, USA).

Sample ID (lot #)	Sex	Age (years)
B605108	Male	71
B903130	Male	77
C705138	Female	77

Following standard procedures, paraffin-embedded sections were deparaffinized using a series of xylene/ethanol washes and were rehydrated with water. A heat-induced epitope retrieval was performed using a microwave for 15 minutes in three 5-minute intervals in a citrate buffer (10 mM sodium citrate, 0.05% Tween 20, pH 6.0). Subsequently, the slides were left to cool at room temperature and blocked in PBS containing 5% BSA (Sigma-Aldrich, St. Louis, Missouri, USA) for 1 hour. The slides were then incubated overnight at 4°C with the primary antibody for P-gp (1:50, P7965, mouse monoclonal, Sigma-Aldrich) or BCRP (1:50, sc-58222, mouse monoclonal, Santa Cruz Biotechnology, Dallas, Texas, USA). Then, the slides were washed and blocked again in PBS containing 5% BSA for 1 hour and incubated with secondary fluorescent antibody (1:1000, anti-mouse Alexa Fluor 488 or Texas Red, ThermoFisher Scientific, Waltham, Massachusetts, USA) for 30 minutes at room temperature. The slides were mounted with VECTASHIELD® Antifade Mounting Medium with DAPI (Vector Laboratories, Burlingame, California, USA) and visualized under a Nikon Eclipse 80i fluorescence microscope (Nikon Instruments Inc., Melville, New York, USA).

For the quantitative analysis of immunofluorescence images, ImageJ Fiji software with JACoP plugin was used (Bolte & Cordelieres, 2006; Schindelin et al., 2012). ImageJ Fiji was used to split each overlay image into the respective channels to isolate the signal resulting from the appropriate antibody, and the JACoP plugin was used to yield the Pearson's correlation coefficient (r) as an indicator of the degree of co-staining of the two antibodies of interest. In brief, the JACoP plugin plots the location and intensity of the two signals of interest along the x- and y-axis, and the Pearson's correlation coefficient is the correlation coefficient of the resulting scatter plot.

2.2 Cell Culture, Subculturing and Maintenance

INS-1 832/13 cells were purchased from Sigma-Aldrich and cultured in 75 cm² Falcon Tissue Culture Flasks (ThermoFisher Scientific) in RPMI-1640 medium containing 2

mM L-glutamine (Sigma-Aldrich), supplemented with 10% FBS (Gibco, ThermoFisher Scientific), 25 mM 4-(2-hydroxyethyl)-1-piperazineethanesulfonic acid (HEPES)(Sigma-Aldrich), 23.8 mM sodium bicarbonate (Gibco), 1 mM sodium pyruvate (Gibco) and 50 μ M 2-mercaptoethanol (Sigma-Aldrich). When the cells reached near confluency, they were washed with Dulbecco's PBS (ThermoFisher Scientific) and incubated with 0.05% trypsin (ThermoFisher Scientific) for 5 minutes at 37°C and 5% CO₂. RPMI-1640 medium was added to neutralize the trypsin, and the cell suspension was centrifuged at 300 x g for 3 minutes to pellet the cells, for further passaging and seeding. Cell passages were kept to under passage 10 for glucose-stimulated insulin secretion studies (Section 2.6), or under passage 20 for all other experiments.

2.3 Adenoviral Transduction as an Overexpression Model for Human OATP2B1

We chose adenoviral transduction as the method for the overexpression of OATP2B1 in INS-1 cells, while other forms of transient transfection such as Lipofectamine 3000 (ThermoFisher Scientific) Xtreme-Gene (Sigma-Aldrich) were tried but were unsuccessful. For adenoviral transduction, ViraPower Adenoviral Expression System (Invitrogen, ThermoFisher Scientific) was previously used to create an adenoviral vector including human OATP2B1 (referred to as Ad-OATP2B1) and LacZ (referred to as Ad-LacZ), the latter used as negative control (Knauer et al., 2010). INS-1 cells were transduced with the adenoviral vectors by diluting appropriate volumes of previously titered adenoviral stock diluted in phenol red-free RPMI-1640 medium (Gibco) to yield the multiplicity of infection (MOI) of 250. The adenoviral mix was aspirated and replaced with RPMI-1640 growth medium 24 hours post-transduction and the cells were incubated for an additional 24 hours for a total transduction time of 48 hours before the experiments were conducted.

2.4 Western Blot of OATP2B1 and OXPHOS Complex

Western blot was conducted to verify OATP2B1 overexpression in INS-1 cells following adenoviral transduction, and to investigate changes in the expression of mitochondrial oxidative phosphorylation complexes following atorvastatin treatment with or without mevalonate pathway substrates.

INS-1 cells were lysed with PierceTM IP Lysis Buffer (ThermoFisher Scientific) and bicinchoninic acid (BCA) assay was conducted using the Pierce BCA Protein Assay Kit (ThermoFisher Scientific) to quantify total protein level in the cell lysates. For the BCA assay, 25 μ L of cell lysate and 200 μ L of the working BCA reagent were added to 96-well microplate in duplicates and were incubated at 37 °C for 30 minutes. The absorbance was read at 562 nm using a MultiSkan Spectrum spectrophotometer and the protein concentrations were determined using a BCA standard curve.

For western blot analysis, 20 μ g of protein was loaded onto a NuPage 10% Bis-Tris Gel (ThermoFisher Scientific) for gel electrophoresis. An XCell SureLock Mini-Cell apparatus was used to run the gel at 120V for 1.5 hours to separate the proteins. The proteins were transferred onto a polyvinylidene fluoride (PVDF) membrane (0.45 μ M pore size) by running the gel at 25 V for 2 hours. Then, the membrane was incubated with 5% skim milk for 1 hour for blocking. The membrane was incubated overnight at 4° C with either the anti-OATP2B1 primary antibody (1:200, H-189, rabbit polyclonal, Santa Cruz Biotechnology) or anti-OXPHOS antibody cocktail (1:500, ab110413, goat polyclonal, Abcam, Toronto, Ontario, Canada) diluted in Tris-buffered saline with 0.1% Tween 20 (TBST). Anti-glyceraldehyde 3-phosphate dehydrogenase (GAPDH)(1:5000, ab8245, mouse monoclonal, Abcam) was used as a loading control. Following overnight incubation with the primary antibody, the membrane was washed with TBST for 10 minutes and incubated with anti-rabbit or anti-mouse horseradish peroxidase (HRP)-conjugated secondary antibody (1:5000, Cell Signaling Technology, Danvers, Massachusetts, USA) for 1 hour at RT. Finally, PierceTM ECL Western Blotting Substrate (ThermoFisher Scientific) was applied to the membrane for one minute and the protein bands were visualized using ImageQuant LAS 500 Imager (GE Healthcare Life Sciences,

Chicago, Illinois, USA). For the quantification of OXPHOS western blot, ImageJ Fiji was used to measure and compare relative band intensities following normalization to GAPDH loading control (Schindelin et al., 2012).

2.5 Statin Transporter Gene Expression Analysis

We used reverse transcription-quantitative polymerase chain reaction (RT-qPCR) to compare statin uptake and efflux transporter expression in INS-1 cells with that of rat liver, the latter used as positive control due to its known abundant expression of such transporters. Rat liver samples (N=2), which were generously provided by Dr. Dan Hardy, along with commercial rat liver total RNA sample (N=1, QS0637, ThermoFisher Scientific) were used as controls. Rat pancreas cDNA (N=3) was also kindly provided by Dr. Dan Hardy for RT-qPCR. As the transporter expression in the rat pancreas was not detectable, data were normalized to rat liver instead. Liver samples were crushed and homogenized, and INS-1 cells were centrifuged and suspended before diluting them in 1 mL of TRIzol® Reagent (Life Technologies, ThermoFisher Scientific). Then, 200 µL of chloroform was added, shaken for 15 seconds, followed by 3-minute incubation at room temperature. The samples were centrifuged at 12 000 x g for 15 minutes and the top aqueous phases were transferred to separate microcentrifuge tubes. Then, 500 µL of isopropanol was added and incubated for 10 minutes at room temperature, followed by 10-minute centrifugation at 12 000 x g. The supernatant was aspirated, and 75% ethanol was added and mixed, followed by 5-minute centrifugation at 7500 x g. The resulting RNA pellet was air-dried and re-suspended in 50 µL of RNase-free water.

Then, RNA concentration was determined by taking the absorbance readings at 260 nm and 280 nm using a DS-11 spectrophotometer (DeNovix, Wilmington, Delaware, USA). For reverse transcription, 4 µL of iScript™ Reverse Transcription Supermix (Bio-Rad, Hercules, California, USA), along with 1 µg total RNA and water was used for a total volume of 20 µL. Then, the samples were incubated in a GeneAmp® PCR System 9700

Thermocycler (Applied Biosystems, ThermoFisher Scientific) for 5 minutes at 25 °C, 20 minutes at 46 °C and 1 minute at 95 °C.

For qPCR, the samples were assessed in triplicates by mixing 12.5 µL of SensiFast SYBR Green Mastermix (FroggaBio, Concord, Ontario, Canada), 1 µL of 100 µM forward primer, 1 µL of 100 µM reverse primer, 9.5 µL of nuclease-free water (Gibco) and 2 µL cDNA containing 100 ng cDNA per well. All primers were obtained from Eurofins Genomics, Toronto, Ontario, Canada, and primer sequences are provided in **Table 2.1**. The qPCR was conducted using 7500 Fast Real-Time PCR System (ThermoFisher Scientific) using 60 °C annealing temperature for 30 seconds and 95 °C denaturation temperature for 3 seconds per cycle, for 40 cycles total. The resulting cycle threshold (C_t) values were obtained and were analyzed using the delta-delta C_t method (Livak & Schmittgen, 2001) to quantitatively compare the mRNA expression of these transporters in INS-1 cells relative to rat liver.

Table 2.2. Forward and reverse sequences of RT-qPCR primers for statin uptake and efflux transporters in INS-1 cells. Primers were designed using the Eurofin Genomics PCR Primer Design Tool, and all primers were obtained from Eurofin Genomics, Toronto, Ontario, Canada.

Gene (rat)	Forward (5` to 3`)	Reverse (5` to 3`)	Reference
Oatp1a1	AGGTCGAGAATGACGGAGAA	ATTCCGGAGGAAGGGAAGT GT	(de Graaf et al., 2011)
Oatp1a4	ATCTCGCTACCCCATTTCT	TGGGATCTGTTTTCCACACA	(de Graaf et al., 2011)
Oatp1a5	TCTGCAGTCCTGGGGTTATG	TGCCAGCGAATACTCTTGTG	(Naud et al., 2007)
Oatp1b2	GACATCACCCACTGGACCTT	AGCATGTTCCCATCAAGA C	(de Graaf et al., 2011)
Oatp2b1	ACGACTTTGCCACCATAGC	CCACGTAAAGGCGTAGCAT GA	(St-Pierre et al., 2004)
Mdr1a	CACCATCCAGAACGCAGACT	ACATCTCGCATGGTCACAGT T	(Ma et al., 2019)
Bcrp	GTA CTTTGCATCAGCAGGTTA CCACT	ATTACAGCCGAAGAATCTC CGTTG	(Xu et al., 2014)

RT-qPCR, reverse transcription-quantitative polymerase chain reaction

2.6 Statin Uptake and Quantification in INS-1 cells using LC-MS/MS

We investigated the effect of OATP2B1 and statin efflux transporters on statin uptake by quantifying cellular uptake of statins in INS-1 cells using liquid chromatography-tandem mass spectrometry (LC-MS/MS).

INS-1 cells were seeded on a 24-well plate at 150 000 cells/well and incubated overnight at 37°C with 5% CO₂. The cells were transduced with Ad-OATP2B1 and Ad-LacZ at 250

MOI for 48 hours. Then, the growth medium was aspirated and replaced with Opti-MEM and incubated for 30 minutes. Stock solutions (1, 10 or 100 mM in DMSO) were prepared by dissolving rosuvastatin- Ca^{2+} , atorvastatin- Na^+ or pravastatin- Na^+ (Toronto Research Chemicals, North York, Ontario, Canada) in appropriate volumes of sterile DMSO and stored at $-20\text{ }^{\circ}\text{C}$. These stock solutions were used to prepare fresh working statin treatment solutions (final concentrations of 1, 10 or 100 μM) by first diluting the stock solution 1:100 in PBS then further diluting it 1:10 in Opti-MEM (0.1% DMSO). Opti-MEM was aspirated from each well, and then the cells were incubated with appropriate statin solutions for 30 minutes or 24 hours to allow for cellular statin uptake. Ice-cold PBS was used to wash (3x) to stop the uptake and the cells were lysed with 200 μL of acetonitrile solution (ThermoFisher Scientific) containing 0.01 $\mu\text{g}/\text{mL}$ D6-rosuvastatin, 0.01 $\mu\text{g}/\text{mL}$ D5-atorvastatin or 0.01 $\mu\text{g}/\text{mL}$ D3-pravastatin as internal standards. The cell lysates were collected and concentrated using a SpeedVac® Vacuum Concentrator (ThermoFisher Scientific) at 45°C for 1 hour.

For the quantification of statin uptake, LC-MS/MS was conducted to measure cellular statin concentrations, as reported previously with modifications (Medwid et al., 2021). Specifically, the concentrated cell lysates were re-suspended in 120 μL of mobile phase consisting of 75% water with 0.1% formic acid and 25% acetonitrile with 0.1% formic acid. The samples were vortexed and centrifuged at 13 000 x g for 10 minutes at room temperature to pellet the cell lysate. For high-performance liquid chromatography, 50 μL of the supernatant was injected into a C18 Liquid Chromatography Column (Hypersil GOLD™, 50 x 3 mm, 5 μm particle size; ThermoFisher Scientific). The mobile phases consisted of 75% water with 0.1% formic acid and 25% acetonitrile with 0.1% formic acid. The statin concentrations were measured using a TSQ Vantage triple-quadrupole mass spectrometer (ThermoFisher Scientific) with D6-rosuvastatin, D5-atorvastatin and D3-pravastatin as internal standards. A HESI II probe (ThermoFisher Scientific) was used for detection, in negative mode for pravastatin and positive mode for rosuvastatin and atorvastatin. Spray voltage was set at 4000V, vaporizer temperature at 350°C , sheath gas pressure at 40 bar, auxiliary gas pressure at 10 bar, and capillary temperature at 350°C .

For the detection of rosuvastatin and atorvastatin, a starting gradient of 75% water with 0.1% formic acid and 25% acetonitrile with 0.1% formic acid was used. This gradient was linearly changed to 40% water with 0.1% formic acid and 60% acetonitrile with 0.1% formic acid from 1 to 6 minutes. The gradient was then linearly reversed back to 75% water with 0.1% formic acid and 25% acetonitrile with 0.1% formic acid until 7 minutes. This final gradient was maintained for a total run time of 9 minutes per sample. The m/z transitions used were 482.1 → 258.2 for rosuvastatin, 488.0 → 264.3 for D6-rosuvastatin, 559.2 → 440.4 for atorvastatin and 564.1 → 255.2 for D5-atorvastatin. A constant flow rate of 0.5 mL/min was maintained.

For the detection of pravastatin, a starting gradient of 90% water with 0.1% formic acid and 10% acetonitrile with 0.1% formic acid was used. From 1 to 4 minutes, the gradient was linearly changed to 10% water with 0.1% formic acid and 90% acetonitrile with 0.1% formic acid, which remained until 4.5 minutes. The gradient was then linearly reversed to 90% water with 0.1% formic acid and 10% acetonitrile with 0.1% formic acid to until 5.25 minutes. This gradient remained for a total run time of 7 minutes per sample. The m/z transitions used were 423.1 → 321.3 for pravastatin and 426.2 → 321.4 for D3-pravastatin. A constant flow rate of 0.5 mL/min was maintained.

Standard curves ranging from 0 to 100 ng/mL, with the lower limit of detection being 2.5 ng/mL, were also prepared for each of rosuvastatin, atorvastatin and pravastatin for absolute statin quantification. A sample standard curve for each statin was generated using GraphPad Prism v.9. using simple linear regression function and is shown below.

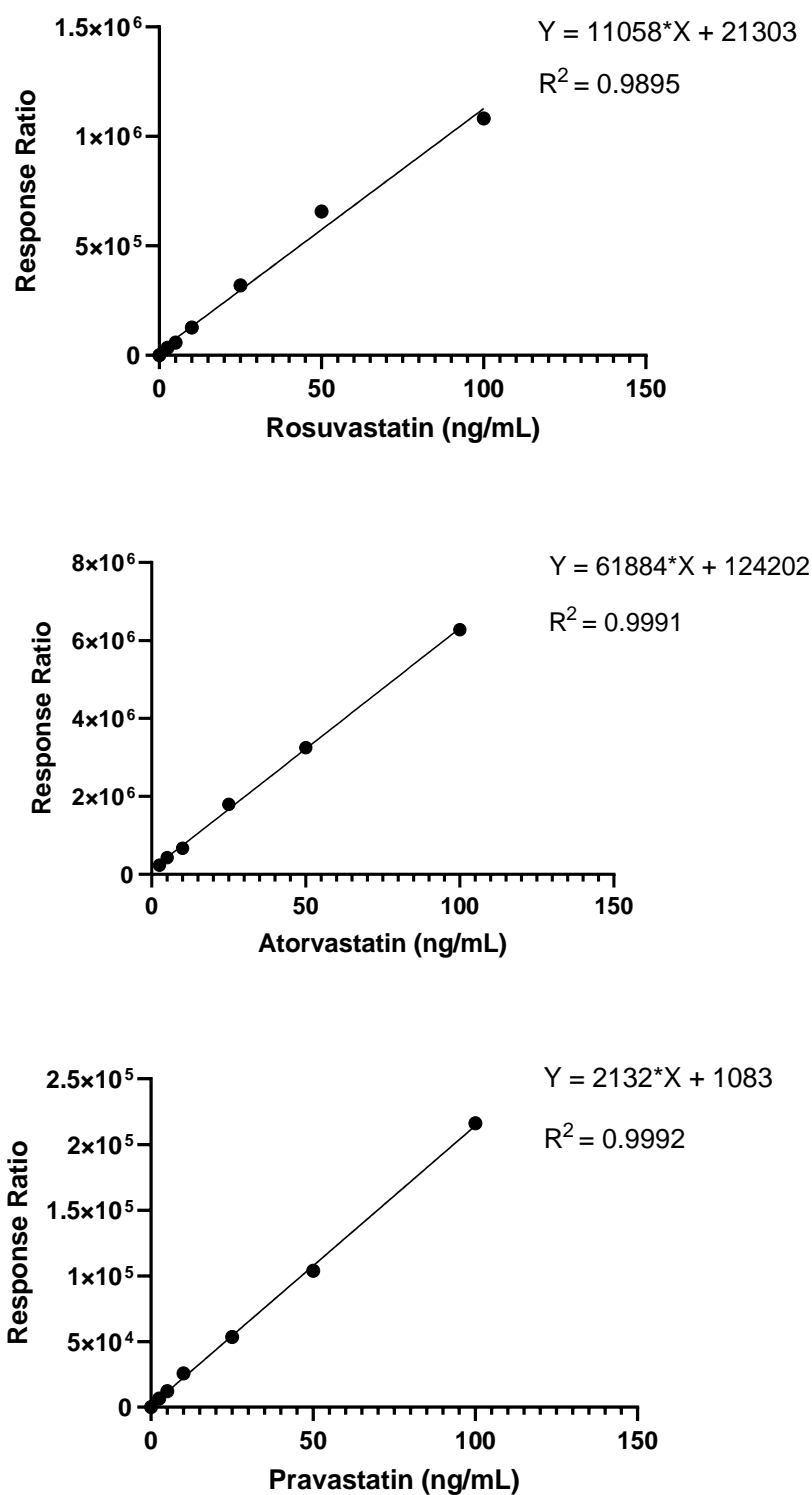


Figure 2.1. Sample standard curves for rosuvastatin, atorvastatin and pravastatin (0-100 ng/mL).

2.7 Glucose-Stimulated Insulin Secretion following 24-hour Statin Treatment

To investigate the effect of statins and mevalonate pathway intermediates on insulin secretion, glucose-stimulated insulin secretion (GSIS) was performed according to the INS-1 832/13 cell product sheet (Millipore-Sigma) with modifications, and insulin was quantified using a rat insulin enzyme-linked immunosorbent assay (ELISA).

Working statin solutions were prepared in phenol red-free RPMI-1640 medium (Gibco) at appropriate final statin concentrations ranging from 0.1 to 10 μ M and 10 μ M substrate concentrations. The experiment was performed in triplicates. In addition, low-glucose (2.2 mM glucose) buffer and high-glucose (22 mM glucose) buffer were prepared fresh on the day of the GSIS experiment, and contained 114 mM NaCl, 4.7 mM KCl, 1.2 mmol/L KH_2PO_4 , 1.16 mM MgSO_4 , 20 mM HEPES, 2.5 mM CaCl_2 and 25.5 mM NaHCO_3 (adjusted pH 7.2).

INS-1 cells were seeded on a 48-well plate at 100 000 cells/well and transduced for 48 hours with Ad-LacZ or Ad-OATP2B1 as described previously (section 2.2). Then, the cells were treated with 300 μ L of the statin alone or in combination with 10 μ M FPP or 10 μ M GGPP for 24 hours, as appropriate. Then, the supernatant was removed and cells were washed twice with 300 μ L of glucose-free Krebs-Ringer HEPES buffer (KRHB). The cells were then incubated with low-glucose KRHB for 2 hours and the supernatant was collected. Next, the cells were incubated with high-glucose KRHB for 2 hours and the supernatant was collected. The supernatant was frozen at -80°C prior to performing rat insulin ELISA.

Insulin content in the supernatants following glucose stimulation was quantified using an Ultra-Sensitive Rat Insulin ELISA Kit (CrystalChem, Elk Grove Village, Illinois, USA) according to the manufacturer's protocol. Rat insulin standards were prepared at final concentrations ranging from 0.1 to 32 ng/mL through a serial dilution of the provided rat insulin stock. In brief, the microplate coated with anti-rat insulin antibody was equilibrated to room temperature. Then, 5 μ L of each standard or supernatant and 95 μ L

of sample diluent was added to each well in duplicates and incubated for 2 hours at 4°C. The wells were washed 5 x in the provided wash buffer and 100 µL of anti-insulin enzyme conjugate was added to each well and incubated for 30 minutes at room temperature. The wells were washed 7 x in wash buffer and 100 µL of enzyme substrate solution was added to each well and allowed to react for 40 minutes at room temperature. Finally, 100 µL of enzyme stop solution was added to arrest the enzyme reaction and absorbance readings at 450 and 630 nm were taken using a MultiSkan Spectrum microplate spectrophotometer (ThermoFisher Scientific).

Insulin standard curve was generated through linear regression of the A_{450} - A_{630} values from the rat insulin standards. Sample insulin concentrations were interpolated from the standard curve. Stimulation Index (SI) was calculated as the ratio of insulin concentration following high-glucose buffer stimulation divided by the insulin concentration following low-glucose buffer stimulation, and this value served as a measure of insulin secretion.

2.8 MTT Assay

In order to assess the effect of statins on NADH-dependent mitochondrial oxidoreductase activity, we performed a dose-response experiment using the 3-(4,5-dimethylthiazol-2-yl)-2,5-diphenyltetrazolium bromide (MTT) assay according to the manufacturer's instructions (Sigma-Aldrich).

INS-1 cells were seeded at 50 000 cells/well on a 96-well plate and transduced with Ad-LacZ or Ad-OATP2B1 at 250 MOI for 48 hours. The cells were then treated with various concentrations of rosuvastatin, atorvastatin and pravastatin ranging from 0.1 to 100 µM for 24 hours. Following statin treatment, growth medium was replaced with 100 µL of Opti-MEM® Reduced Serum Medium (ThermoFisher Scientific). Subsequently, 10 µL of 12 mM stock MTT solution (Sigma-Aldrich) was added to each well and incubated at 37°C for 2 hours. Then, 85 µL of the solution was aspirated, and 50 µL of DMSO was

added to the MTT-containing media solution in each well to solubilize the formazan product. The plate was then incubated at 37°C for 10 minutes and absorbance was taken at 540 nm using a MultiSkan Spectrum microplate spectrophotometer (ThermoFisher Scientific).

Absorbance readings were normalized as percentage of DMSO control for both the Ad-LacZ- and Ad-OATP2B1-transduced INS-1 cells. A curve of best fit was generated using GraphPad Prism v.9 using log(inhibitor) vs. response function, variable slope with four parameters. Estimated IC₅₀ (eIC₅₀) values, the concentration of statin that results in half-maximal inhibition of formazan formation, were determined through interpolation from the curve of best fit.

2.9 ATP Assay

In order to investigate the effect of statins on the level of ATP, a critical signaling molecule in insulin secretion, in INS-1 cells, a luminescent assay was performed according to the manufacturer's instructions. The cells were seeded at 50 000 cells/well on opaque-walled 96-well plate. The cells were transduced with Ad-LacZ or Ad-OATP2B1 at 250 MOI for 48 hours. The cells were then treated with each statin at specified concentrations, with or without substrates, for 24 hours. Then, the plates were equilibrated to room temperature and CellTiter-Glo Luminescent Cell Viability Assay Kit (Promega, Madison, Wisconsin, USA) was used to assess cellular ATP level. Briefly, CellTiter-Glo buffer and CellTiter-Glo substrate were equilibrated to room temperature and thoroughly mixed to yield the working reagent. Then, 100 µL of this working reagent was added to each cell and mixed for 2 minutes on an orbital shaker to lyse the cells. The plates were incubated at room temperature for 10 minutes, and each well content was transferred to a microcentrifuge tube, and luminescence readings were taken using a GloMax 20/20 Luminometer (Promega) with 1 second integration time.

2.10 Caspase 3/7 and Caspase 9 Assay

INS-1 832/13 cells were seeded at 50 000 cells/well on opaque-walled 96-well plate. The cells were transduced with Ad-OATP2B1 or Ad-LacZ control (**Section 2.2**) for 48 hours. The cells were then treated with each statin at specified concentrations, with or without substrates, for 24 hours. Then, the plates were equilibrated to room temperature and Caspase-Glo 3/7 Assay Kit (Promega) or a separate Caspase-Glo 9 Assay Kit (Promega) were used to assess caspase-3/7 or caspase 9 activity, respectively. Caspase-Glo 3/7/9 buffer and Caspase-Glo 3/7/9 substrate were equilibrated to room temperature and thoroughly mixed to yield the working reagent. Then, 100 μ L of this working reagent was added to each cell and incubated at room temperature for 1 hour. Each well content was transferred to a microcentrifuge tube, and luminescence readings were taken using a GloMax 20/20 Luminometer with 1 second integration time.

2.11 Graphing and Statistical Analyses

All data were analyzed using Microsoft Excel and graphed using GraphPad Prism v.9 (GraphPad Software Inc., La Jolla, CA, USA). Two-tailed unpaired t test, one-way analysis of variance (ANOVA) or two-way ANOVA followed by Dunnett's multiple comparisons test, Tukey's post-hoc, or Sidak's multiple comparisons test were performed as appropriate using GraphPad Prism v.9. P values less than 0.05 were considered statistically significant.

Chapter 3

3 Results

3.1 Characterization of the Endogenous Expression of Statin Transporters in the Human Pancreas

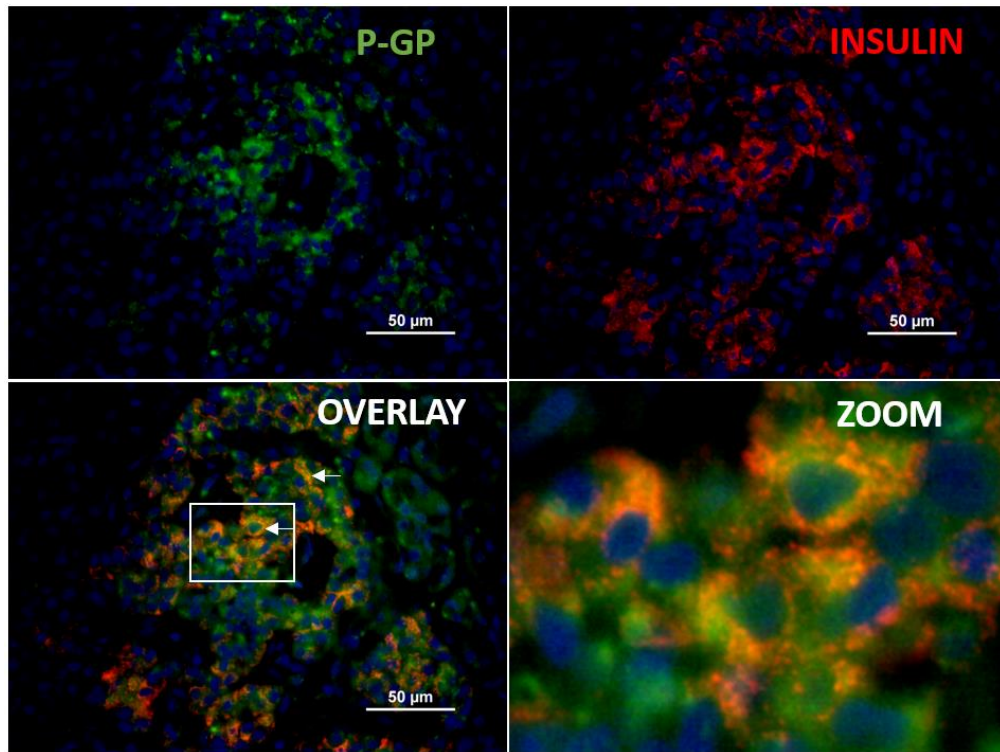
After we previously reported the expression of OATP2B1 in human islets with predominant localization to the beta cells (Kim et al., 2017), we sought to further characterize the localization of statin efflux transporters in beta cells. RNA expression of P-gp and BCRP in human islets had been previously observed (Kim, 2017).

Using immunofluorescent staining of normal pancreatic sections from three adult individuals, we observed abundant expression of P-gp and BCRP within human islets. Specifically, P-gp co-localized with both alpha and beta cells, as indicated by co-staining for glucagon (alpha cells) or insulin (beta cells) (**Figures 3.1, 3.3**). A similar result was observed for BCRP, where marked co-localization of BCRP occurred with alpha and beta cells (**Figures 3.2, 3.4**). Representative immunofluorescence images are shown below, illustrating the observed staining pattern (**Figures 3.1-3.4**).

Quantitative analysis for co-localization using the Pearson's correlation coefficient showed that P-gp and BCRP were highly co-localized to both alpha and beta cells (**Figure 3.5A**). Mean Pearson's correlation coefficients for P-gp with beta cells ($r=0.722$) and that with alpha cells ($r=0.756$) were not statistically different. For BCRP, the mean Pearson's correlation coefficient with beta cells ($r=0.643$) was higher than that with alpha cells ($r=0.545$, $p<0.01$), indicating a preferential distribution of BCRP to the beta cells (**Figure 3.5B**).

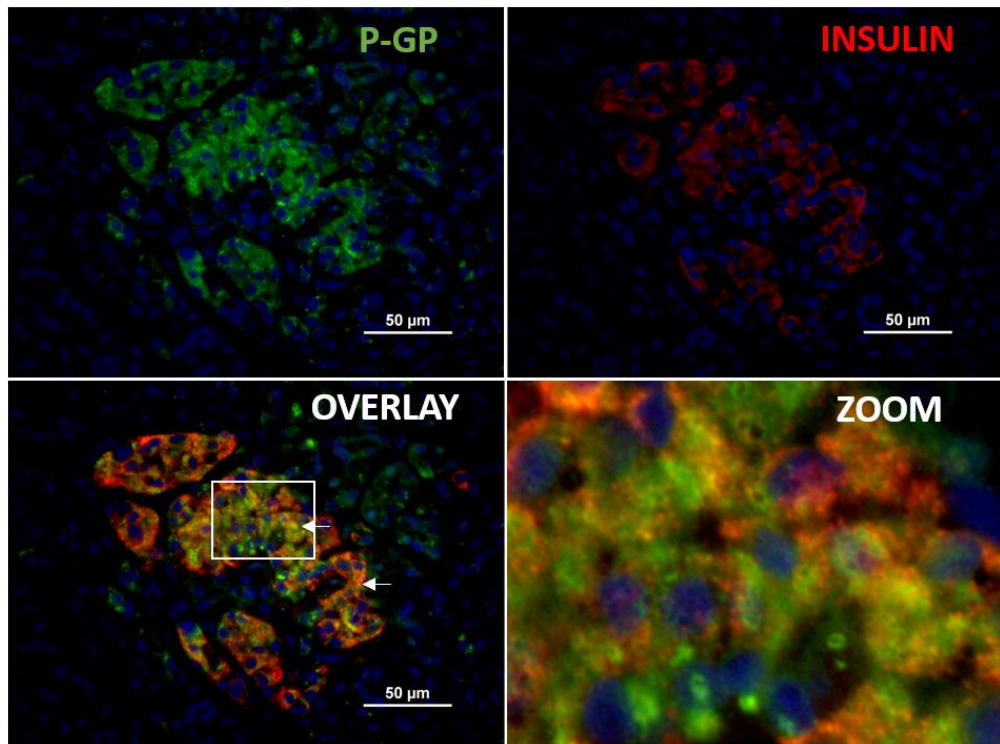
A

Female, 77 years old, Islet #1



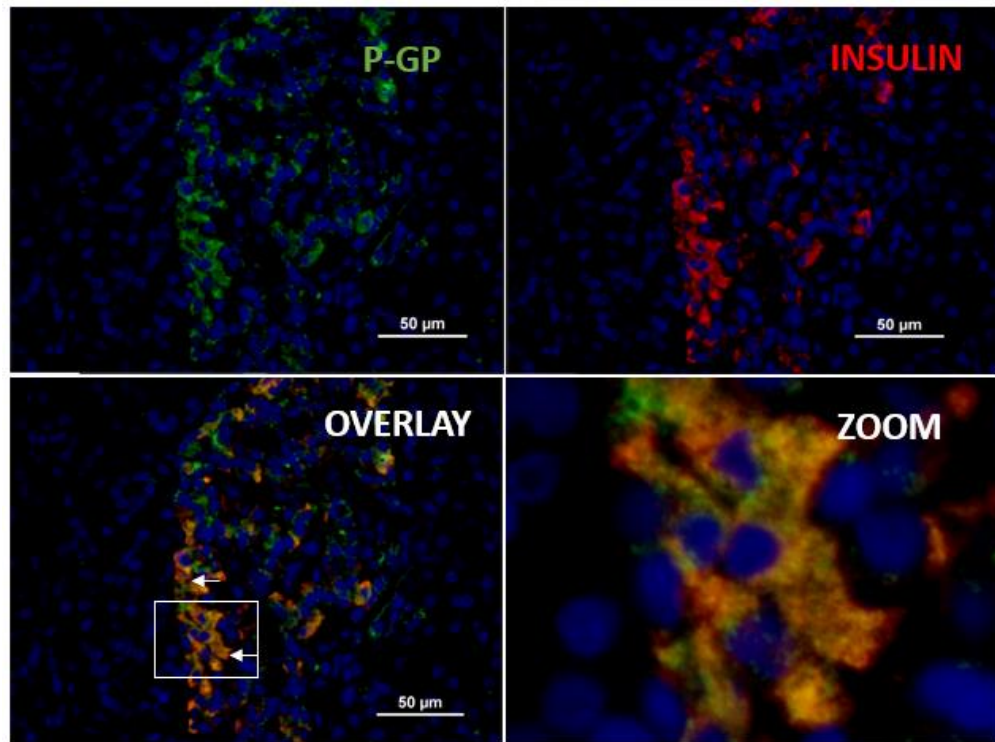
B

Female, 77 years old, Islet #2



C

Male, 71 years old, Islet #1



D

Male, 71 years old, Islet #2

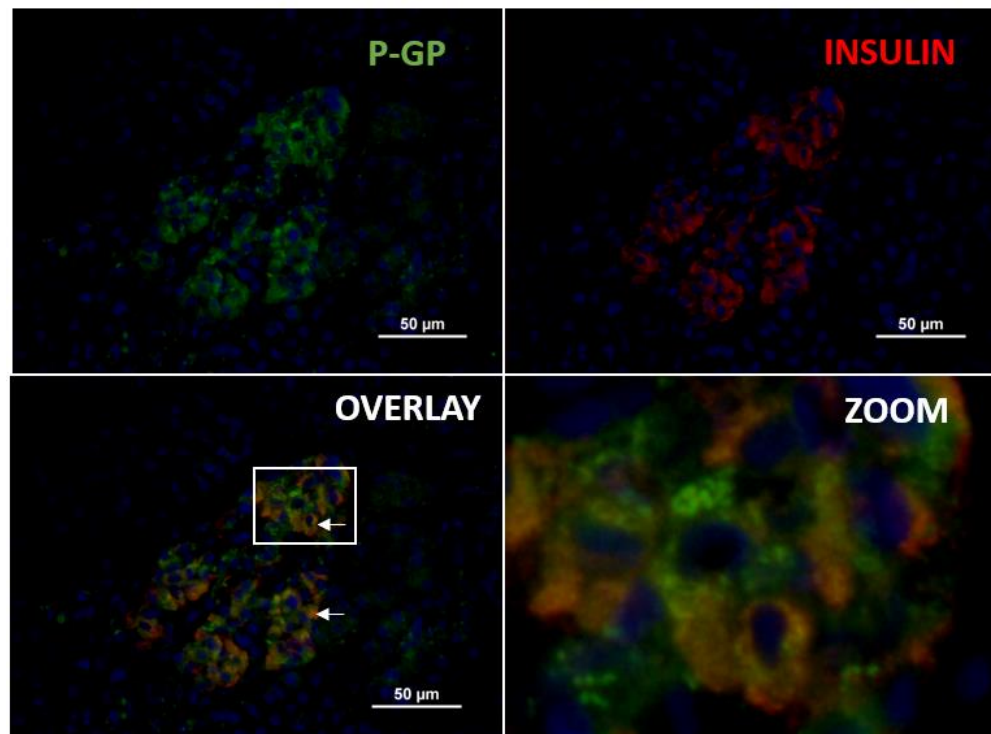
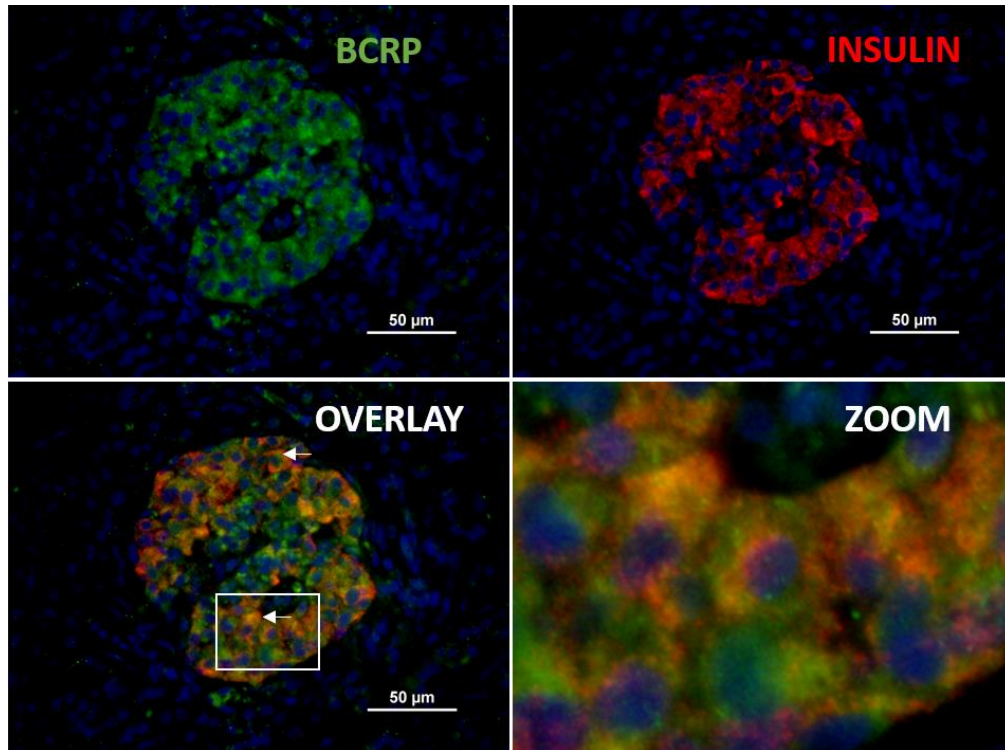


Figure 3.1. Representative images of P-glycoprotein (P-gp) co-localization with insulin-producing beta cells in normal adult human pancreas. Immunofluorescent staining was performed on paraffin-embedded pancreatic tissue sections of a 77-year old female (**A, B**) and 71-year old male (**C, D**) subjects with dual-staining for P-gp (green) and insulin (red). Individual, merged (overlay) and magnified (zoom) images shown (40x objective). White arrows indicate areas of co-localization.

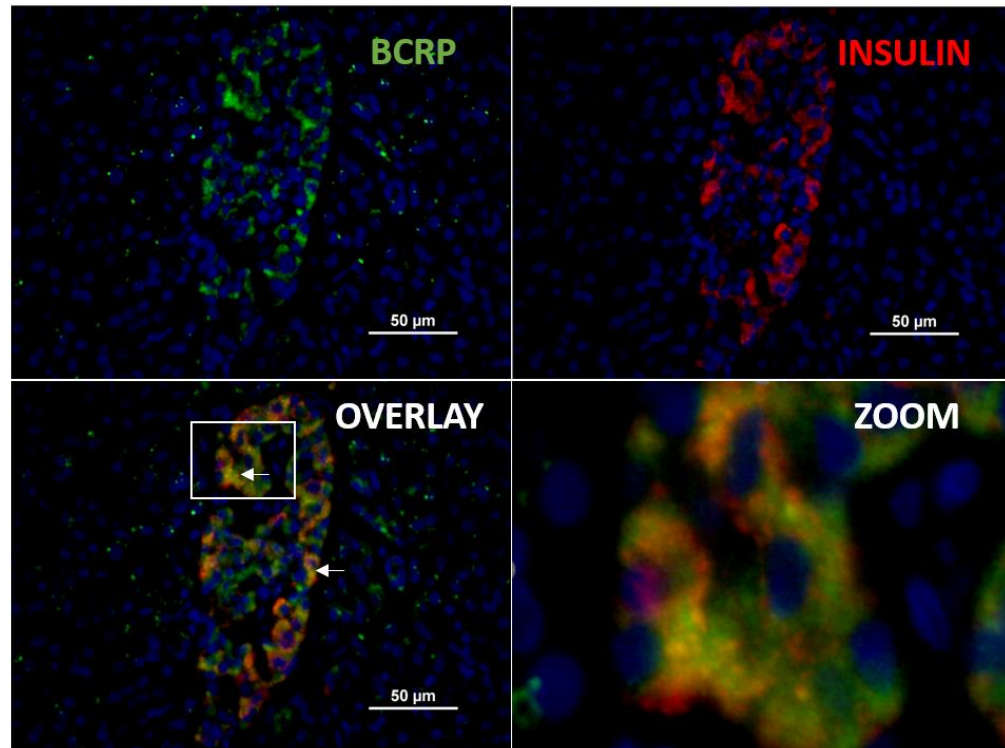
A

Female, 77 years old, Islet #1



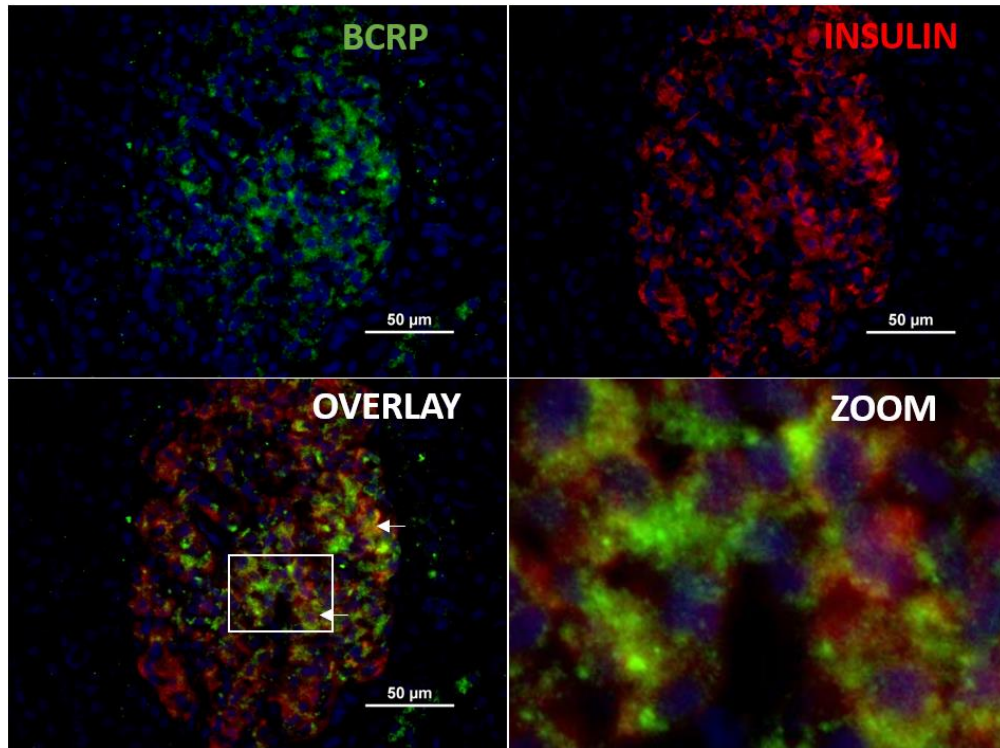
B

Female, 77 years old, Islet #2



C

Male, 77 years old, Islet #1



D

Male, 77 years old, Islet #2

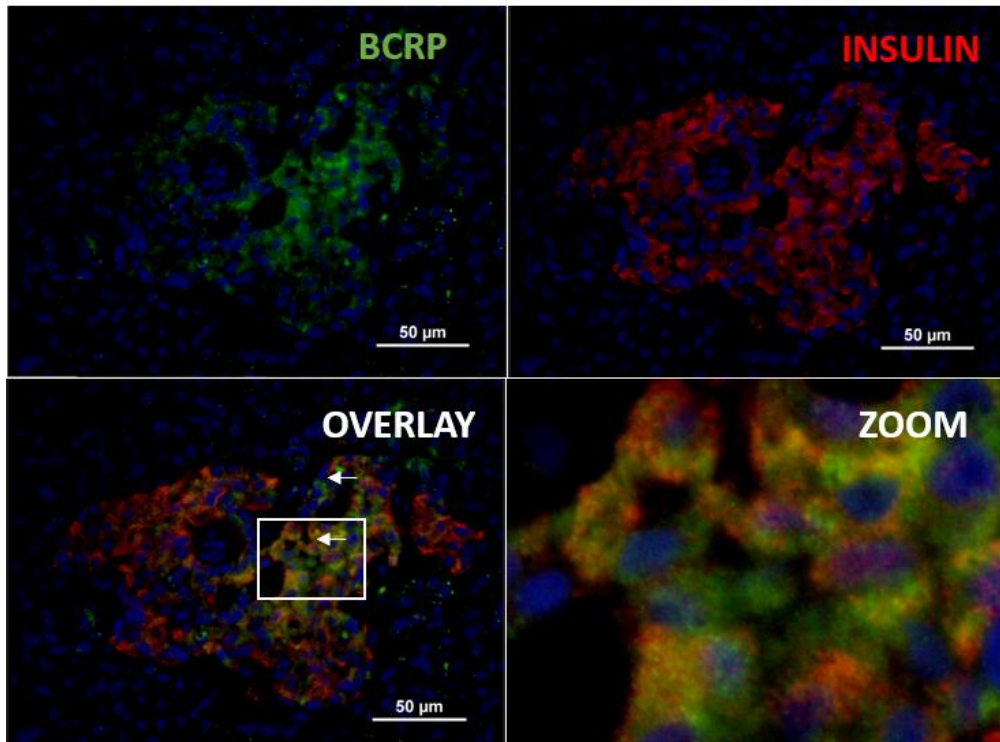
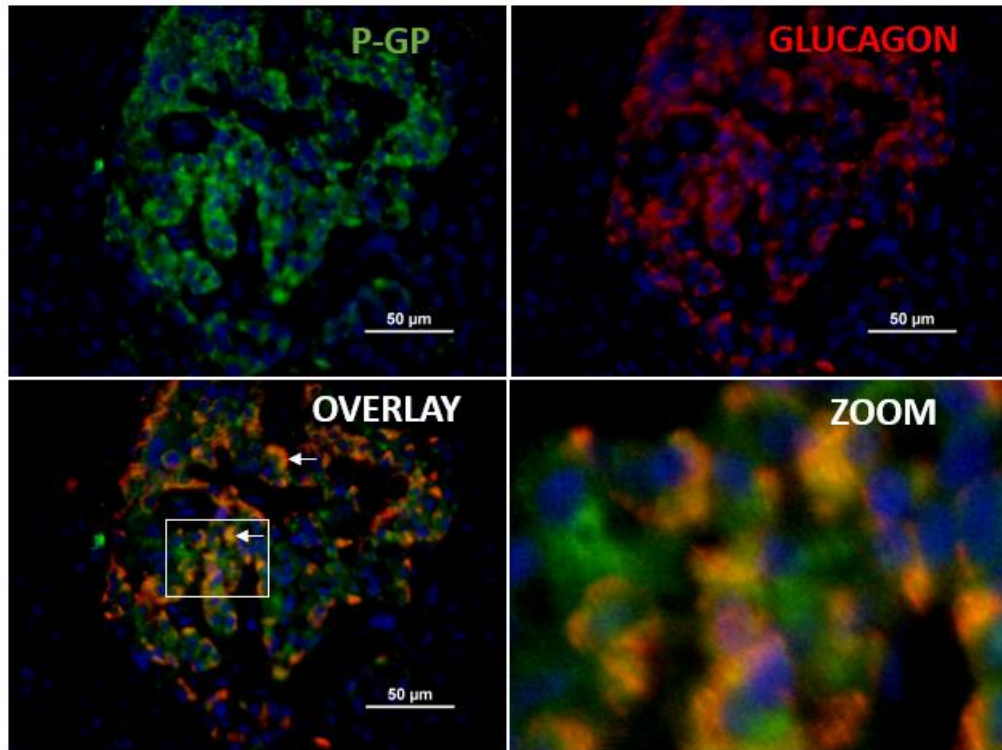


Figure 3.2. Representative images of breast cancer resistance protein (BCRP) co-localization with insulin-producing beta cells in normal adult human pancreas.

Immunofluorescent staining was performed on paraffin-embedded pancreatic tissue sections of a 77-year old female (**A, B**) and 77-year old male (**C, D**) subjects with dual-staining for BCRP (green) and insulin (red). Individual, merged (overlay) and magnified (zoom) images shown (40x objective). White arrows indicate areas of co-localization.

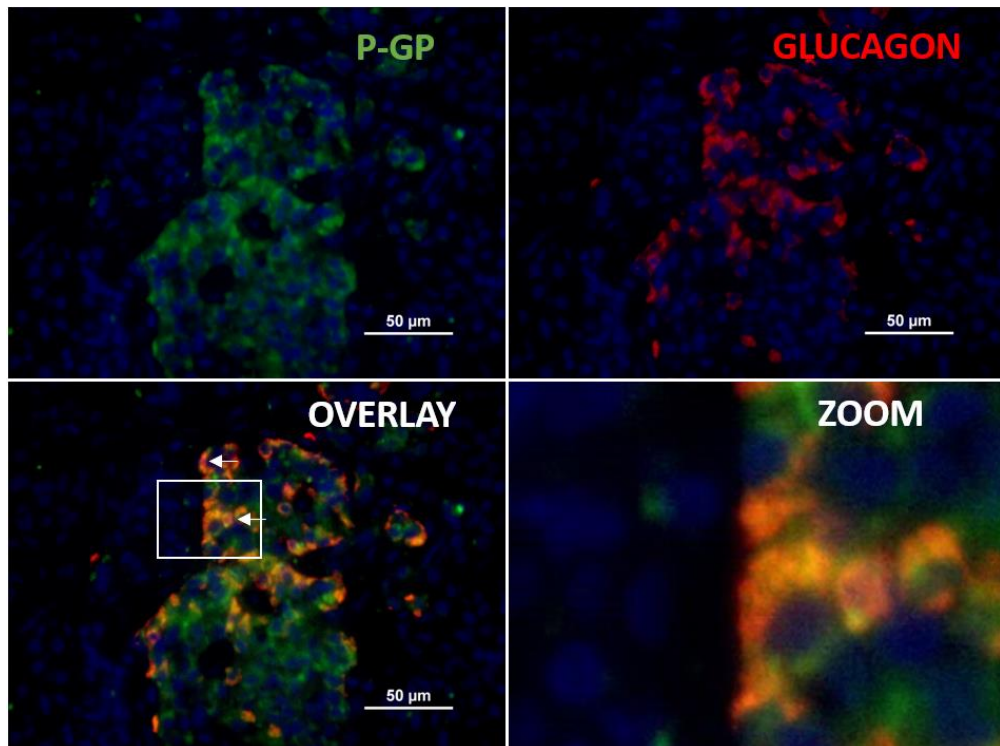
A

Female, 77 years old, Islet #1



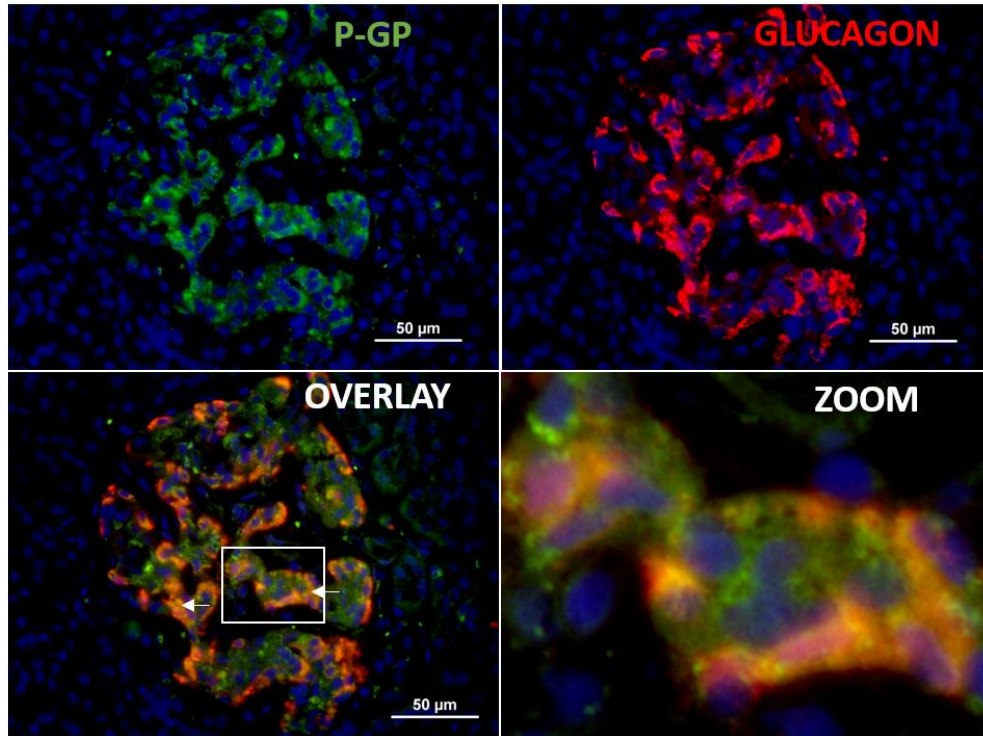
B

Female, 77 years old, Islet #2



C

Male, 71 years old, Islet #1



D

Male, 71 years old, Islet #2

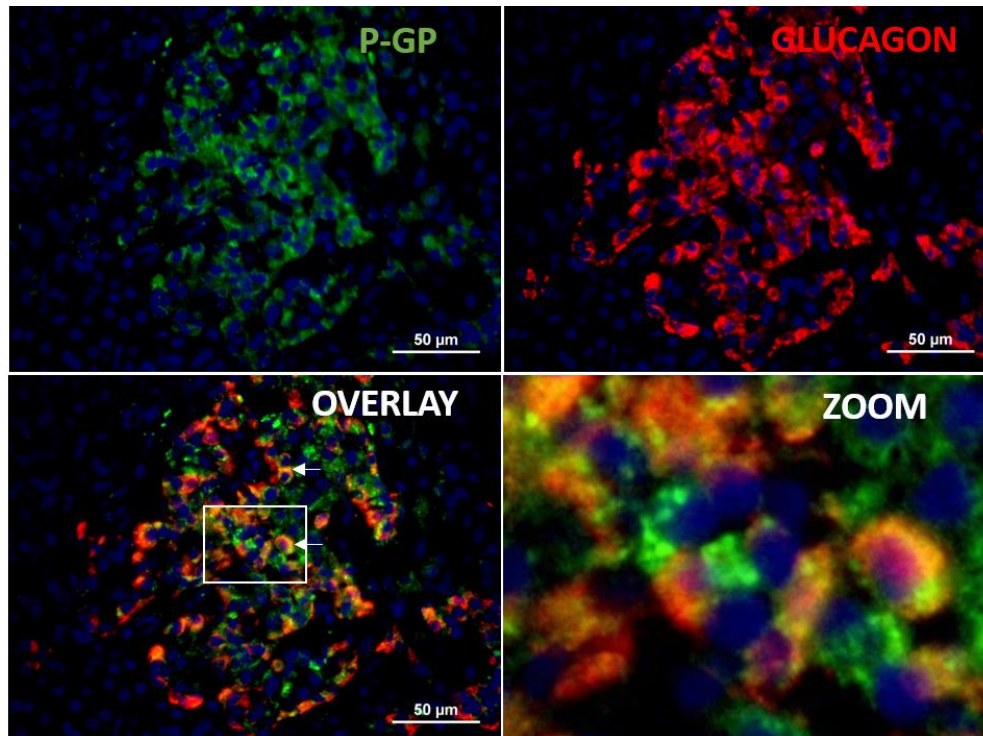
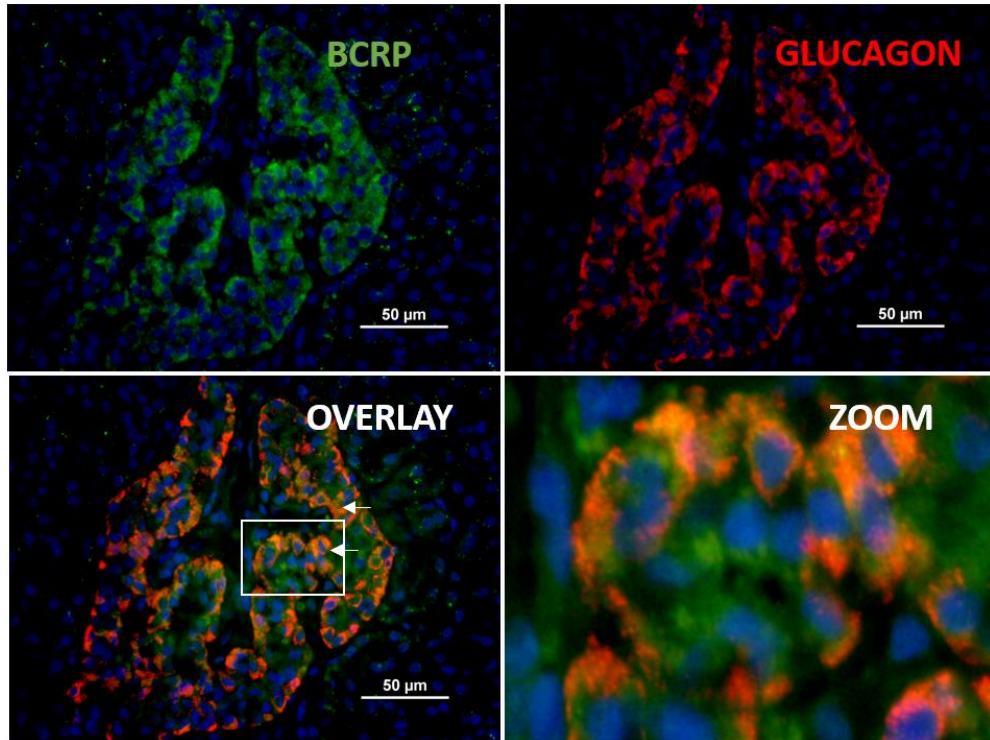


Figure 3.3. Representative images of P-glycoprotein (P-gp) co-localization with glucagon-producing alpha cells in normal adult human pancreas. Immunofluorescent staining was performed on paraffin-embedded pancreatic tissue sections of a 77-year old female (**A, B**) and 71-year old male (**C, D**) subjects with dual-staining for P-gp (green) and glucagon (red). Individual, merged (overlay) and magnified (zoom) images shown (40x objective). White arrows indicate areas of co-localization.

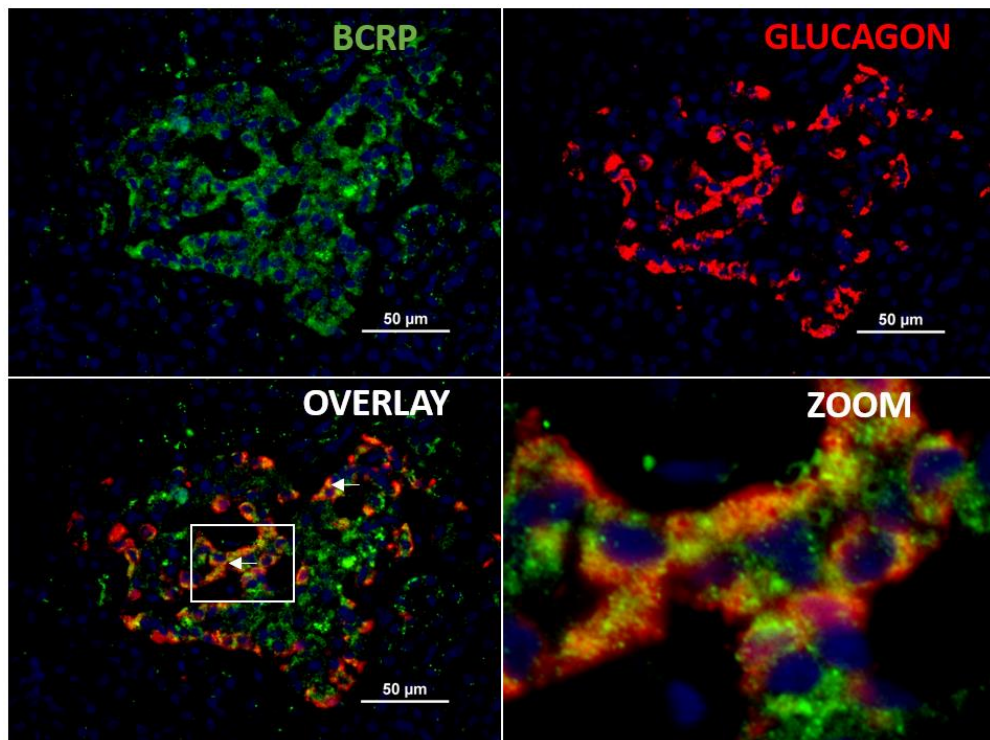
A

Female, 77 years old, Islet #1



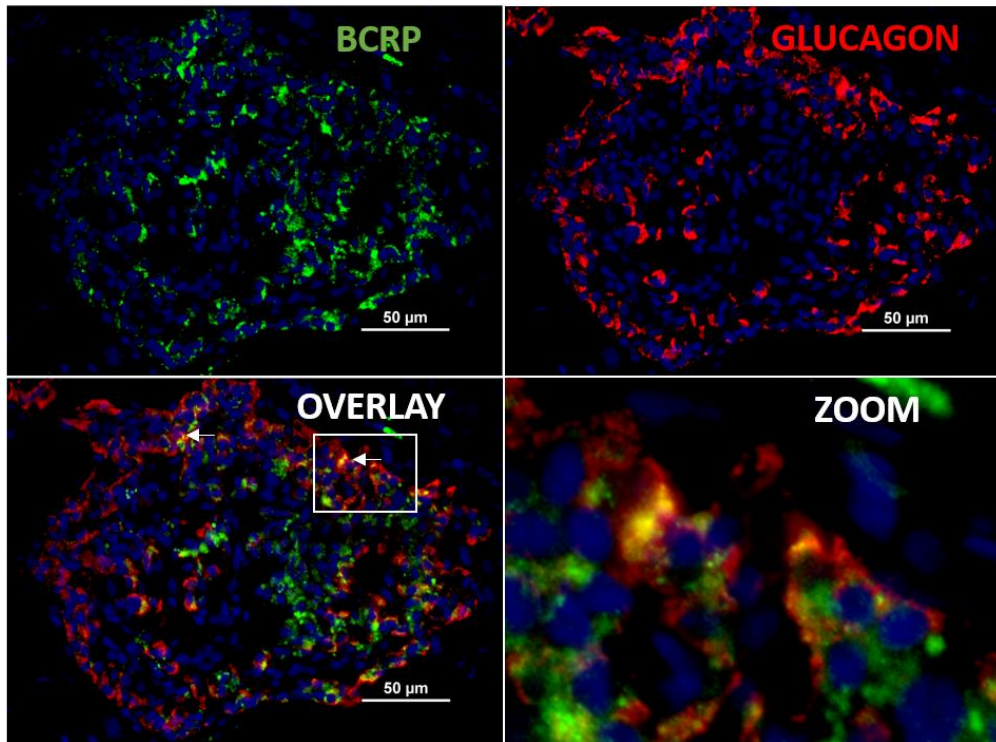
B

Female, 77 years old, Islet #2



C

Male, 77 years old, Islet #1



D

Male, 77 years old, Islet #2

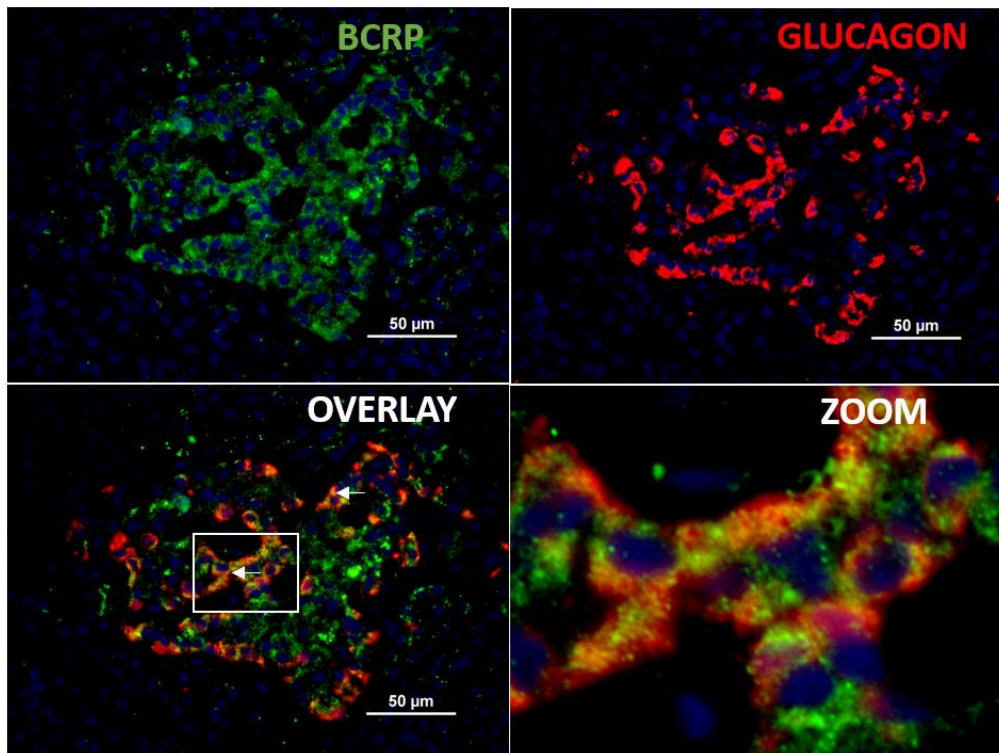


Figure 3.4. Representative images of breast cancer resistance protein (BCRP) co-localization with glucagon-producing alpha cells in normal adult human pancreas. Immunofluorescent staining was performed on paraffin-embedded pancreatic tissue sections of a 77-year old female (**A, B**) and 77-year old male (**C, D**) subjects with dual-staining for BCRP (green) and glucagon (red). Individual, merged (overlay) and magnified (zoom) images shown (40x objective). White arrows indicate areas of co-localization.

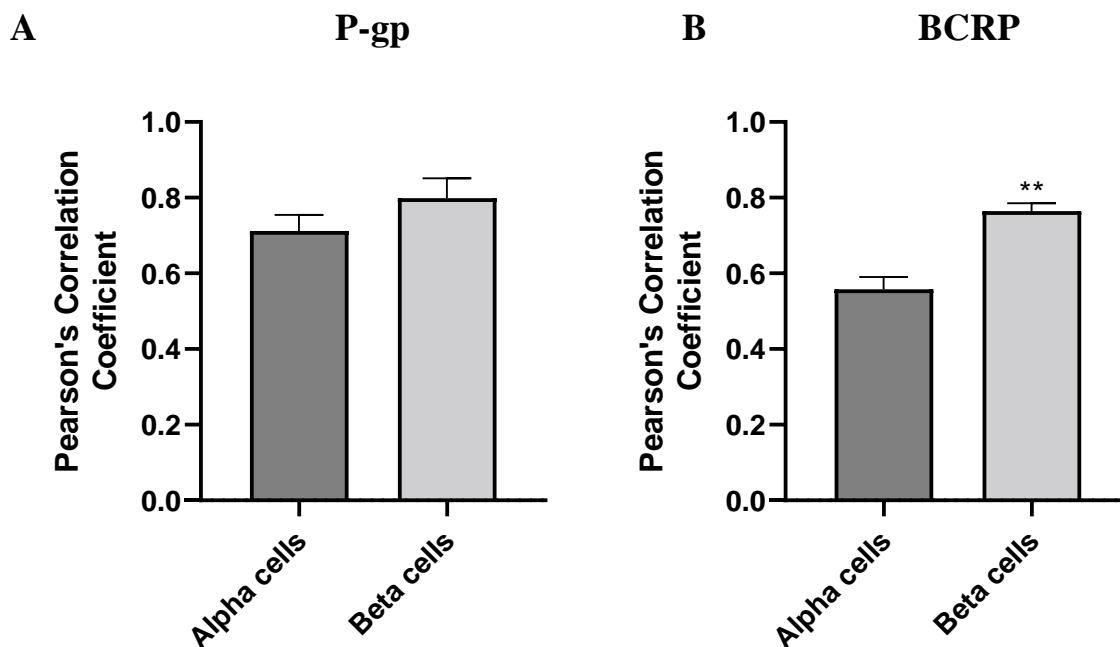


Figure 3.5. Quantitative co-localization analysis of P-glycoprotein (P-gp) and breast cancer resistance protein (BCRP). ImageJ Fiji software and JACoP plugin was used to obtain the Pearson's correlation coefficient (r) as an indicator of co-localization of P-gp with alpha cells or beta cells (**A**) and BCRP with alpha cells or beta cells (**B**). Dual-stained immunofluorescent images of normal adult human pancreatic sections were analyzed (refer to **Figures 3.1-3.4**). Pancreatic sections from each of the four groups (staining with insulin and P-gp, insulin and BCRP, glucagon and P-gp, or glucagon and BCRP) were assessed using two different individuals considering a total of 10 islets per group or 5 islets per individual. Data shown are mean Pearson's correlation coefficient \pm SEM with individual values for each islet shown, and were analyzed using a two-tailed t test. * $p < 0.05$.

3.2 Characterization of the Endogenous Expression of Statin Transporters in INS-1 Cells

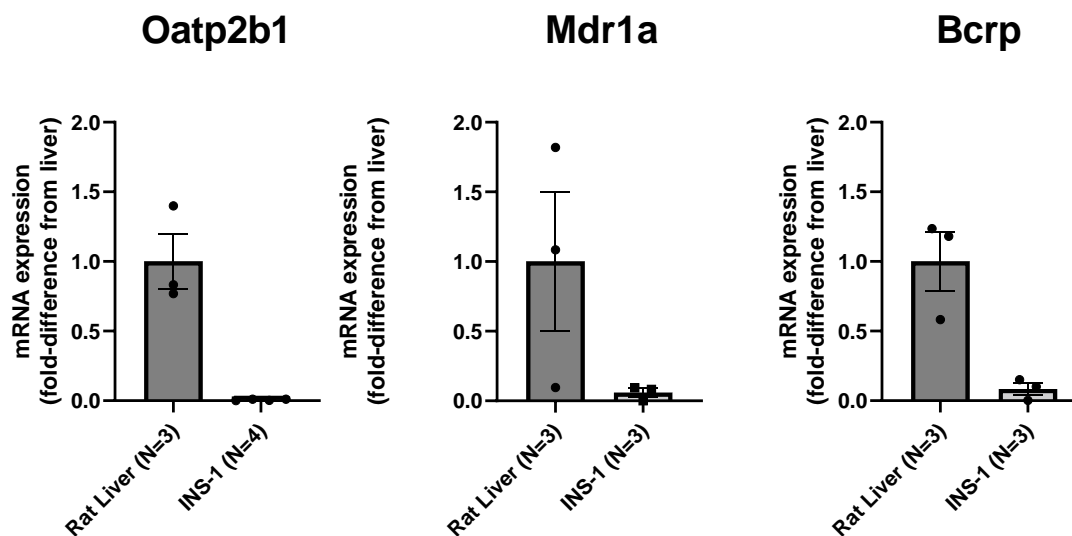
Using qPCR, we next confirmed the absence of endogenous mRNA expression of statin uptake transporters including rat Oatp1a1, Oatp1a4, Oatp1a5 and Oatp2b1 as previously shown (Kim, 2017) in newly obtained INS-1 cells. We also aimed to determine the expression of various two key statin efflux transporters, rat P-gp and Bcrp, in INS-1 cells.

As expected, the expression of Oatp1a1, Oatp1a4 and Oatp1a5 was very low or absent (results not shown, as C_t values were below threshold). Similarly, relative to rat liver, INS-1 cells showed very low or negligible expression of Oatp2b1 (**Figure 3.6A**).

Interestingly, efflux transporters of potential relevance to cellular statin accumulation were found to be abundant in INS-1 cells with 11.8-fold and 16.7-fold lower Bcrp and Mdr1a (P-gp) mRNA expression compared to rat liver, a tissue known for its high expression of these carriers. We were unable to quantify RNA expression of any herein assessed statin transporters in rat pancreas (N=3), likely due to the overall very low proportion of islets in the pancreas.

We also conducted dual immunofluorescent staining of INS-1 cells with insulin and P-gp or Bcrp antibodies (**Figure 3.6B**), showing that both transporters were expressed in the insulin-secreting INS-1 cells, as observed by the co-staining of insulin with P-gp or Bcrp, supporting our qPCR findings.

A



B

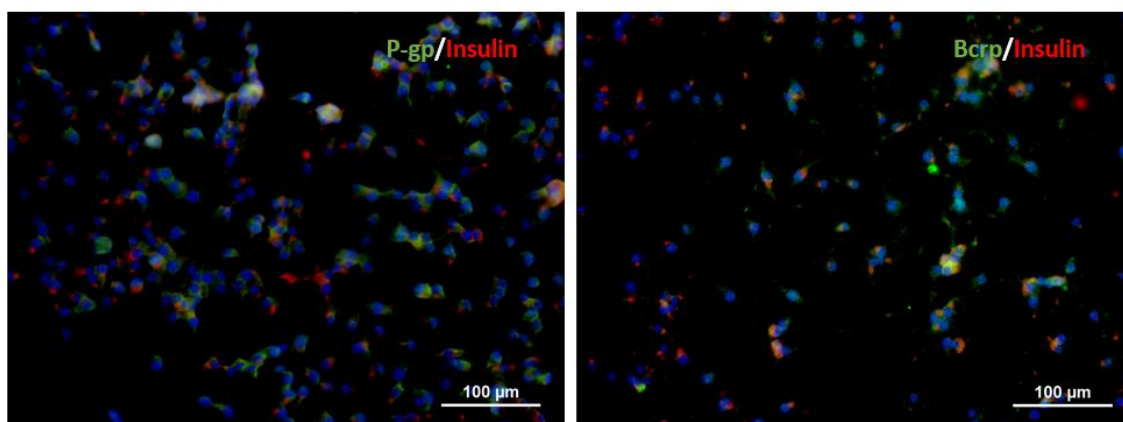
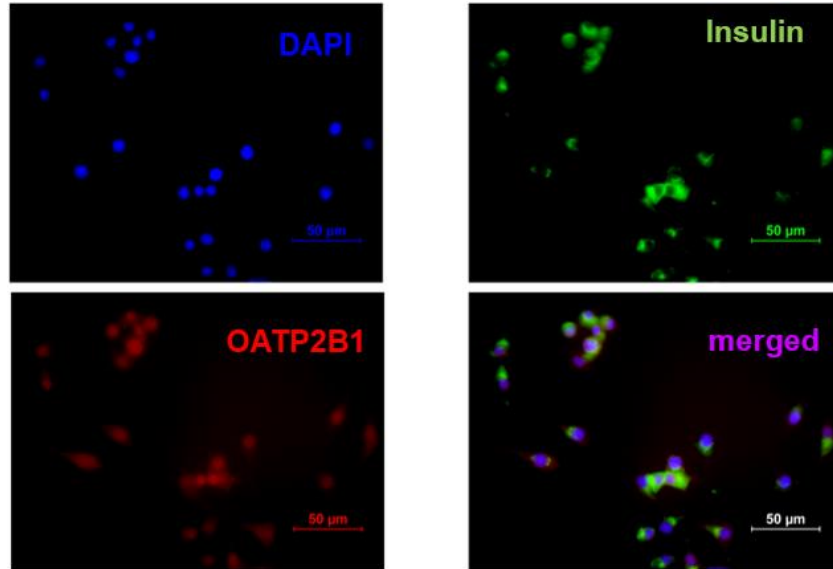


Figure 3.6. Statin efflux transporter expression in INS-1 cells. RNA was extracted from INS-1 cells (N=3) or rat liver samples (N=3), and RT-qPCR was performed to quantify mRNA levels of rat Oatp2b1, P-gp (measured as Mdr1a) and Bcrp, with β -actin as the internal control (A). Data are shown as mean \pm SEM, expressed as a fold-difference from the liver. INS-1 cells were also dual-fluorescence stained for P-gp (B, left, in green) or Bcrp (B, right, in green) and insulin (B, in red). The overlay images are shown, taken at 20x objective magnification.

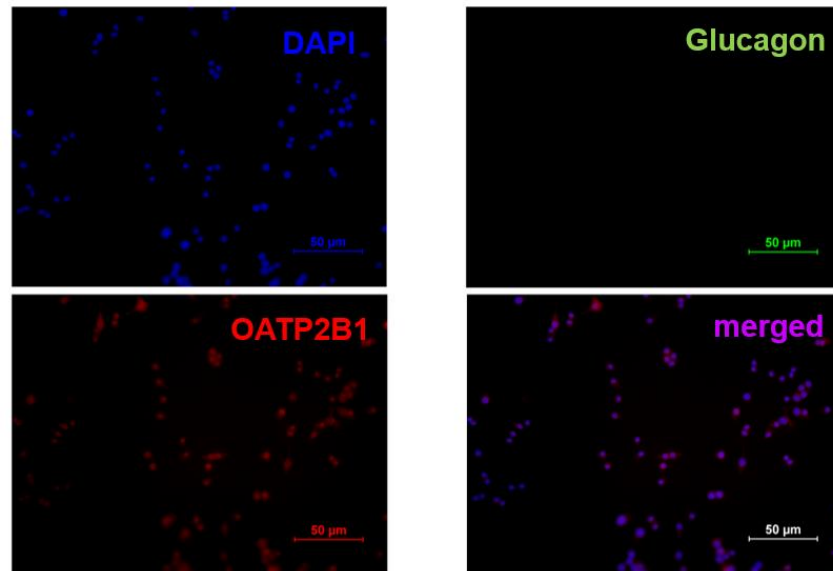
3.3 OATP2B1 overexpression model in INS-1 cells

After demonstrating the absence of endogenous *Oatp2b1*, as well as other relevant *Oatps* for statin uptake in INS-1 cells (Kim, 2017), a transient overexpression model for human OATP2B1 was established using adenoviral transduction to study the effect of OATP2B1-mediated statin transport on beta cell function. We used 48-hour adenoviral transduction to overexpress OATP2B1 in INS-1 cells (Ad-OATP2B1) as previously established (**Section 2.3**). To verify the expression, we performed western blotting and dual immunofluorescent staining for OATP2B1 and insulin or glucagon. We observed co-staining for OATP2B1 and insulin, while there was no glucagon staining observed, indicating lack of glucagon-secreting cells in our INS-1 cell model (**Figure 3.7A, B**). We observed abundant OATP2B1 expression in INS-1 cells transduced with Ad-OATP2B1, which increased with the amount of protein loaded; as expected, no OATP2B1 expression was observed in Ad-LacZ control (**Figure 3.7C**). We attempted two other methods of transient OATP2B1 transfection in INS-1 cells, including Lipofectamine 3000 and Xtreme-GENE, but both were unsuccessful.

A



B



C

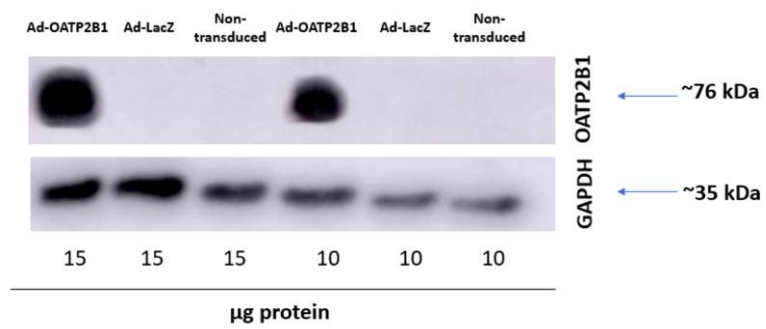


Figure 3.7. Characterization of OATP2B1 overexpression in INS-1 cells using immunofluorescent staining (A, B) and western blot (C). INS-1 cells were transduced with Ad-OATP2B1 at MOI of 250 for 48 hours, and after fixation with 4% formaldehyde, stained for insulin (**A**) or glucagon (**B**) (green) and OATP2B1 (red) at 40x objective. DAPI, insulin or glucagon, OATP2B1 and merged images are shown. Western blot analysis for OATP2B1 and GAPDH as loading control was also conducted following the 48-hour adenoviral transduction with Ad-LacZ or Ad-OATP2B1, with Ad-LacZ and non-transduced cells as negative controls (**C**).

3.4 The Effect of OATP2B1 and Inhibition of Statin Efflux Transporters on Cellular Statin Accumulation

Overall, OATP2B1 overexpression, as well as statin treatment (pravastatin, rosuvastatin or atorvastatin) had a significant effect on cellular statin accumulation in INS-1 cells (**Figure 3.8**). Specifically, OATP2B1-overexpressing cells had a 2.5-fold higher rosuvastatin uptake ($p < 0.0001$) and 2-fold higher atorvastatin uptake ($p < 0.0001$) relative to Ad-LacZ control, while there was only a trend for higher pravastatin uptake (**Figure 3.8A**). Absolute cellular statin concentration was overall highest in the atorvastatin group, in comparison to rosuvastatin and pravastatin, and OATP2B1 led to a significantly higher cellular statin accumulation (2.0-fold, $p = 0.004$) relative to Ad-LacZ control following atorvastatin treatment only (**Figure 3.8B**).

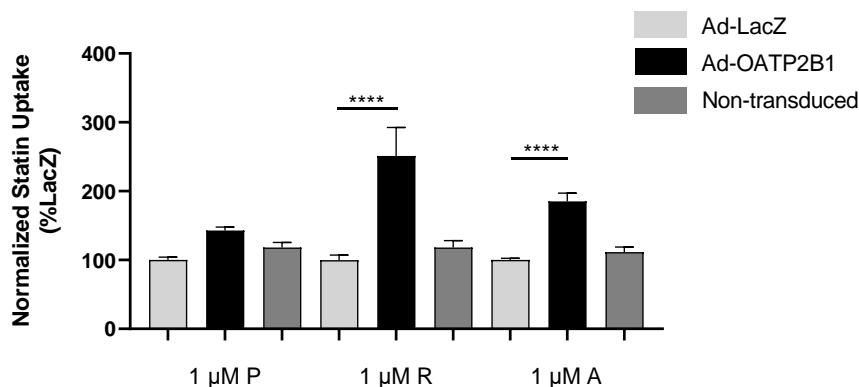
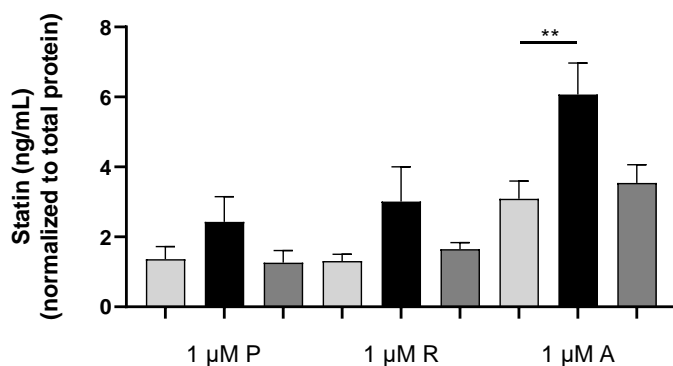
A**B**

Figure 3.8. Statin uptake in Ad-OATP2B1 INS-1 cells compared to Ad-LacZ. INS-1 cells were transduced with Ad-LacZ (control), Ad-OATP2B1 or left non-transduced for 48 hours (MOI 250). Then, the cells were treated with 1 μM of pravastatin (P), rosuvastatin (R) or atorvastatin (A) for 30 minutes to allow for uptake, washed, lysed, and cellular statin concentrations were quantified using LC-MS/MS. Data shown are mean statin concentration \pm SEM (N=4 independent experiments, measured in triplicates), normalized to total protein, expressed as %LacZ control (A) or as absolute concentration (ng/mL)(B), and were analyzed using a two-way ANOVA with Tukey's post-hoc test. Significant main effects of OATP2B1 ($p < 0.0001$ for A, $p < 0.01$ for B), statin treatment ($p < 0.01$ for A, $p < 0.0001$ for B), and their interaction were found ($p < 0.001$ for A). ** $p < 0.01$, **** $p < 0.0001$.

We next investigated the role of statin concentration and time of treatment on OATP2B1-mediated statin uptake using rosuvastatin as the prototypic OATP2B1 substrate (**Figure 3.9**). Ad-OATP2B1 INS-1 cells were assessed following 30-minute rosuvastatin treatment at different concentrations (1, 10 or 100 μM) or following 24-hour treatment with 1 μM rosuvastatin. A potential role of the efflux transporters P-gp and Bcrp was also investigated through co-administration of 1 μM rosuvastatin with either fumitremorgin C, a known inhibitor of Bcrp or verapamil, a relatively unspecific inhibitor of various efflux transporters including P-gp.

As shown in **Figure 3.9A**, as rosuvastatin concentration increased from 1, 10 to 100 μM , the effect of OATP2B1 on cellular rosuvastatin accumulation was diminished. At 1 μM , cellular rosuvastatin accumulation was 2.8-fold higher in OATP2B1-overexpressing cells relative to Ad-LacZ cells ($p < 0.0001$), which was decreased to 2.2-fold at 10 μM ($p < 0.0001$) and 1.7-fold ($p < 0.05$) at 100 μM . Additionally, as 1 μM rosuvastatin treatment duration increased from 30 minutes to 24 hours, the effect of OATP2B1 decreased (**Figure 3.9B**). Cellular rosuvastatin accumulation was 2.8-fold higher in OATP2B1-overexpressing INS-1 cells relative to Ad-LacZ cells ($p < 0.0001$) at 30 minutes, whereas at 24 hours, there was only a trend for an increase in Ad-OATP2B1 vs. Ad-LacZ.

To assess a potential effect of statin efflux inhibitors, rosuvastatin uptake was assessed at different concentrations or times in Ad-OATP2B1 and Ad-LacZ compared to no-inhibitor (DMSO) control. Following 30-minute treatment with 1 μM rosuvastatin, co-treatment with fumitremorgin C (5 μM) and verapamil (40 μM) led to a 1.8-fold ($p > 0.05$) and 3.6-fold higher rosuvastatin uptake ($p < 0.0001$), respectively, relative to no-inhibitor (DMSO) control in Ad-LacZ cells (**Figure 3.9C**). In OATP2B1-overexpressing cells, only verapamil co-treatment had a significant effect on rosuvastatin uptake, but not fumitremorgin C (**Figure 3.9C**). A main effect of OATP2B1 ($p < 0.0001$), statin efflux inhibition ($p < 0.0001$) and their interaction ($p < 0.01$) was found.

Following 30-minute treatment with 10 μM rosuvastatin, co-treatment verapamil led to a 2.5-fold higher rosuvastatin uptake ($p < 0.05$) relative to no-inhibitor (DMSO) treatment in

Ad-LacZ cells, while there was no effect of fumitremorgin C (**Figure 3.9D**). In OATP2B1-overexpressing INS-1 cells, co-treatment with fumitremorgin C led to a 2.1-fold higher rosuvastatin uptake ($p < 0.001$), and co-treatment with verapamil led to a 2-fold higher rosuvastatin uptake ($p < 0.001$) relative to no-inhibitor (DMSO) control (**Figure 3.9D**). A main effect of OATP2B1 ($p < 0.0001$) and statin efflux inhibition ($p < 0.0001$) but no interaction was found.

Following 30-minute treatment with 100 μM rosuvastatin, co-treatment with fumitremorgin C and verapamil led to a 2.3-fold ($p < 0.01$) and a 3.3-fold ($p < 0.0001$) increased rosuvastatin uptake relative to no-inhibitor treatment in Ad-LacZ cells (**Figure 3.9E**). In OATP2B1-overexpressing INS-1 cells, co-treatment with verapamil led to a 2.3-fold higher rosuvastatin uptake ($p < 0.0001$) relative to no-inhibitor treatment, whereas fumitremorgin C did not have a significant effect (**Figure 3.9E**). A main effect of statin efflux inhibition ($p < 0.0001$) was found, but no effect of OATP2B1 alone. Their interaction was significant ($p < 0.05$).

Finally, following 24-hour treatment with 1 μM rosuvastatin, co-treatment with verapamil led to a 1.6-fold ($p < 0.05$) and 1.4-fold greater rosuvastatin uptake ($p < 0.05$) relative to no-inhibitor treatment within Ad-LacZ control and OATP2B1-overexpressing cells, respectively, whereas fumitremorgin C had no significant effect (**Figure 3.9F**). A main effect of OATP2B1 ($p < 0.0001$) and statin efflux inhibition ($p < 0.0001$) but no interaction was found.

Taken together, while these results support a role of OATP2B1 on cellular statin accumulation after 30-minute treatment, the effect decreased with increasing rosuvastatin concentration, as well as longer treatment time. Moreover, our results suggest that co-treatment with statin efflux inhibitors may further enhance rosuvastatin uptake compared to no-inhibitor control, with a more pronounced effect for verapamil, an unspecific P-gp inhibitor compared to fumitremorgin C, an inhibitor of BCRP. This effect was more pronounced in Ad-LacZ control than in OATP2B1-overexpressing cells, and decreased over time.

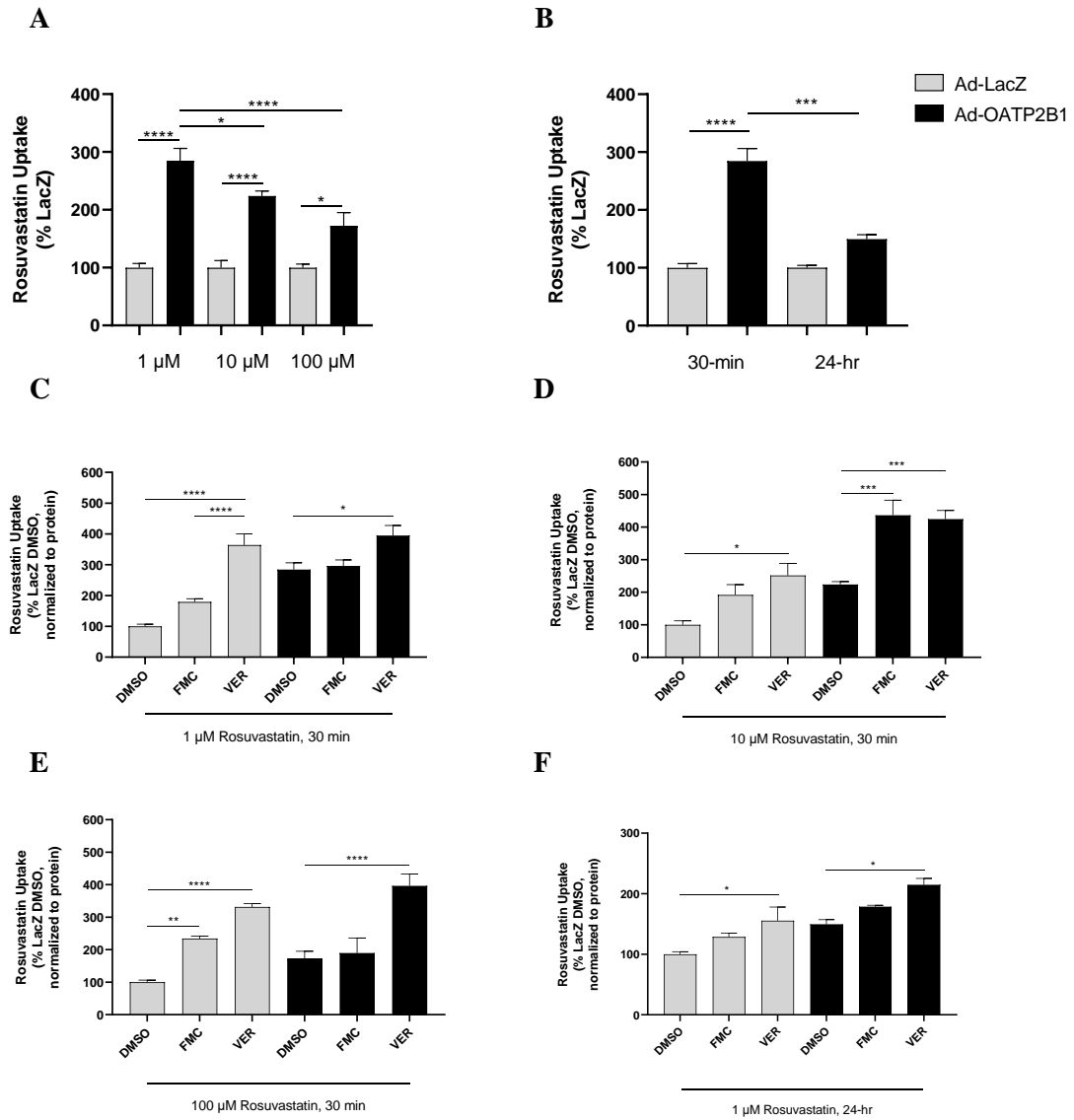


Figure 3.9. Effect of statin concentration and time on rosuvastatin uptake with or without inhibitors of statin efflux transporters in Ad-OATP2B1 INS-1 cells compared to Ad-LacZ.

The INS-1 cells were transduced with Ad-LacZ (control) or Ad-OATP2B1 for 48 hours, and subsequently treated with 1 μ M (**C**), 10 μ M (**D**) or 100 μ M (**E**) of each statin for 30 minutes, or 1 μ M rosuvastatin for 24 hours (**F**) with 5 μ M fumitremorgin C (FMC) or 40 μ M verapamil (VER) or DMSO control. Data were also separately graphed to assess the effect of concentration (**A**) or treatment time (**B**).

Relative differences in statin concentrations were determined using LC-MS/MS. Data shown are mean statin uptake \pm SEM, normalized to total protein (measured in triplicates, N=3 independent experimental days, except N=2 for DMSO/FMC for Ad-OATP2B1 in **C**, N=1 in triplicates for 24-hour data) and analyzed using a two-way ANOVA with Tukey's post-hoc test. A significant main effect of OATP2B1 ($p < 0.0001$ for **A**, **B**, **C**, **D** and **F**), statin treatment ($p < 0.0001$ for **A**, **B**, **C**, **D** and **E**, $p < 0.001$ for **F**) and their interaction ($p < 0.01$ for **A**, **B**, **C**, $p < 0.05$ for **E**) were found. * $p < 0.05$, ** $p < 0.01$, *** $p < 0.001$, **** $p < 0.0001$.

3.5 Role of OATP2B1 in Statin-Induced Impairment of Glucose-Stimulated Insulin Secretion and the Involvement of the Mevalonate Pathway

As described above, OATP2B1 markedly increased cellular concentration of rosuvastatin and atorvastatin but not pravastatin after 1 μ M treatment in our INS-1 cell model (**Figure 3.8**). In order to study the effect of OATP2B1 and increasing concentrations of rosuvastatin, atorvastatin and pravastatin after 24-hour incubation on insulin secretion, we next performed a glucose-stimulated insulin secretion (GSIS) experiment. Simultaneously, we investigated a potential reversal of statin-induced impaired insulin secretion with co-administration of mevalonate pathway substrates in INS-1 cells.

Under DMSO control conditions for all experiments (**Figures 3.10-12**), insulin secretion increased about 4-fold in OATP2B1-overexpressing cells and 3-fold in Ad-LacZ cells after high-glucose stimulation at 22 mM compared to low-glucose stimulation at 2.2 mM, as indicated by a comparable stimulation index (SI) of about 3 in Ad-LacZ control, confirming functional INS-1 cells. Stimulation index was calculated as the ratio of insulin secretion following high-glucose stimulation divided by that of the low-glucose stimulation. Unexpectedly, we observed a significant increase in insulin secretion following high-glucose stimulation in OATP2B1-overexpressing cells relative to Ad-LacZ cells in DMSO control ($p < 0.05$) (**Figures 3.10C, 11C, 12C**)

Following 24-hour rosuvastatin treatment, OATP2B1 expression as well as various rosuvastatin concentrations and substrates (FPP and GGPP) had a significant main effect on insulin secretion following low and high glucose stimulation. When represented as SI or normalized SI (% DMSO), we observed a significant main effect of statin concentration and substrate treatment. Interaction was found following high-glucose stimulation and normalized SI with substrate treatment only. Specifically, insulin secretion following low-glucose stimulation at 2.2 mM (**Figure 3.10A**) and high-glucose stimulation at 22 mM (**Figure 3.10C**) was variable. In OATP2B1-overexpressing cells, insulin secretion following high-glucose stimulation, as well as stimulation index,

showed a dose-dependent decrease as rosuvastatin concentration increased from 0.1, 1 to 10 μ M compared to DMSO control. When stimulation index was normalized to % DMSO, we observed a dose-dependent reduction in insulin secretion as statin concentration increased, with a 59% reduction ($p < 0.05$) in SI following 10 μ M treatment in OATP2B1-overexpressing cells compared to DMSO control (**Figure 3.10G**). The same trend was observed in Ad-LacZ cells, which seemed to be rescued when supplemented with FPP or GGPP (**Figure 3.10C, D**). Co-treatment with GGPP resulted in a marked increase in stimulation index compared to co-treatment with FPP ($p < 0.05$) (**Figure 3.10F, H**). There was no difference in insulin or stimulation index comparing OATP2B1-overexpressing cells versus Ad-LacZ control for any of the assessed rosuvastatin concentrations.

Following 24-hour atorvastatin treatment, we observed an overall main effect of OATP2B1 expression following high glucose stimulation, and an effect of atorvastatin concentration following high-glucose stimulation and stimulation index (**Figure 3.11**). Interaction was found following high-glucose stimulation only. Insulin secretion following low-glucose stimulation was variable (**Figure 3.11A**), but following high-glucose stimulation, we observed a dose-dependent decrease in insulin secretion compared to DMSO control (**Figure 3.11C**), similar to rosuvastatin. We also observed a trend towards decreased insulin secretion following high-glucose stimulation as atorvastatin concentration increased, with a 64% reduction in stimulation index at 10 μ M compared to DMSO control (**Figure 3.11G**). Co-treatment with FPP or GGPP did not rescue insulin secretion, and similar to rosuvastatin treatment, there was no difference in SI comparing OATP2B1-overexpressing cells and Ad-LacZ control for any of the assessed atorvastatin concentrations.

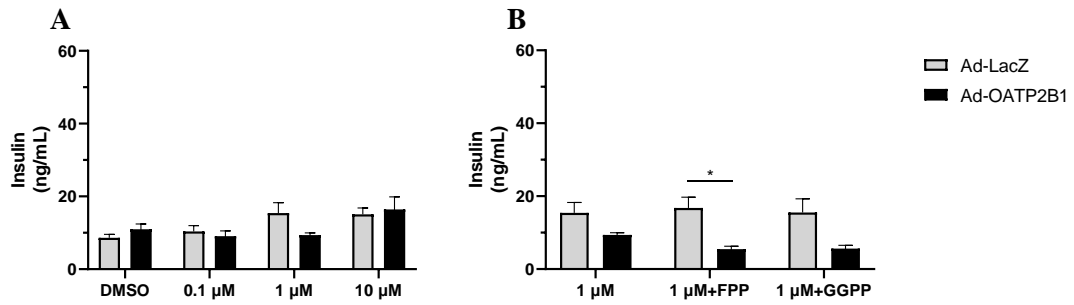
Following 24-hour pravastatin treatment, we observed a main effect of pravastatin concentration at low-glucose stimulation, and an overall effect of OATP2B1 following low- and high-glucose stimulation. No interaction was found. Co-treatment with FPP and GGPP did not affect insulin secretion. When represented as SI or normalized SI values, the trend was quite variable, and like rosuvastatin and atorvastatin, no effect of

OATP2B1 was observed relative to Ad-LacZ control in any of our concentrations tested (**Figure 3.12E-H**).

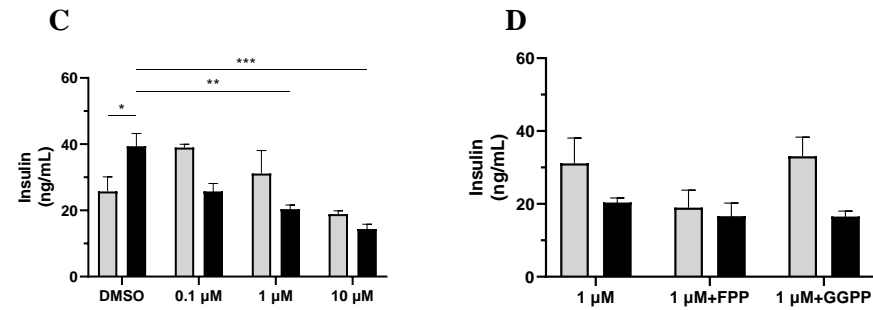
In summary, while a dose-dependent reduction in insulin secretion was observed with rosuvastatin and atorvastatin compared to DMSO control, OATP2B1 did not affect insulin secretion in any of the statin concentrations tested after 24-hour treatment.

24-hour rosuvastatin

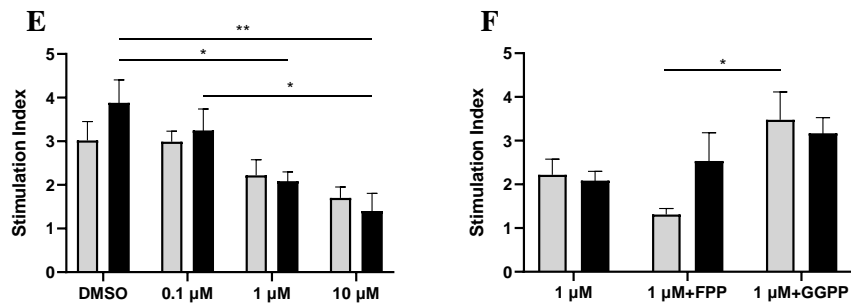
Low-glucose



High-glucose



SI



SI (%)

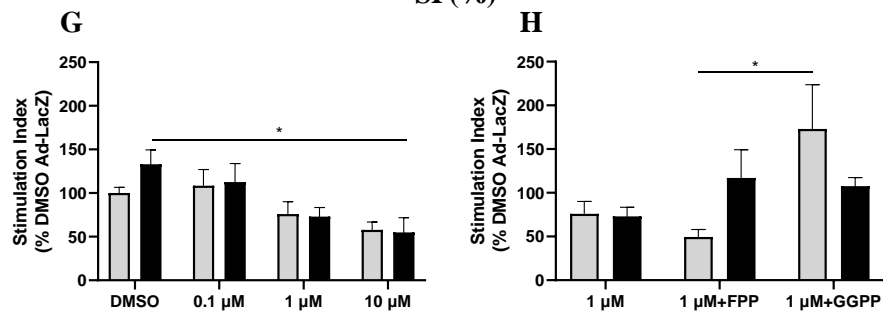


Figure 3.10. Insulin concentration following low-glucose stimulation (A, B), high-glucose stimulation (C, D), stimulation index (E, F) and normalized stimulation index (%DMSO) (G, H) after 24-hour rosuvastatin treatment. INS-1 cells were transduced with Ad-LacZ (control) or Ad-OATP2B1 for 48 hours and treated with various concentrations of rosuvastatin (0.1 μ M, 1 μ M, 10 μ M) or DMSO control, or 1 μ M rosuvastatin with 10 μ M farnesyl pyrophosphate (FPP) or geranylgeranyl pyrophosphate (GGPP) for 24 hours. They were then incubated with low-glucose (2.2 mM) and then subsequently high-glucose (22 mM) buffer for 2 hours each. Supernatant was collected and insulin content was quantified using an enzyme-linked immunosorbent assay (ELISA). Stimulation index was calculated as the ratio of GSIS after high-glucose divided by low-glucose stimulation for each independent experiment using paired values for insulin concentration after high and low glucose stimulation. Data shown are mean \pm SEM (N=3 independent experiments in duplicates, except N=2 for SI at 0.1 μ M due to lack of paired data) and were analyzed using a two-way ANOVA followed by Tukey's post-hoc test. A significant main effect of statin concentration ($p < 0.05$ for **A**, $p < 0.0001$ for **C**, $p < 0.0001$ for **E**, $p < 0.001$ for **G**), FPP or GGPP treatment ($p < 0.01$ for **F**, $p < 0.05$ for **H**) and OATP2B1 ($p < 0.0001$ for **B**, $p < 0.05$ for **D**), and their interaction ($p < 0.01$ for **C**, $p < 0.05$ for **H**) was found. * $p < 0.05$, ** $p < 0.01$, *** $p < 0.001$, **** $p < 0.0001$.

24-hour atorvastatin

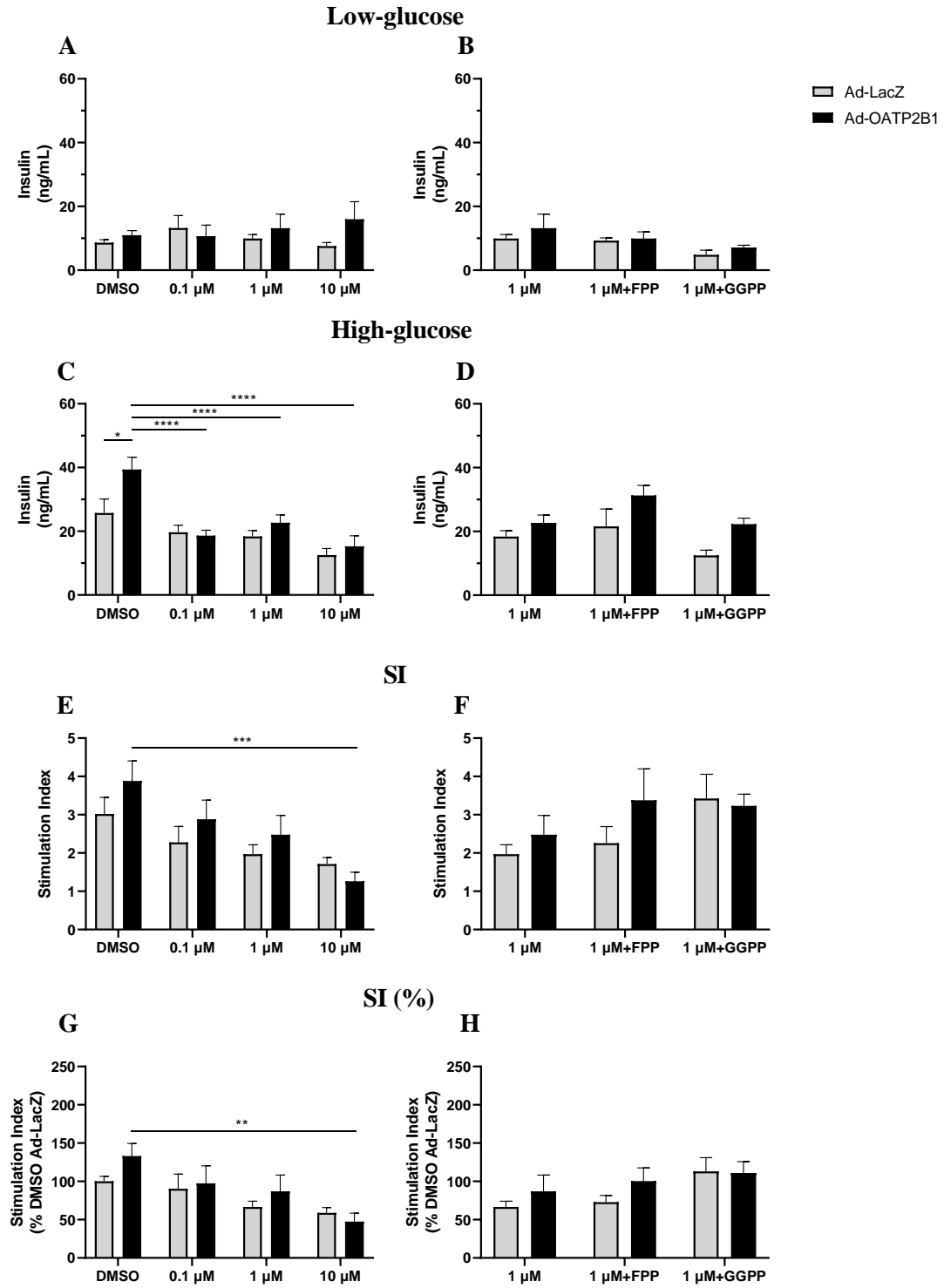


Figure 3.11. Insulin concentration following low-glucose stimulation (A, B), high-glucose stimulation (C, D), stimulation index (E, F) and normalized stimulation index (%DMSO) (G, H) after 24-hour atorvastatin treatment. INS-1 cells were transduced with Ad-LacZ (control) or Ad-OATP2B1 for 48 hours and treated with various concentrations of atorvastatin (0.1 μ M, 1 μ M, 10 μ M) or DMSO control, or 1 μ M atorvastatin with 10 μ M farnesyl pyrophosphate (FPP) or geranylgeranyl pyrophosphate (GGPP) for 24 hours. They were then incubated with low-glucose (2.2 mM) and then subsequently high-glucose (22 mM) buffer for 2 hours each. Supernatant was collected and insulin content was quantified using an enzyme-linked immunosorbent assay (ELISA). Stimulation index was calculated as the ratio of GSIS after high-glucose divided by low-glucose stimulation. Data shown are mean \pm SEM (N=3 independent experiments performed in duplicates) and were analyzed using a two-way ANOVA followed by Tukey's post-hoc test. A significant main effect of statin concentration ($p < 0.0001$ for **C**, $p < 0.001$ for **E** and $p < 0.001$ for **G**), FPP or GGPP treatment ($p < 0.05$ for **B** and **D**) and OATP2B1 ($p < 0.05$ for **C**, $p < 0.01$ for **D**) was found. Interaction was found ($p < 0.0001$) in **C**. ** $p < 0.01$, *** $p < 0.001$, **** $p < 0.0001$.

24-hour pravastatin

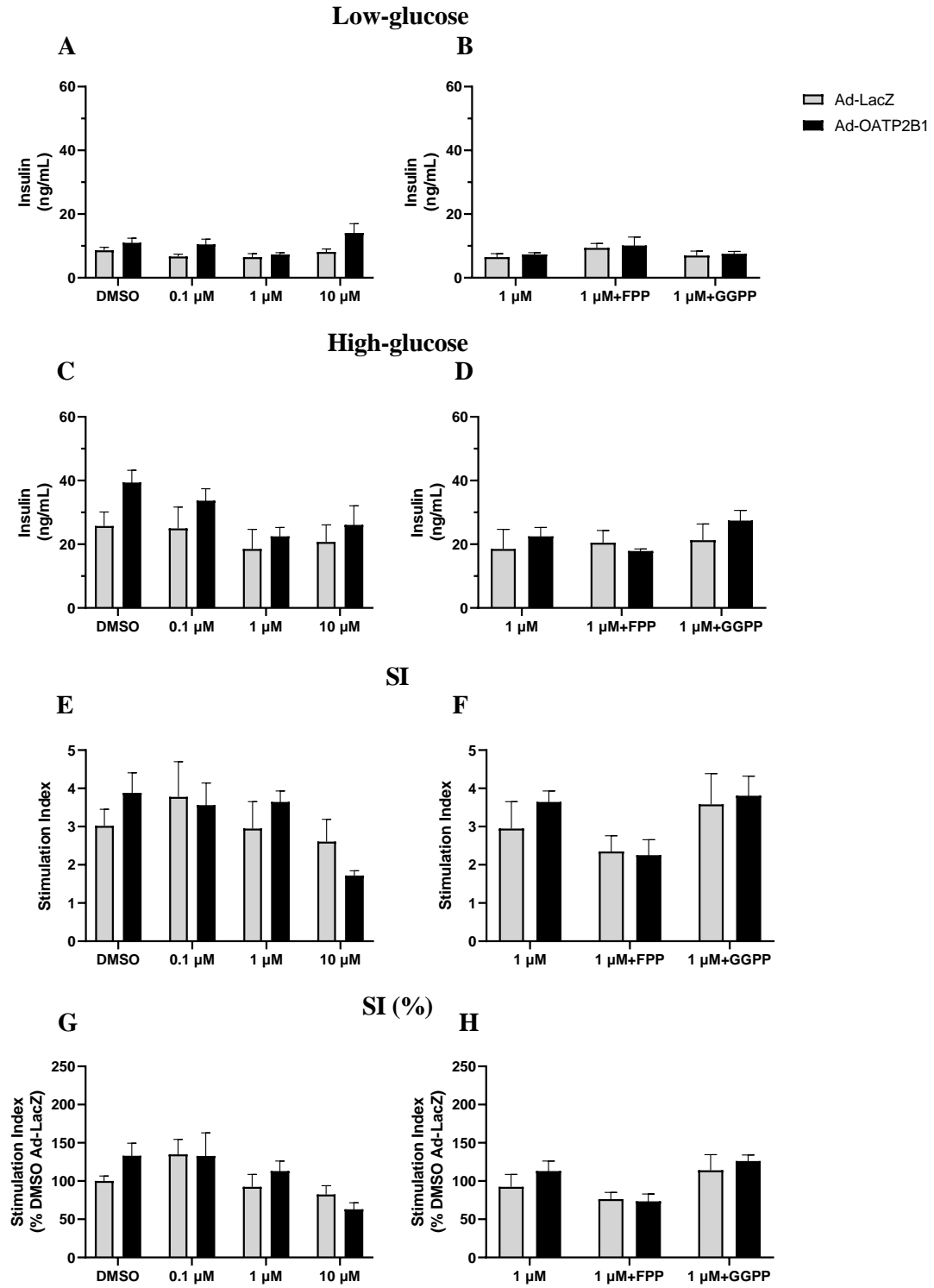
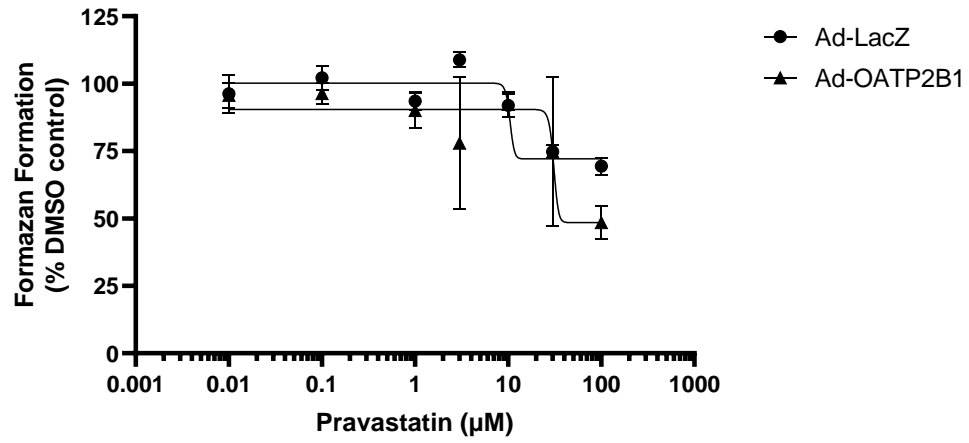


Figure 3.12. Insulin concentration following low-glucose stimulation (A, B), high-glucose stimulation (C, D), stimulation index (E, F) and normalized stimulation index (%DMSO) (G, H) after 24-hour pravastatin treatment. INS-1 cells were transduced with Ad-LacZ (control) or Ad-OATP2B1 for 48 hours and treated with various concentrations of pravastatin (0.1 μ M, 1 μ M, 10 μ M) or DMSO control, or 1 μ M pravastatin with 10 μ M farnesyl pyrophosphate (FPP) or geranylgeranyl pyrophosphate (GGPP) for 24 hours. They were then incubated with low-glucose (2.2 mM) and then subsequently high-glucose (22 mM) buffer for 2 hours each. Supernatant was collected and insulin content was quantified using an enzyme-linked immunosorbent assay (ELISA). Stimulation index was calculated as the ratio of GSIS after high-glucose divided by low-glucose stimulation. Data shown are mean \pm SEM (N=3 independent experiments performed in duplicates, except N=2 experiments in duplicates for stimulation index at 1 μ M) and were analyzed using a two-way ANOVA followed by Tukey's post-hoc test. A significant main effect of statin concentration ($p < 0.05$ for **A** and **G**), FPP or GGPP treatment ($p < 0.01$ for **H**) and OATP2B1 ($p < 0.01$ for **A** and $p < 0.05$ for **C**) was found, but no interaction was detected.

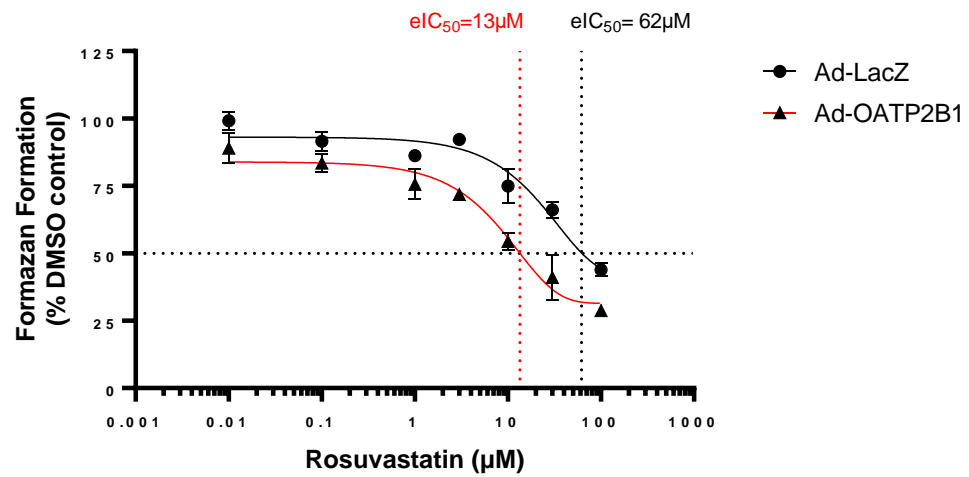
3.6 Role of OATP2B1 in Statin-Mediated Effect on Mitochondrial Function

First, we assessed the effect of statin treatment on mitochondrial toxicity using an MTT test. Formazan formation, which is catalyzed by complex III of the electron transport chain and thus represents a measure of mitochondrial function, was measured after 24-hour statin treatment. Using increasing statin concentrations, a formazan dose response curve was fitted for each statin (**Figure 3.13**). Due to the overall modest reduction in formazan formation even at the highest statin concentration of 100 μM , only an estimate of the IC_{50} (eIC_{50}) could be interpolated from the graph. In OATP2B1-overexpressing INS-1 cells, eIC_{50} values for rosuvastatin and atorvastatin were markedly decreased to 13 μM and 19 μM , respectively, from 62 μM and 63 μM , respectively, in Ad-LacZ control. Estimating the eIC_{50} the pravastatin dose-response curves was not feasible due to the highest pravastatin concentration not resulting in formazan formation below the half-maximal point. Accordingly, our results suggest that OATP2B1 overexpression resulted in a left-shift of the statin dose response curve for formazan formation, with a marked decrease in eIC_{50} following 24-hour rosuvastatin (about 5-fold) and atorvastatin (about 3-fold) treatment in INS-1 cells, suggesting that statin-mediated mitochondrial toxicity is enhanced due to the presence of OATP2B1.

A



B



C

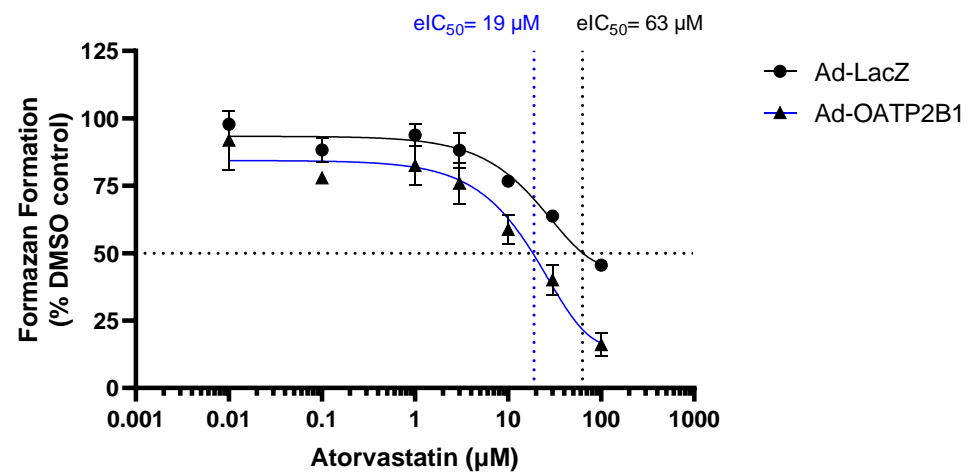
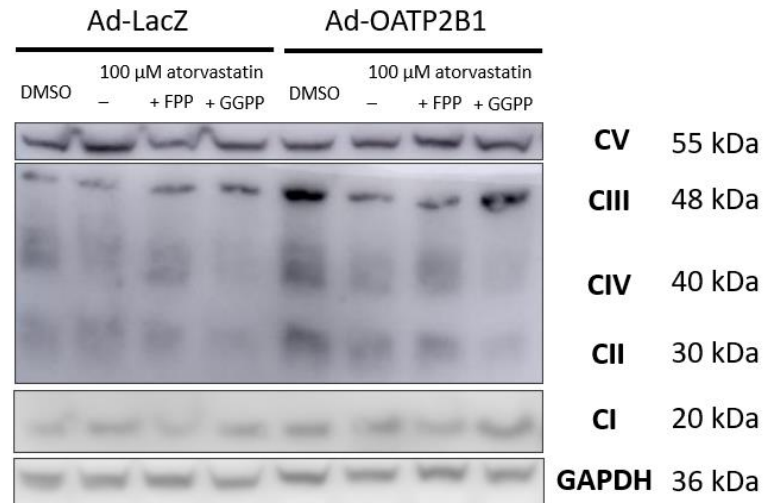


Figure 3.13. Dose-response curves for formazan formation following 24-hour treatment with increasing statin concentrations in Ad-OATP2B1 or Ad-LacZ INS-1 cells. INS-1 cells were transduced with Ad-OATP2B1 or Ad-LacZ control for 48 hours and then treated with 0.01, 0.1, 1, 3, 10, 30 and 100 μM pravastatin (**A**), rosuvastatin (**B**) or atorvastatin (**C**) for 24 hours. Formazan formation was measured using an MTT assay. Data shown are mean formazan formation (% DMSO control) \pm SEM (N=3 independent experiments, measured in triplicates). Estimated IC_{50} (eIC_{50}) values were interpolated from the dose-response curve (log dose) of best fit with non-linear regression (curve fit) using the variable slope-four parameter function in GraphPad Prism v.9.

Mitochondrial function was also assessed by evaluating changes in the protein expression of mitochondrial electron transport chain complexes I-V after 100 μM atorvastatin treatment using western blotting. Atorvastatin at 100 μM was chosen because it led to the greatest decrease in statin-mediated mitochondrial function in OATP2B1-overexpressing cells, as shown in **Figure 3.13**. Although the blots showed a trend of decreased expression of complex III following 100 μM atorvastatin treatment vs. DMSO in OATP2B1-overexpressing cells, quantitative analysis of three independent experiments yielded no significant differences for any of the complexes, as well as no effect of OATP2B1. A representative image of the western blot results is shown below (**Figure 3.14A**), with the quantitative analysis for each complex using ImageJ (**Figure 3.14B**).

A



B

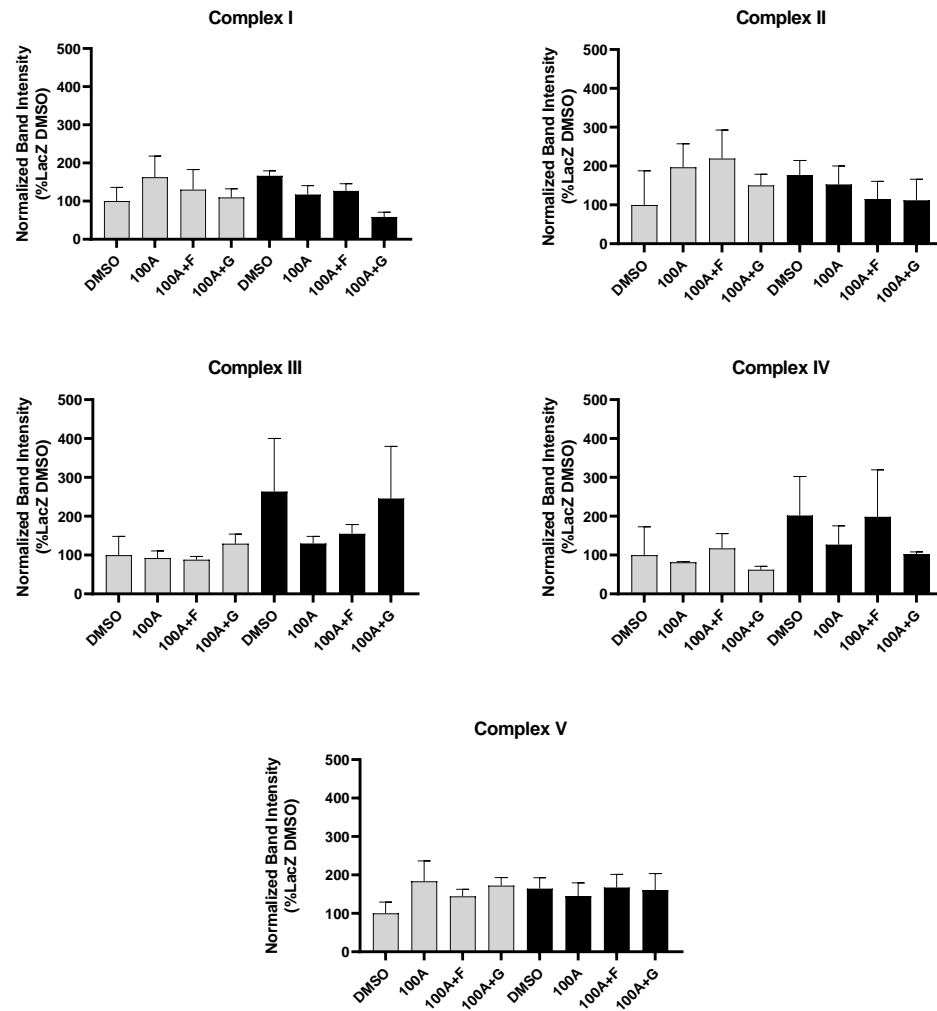


Figure 3.14. Representative western blot (A) and quantification of band intensity (B) for mitochondrial complexes I-V following atorvastatin treatment in Ad-OATP2B1 or Ad-LacZ INS-1 cells. INS-1 cells were treated with DMSO (control) or 100 μ M atorvastatin with or without 10 μ M farnesyl pyrophosphate (FPP) or geranylgeranyl pyrophosphate (GGPP) for 24 hours, and protein expression of mitochondrial complexes I, II, III, IV and V was visualized using western blot (N=3 independent experiments) after loading of 20 μ g total protein. Relative band intensities were quantified using ImageJ, and mean normalized band intensities were graphed and analyzed using a two-way ANOVA followed by Tukey's post hoc. No main effect of atorvastatin or substrate treatment, OATP2B1, nor their interaction was found.

3.7 Role of OATP2B1 in Statin-Mediated Effect on Cellular ATP Concentration

To examine a potential effect of statins on the cellular level of ATP, an important signaling molecule involved in insulin secretion, we performed a luminescent ATP assay following 24-hour treatment with 10 μ M or 100 μ M statin compared to DMSO control in OATP2B1-overexpressing, Ad-LacZ control or non-transduced INS-1 cells.

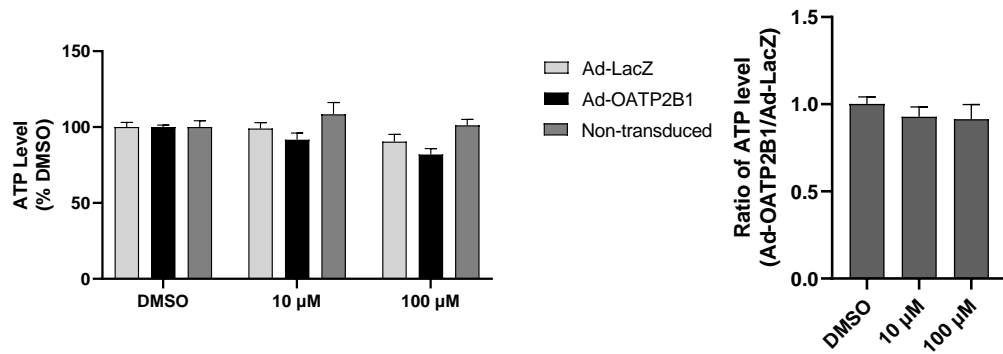
An overall effect of OATP2B1 and statin concentration was found after pravastatin, rosuvastatin and atorvastatin treatment, yet an interaction was found only after rosuvastatin and atorvastatin treatments. In OATP2B1-overexpressing INS-1 cells, 100 μ M rosuvastatin and atorvastatin treatment led to a 43% ($p < 0.01$) and 61% ($p < 0.0001$) reduction in ATP level, respectively, compared to DMSO control (**Figure 3.15B and C**). OATP2B1 overexpression led to a further 1.7-fold decrease in ATP level relative to Ad-LacZ control at 100 μ M atorvastatin (66% of DMSO for Ad-LacZ, 39% of DMSO for Ad-OATP2B1, $p < 0.01$) (**Figure 3.15C**), while there was only a trend at 100 μ M rosuvastatin (79% of DMSO for Ad-LacZ and 56% of DMSO for Ad-OATP2B1,

$p=0.09$). We did not observe any changes in ATP level following 10 μM and 100 μM pravastatin (**Figure 3.15A**).

To better visualize a potential effect of OATP2B1, ATP level was also graphed and assessed as the ratio of ATP level in Ad-OATP2B1 divided by that in Ad-LacZ cells at each concentration. We observed a dose-dependent trend in the reduction of ATP level ratio with rosuvastatin and atorvastatin treatment, while significance was found following 100 μM atorvastatin only (ratio=0.59, $p<0.05$), suggesting a role of OATP2B1 in facilitating the statin-mediated reduction in ATP level at the highest atorvastatin concentration (100 μM).

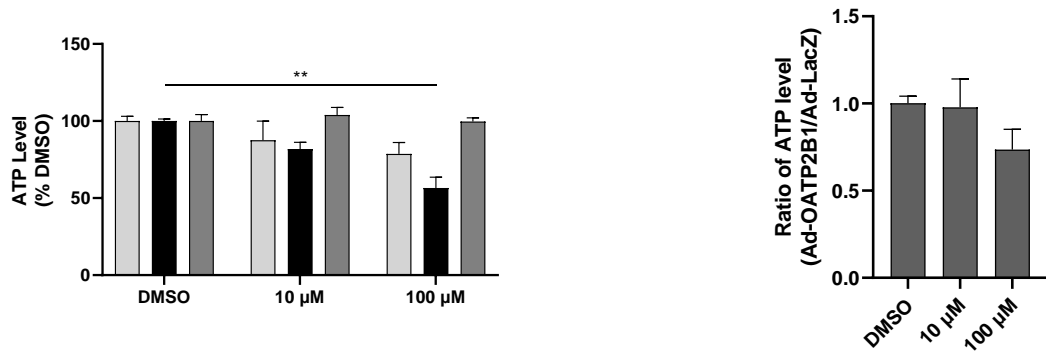
A

Pravastatin Treatment



B

Rosuvastatin Treatment



C

Atorvastatin Treatment

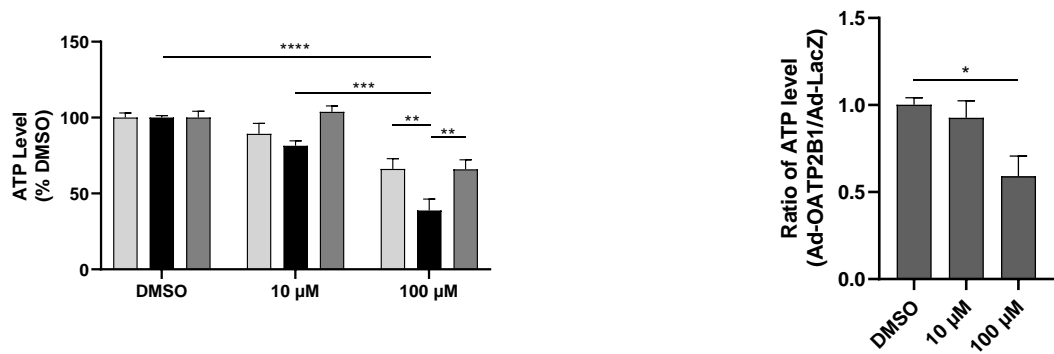


Figure 3.15. ATP level (represented as % DMSO) following 24-hour statin treatment in Ad-LacZ control, OATP2B1-overexpressing and non-transduced INS-1 cells. INS-1 cells were transduced with Ad-LacZ (control) or Ad-OATP2B1 or left non-transduced for 48 hours and treated with DMSO, 10 μ M or 100 μ M of pravastatin (**A**), rosuvastatin (**B**) or atorvastatin (**C**) for 24 hours. Data shown are mean ATP level \pm SEM (left) and mean ratio of ATP level, calculated as ATP level for Ad-OATP2B1 divided by that for Ad-LacZ (right), measured in triplicates over N=3 independent experiments. Data were analyzed using a two-way ANOVA followed by Tukey's post-hoc test (left) or a one-way ANOVA followed by Tukey's post-hoc test (right). A significant effect of statin treatment ($p < 0.01$ for **A** and **B**, $p < 0.05$ for **C**), OATP2B1 ($p < 0.01$ for **A**, $p < 0.0001$ for **B**, $p < 0.05$ for **C**) and interaction was found ($p < 0.05$ for **A** and **B**). One-way ANOVA yielded significance only for **B**. * $p < 0.05$, ** $p < 0.01$, **** $p < 0.0001$.

3.8 Role of OATP2B1 in Statin-Mediated Effects on Caspase 3/7 and 9 Activity

We used a colorimetric assay to assess the effect of statin treatment (10 μ M) for 24 hours on caspase 3/7, two effector caspases indicative of apoptosis, and caspase 9, a mitochondria-mediated initiator caspase, in our INS-1 cell model.

Treatment with 10 μ M rosuvastatin resulted in a 2.9-fold increase in caspase 3/7 activity in OATP2B1-overexpressing INS-1 cells relative to DMSO ($p < 0.01$). Caspase 3/7 activity was also 1.4-fold higher in OATP2B1-overexpressing cells compared to Ad-LacZ control ($p < 0.05$), suggesting a role of OATP2B1 (**Figure 3.16A**). Treatment with 10 μ M atorvastatin led to a 3.6-fold increase in caspase 3/7 activity in OATP2B1-overexpressing INS-1 relative to DMSO ($p < 0.001$), which was also 1.6-fold higher than Ad-LacZ control ($p < 0.01$). Furthermore, in OATP2B1-overexpressing INS-1 cells, co-treatment of 10 μ M atorvastatin with FPP or GGPP significantly decreased caspase 3/7 activity compared to 10 μ M atorvastatin treatment alone ($p < 0.05$ and $p < 0.01$,

respectively). Pravastatin treatment had no effect on caspase 3/7 activity in Ad-LacZ control and OATP2B1-overexpressing INS-1 cells.

In comparison, treatment with 10 μ M rosuvastatin resulted in a less pronounced but still significant 1.5-fold increase in caspase 9 activity ($p < 0.05$) relative to DMSO control in OATP2B1-overexpressing cells (**Figure 3.16B**). Furthermore, 10 μ M atorvastatin resulted in higher caspase 9 activity relative to DMSO in both Ad-LacZ control (1.8-fold, $p < 0.05$) and OATP2B1-overexpressing INS-1 cells (2.5-fold, $p < 0.0001$). These values were also significantly different ($p < 0.05$), suggesting a role of OATP2B1 in amplifying the statin-induced increase in caspase 9 activity. In addition, in OATP2B1-overexpressing cells, this 2.5-fold increase in caspase 9 activity was significantly reduced to 1.6-fold ($p < 0.01$) and 1.4-fold ($p < 0.001$) when co-treated with FPP and GGPP, respectively. Similar to caspase 3/7 activity, pravastatin had no effect on caspase 9 activity in Ad-LacZ control and OATP2B1-overexpressing INS-1 cells.

Overall, 10 μ M atorvastatin resulted in the greatest increase in caspase 3/7 and 9 activities followed by rosuvastatin but not pravastatin in OATP2B1-overexpressing cells, which was rescued when co-treated with FPP or GGPP. We also noted an effect of OATP2B1 on both caspase 3/7 and 9 activities following 10 μ M atorvastatin and 10 μ M rosuvastatin treatment.

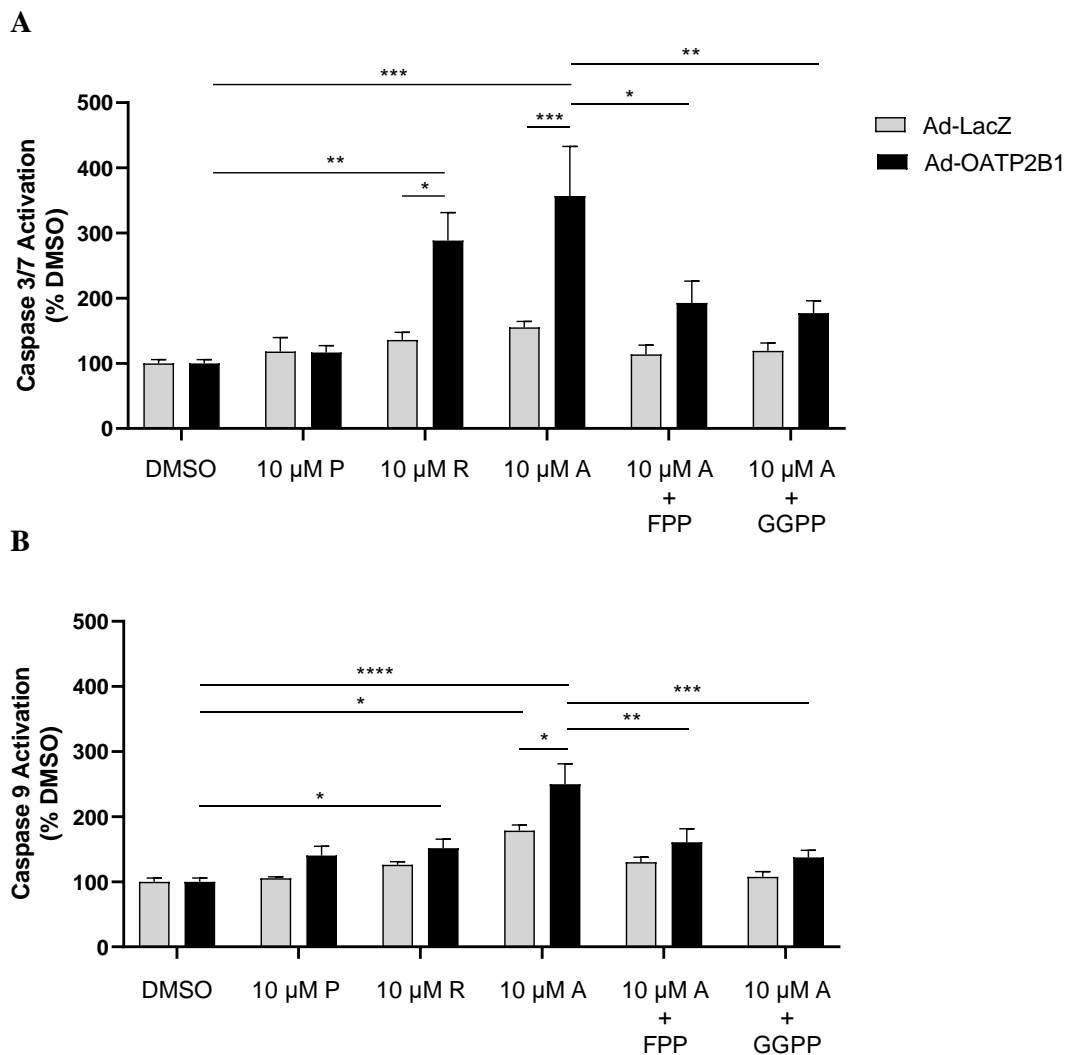


Figure 3.16. Caspase 3/7 (A) or 9 (B) activity in OATP2B1-overexpressing versus Ad-LacZ INS-1 cells following 24-hour statin/substrate treatment. INS-1 cells were transduced with Ad-LacZ or Ad-OATP2B1 for 48 hours and then treated with DMSO control, 10 μM rosuvastatin (R), 10 μM atorvastatin (A) or 10 μM pravastatin (P) with or without 10 μM farnesyl pyrophosphate (FPP) or geranylgeranyl pyrophosphate (GGPP), for 24 hours. Data shown are mean caspase 3/7 (A) or 9 (B) activity as %DMSO ± SEM (performed in triplicates, N=3 independent experiments) and analyzed using a two-way ANOVA with Tukey's post-hoc test. A significant effect of statin treatment ($p < 0.0001$ for **A**, $p < 0.001$ for **B**), OATP2B1 ($p < 0.001$ for **A**, $p < 0.0001$ for **B**) and interaction was found ($p < 0.05$ for **A**). * $p < 0.05$, ** $p < 0.01$, *** $p < 0.001$, **** $p < 0.0001$.

Chapter 4

4 Discussion and Conclusion

4.1 Summary of Key Findings

Cholesterol-lowering statins are subject to the interplay of uptake and efflux by OATPs and ABC efflux transporters, respectively, and these transporters are recognized as important determinants of statin disposition in hepatocytes. Statin therapy has been linked to an increase in the risk of new-onset diabetes mellitus, and potential mechanisms may include inhibition of the mevalonate pathway leading to mitochondrial dysfunction and beta cell apoptosis (Betteridge & Carmena, 2016; Deichmann et al., 2010; Mollazadeh et al., 2021; Yada et al., 1999).

Our lab previously demonstrated OATP2B1 expression in human pancreatic islets and its localization within beta cells, while gene expression of P-gp and BCRP, two ABC efflux transporters, in islets was suggested by initial results (Kim, 2017). This project aimed to explore the link between OATP2B1-mediated statin transport and beta cell function using a rat beta cell model. We hypothesized that OATP2B1 are localized on the human beta cell, facilitates the cellular accumulation of statins in a rat beta cell model, and that it augments statin-associated impairment in beta cell function.

We first investigated the localization of statin efflux transporters, P-gp and BCRP, within the adult human pancreas. We next characterized the expression of various statin-transporting Oatps as well as P-gp and Bcrp in INS-1 cells, a rat insulinoma cell line. We then used adenoviral transduction to transiently overexpress human OATP2B1 to study its effect on cellular statin accumulation and statin-mediated toxicity in a transient INS-1 cell model. Specifically, we assessed the role of OATP2B1-mediated statin uptake in INS-1 cells on insulin secretion, mitochondrial function, cellular ATP level and caspase 3/7 and 9 activities, and whether some of these toxicities could be mitigated through co-treatment with mevalonate pathway intermediates, FPP and GGPP. Key results are summarized below.

4.1.1. Specific Aim 1: To characterize the endogenous expression of statin uptake and efflux transporters in human pancreatic islets and INS-1 cells.

In normal adult human pancreas, we observed abundant expression of key statin efflux transporters, P-gp and BCRP, in both alpha and beta cells (**Figures 3.1-3.4**). We showed that BCRP is pre-dominantly co-localized to beta cells, whereas P-gp was equally distributed to alpha and beta cells (**Figure 3.5**).

Prior to establishing an INS-1 cell model with transient overexpression of OATP2B1, we confirmed the absence of key statin Oatp transporters, including Oatp2b1; however, marked expression of P-gp and Bcrp was found at both mRNA and protein level (**Figures 3.6**).

4.1.2. Specific Aim 2: To establish a transient OATP2B1-overexpression model in INS-1 cells and characterize the role of OATP2B1 on cellular statin accumulation with or without known pharmacological inhibitors of statin efflux transporters expressed in INS-1 cells.

To study the effect of OATP2B1 on statin accumulation, we used adenoviral transduction with Ad-OATP2B1 compared to Ad-LacZ control in INS-1 cells, and subsequently characterized OATP2B1 expression following adenoviral transduction through western blotting and dual immunofluorescent staining (**Figures 3.7**).

We showed that OATP2B1 overexpression resulted in higher cellular accumulation of rosuvastatin and atorvastatin, but not pravastatin, relative to Ad-LacZ control following 1 μ M statin treatment for 30 minutes, suggesting that OATP2B1 primarily facilitates the uptake of rosuvastatin and atorvastatin in our INS-1 cell model (**Figure 3.8A**). Moreover, atorvastatin reached the highest absolute concentration in cells (**Figure 3.8B**), likely due to its lipophilicity which also allows for passive diffusion through the plasma membrane, in contrast to rosuvastatin and pravastatin, which are hydrophilic statins that do not readily diffuse and are more reliant on membrane transporters. Furthermore, we observed a dose- and time-dependent decrease in cellular rosuvastatin accumulation, likely due to transporter saturation and active statin efflux at higher statin concentration and longer

treatment duration (**Figure 3.9A, B**). We also noted that verapamil, an unspecific inhibitor of P-gp, led to the greatest increase in rosuvastatin uptake in both, OATP2B1-overexpressing and Ad-LacZ control cells, indicating the importance of P-gp-mediated efflux of statins on cellular statin accumulation (**Figure 3.9**).

4.1.3. Specific Aim 3: To elucidate the role of OATP2B1 in statin-induced impairment of beta cell function using INS-1 cells by assessing insulin secretion, cellular ATP level, mitochondrial function, and apoptosis activation.

We observed an increase in insulin secretion following high-glucose stimulation in OATP2B1-overexpressing cells relative to Ad-LacZ cells treated with DMSO control (**Figure 3.10-12**). Following 24-hour rosuvastatin and atorvastatin treatment, we observed a dose-dependent reduction in insulin secretion (**Figure 3.10E**), while a trend was observed following with a significant reduction at 10 μ M treatment (**Figure 3.11E, 12E**). However, OATP2B1 overexpression did not result in a significant difference within any of the concentrations tested (0.1-10 μ M). In Ad-LacZ cells, 1 μ M rosuvastatin treatment with GGPP showed a significant increase relative to 1 μ M rosuvastatin with FPP, demonstrating a possible role of GGPP in rescuing statin-induced impairment in insulin secretion (**Figure 3.10G, H**). Co-treatment with FPP and GGPP had a main effect on insulin secretion with rosuvastatin treatment, but had no effect following atorvastatin and pravastatin treatment (**Figure 3.10~12F**).

In terms of mitochondrial toxicity, we showed a dose-dependent decrease in formazan formation, a marker of mitochondrial function and cell viability, following 24-hour rosuvastatin and atorvastatin treatment but not pravastatin (**Figure 3.13**). OATP2B1 overexpression resulted in a left- and downward-shift in the dose response curve with a corresponding decrease in eIC_{50} , indicating an effect of OATP2B1 on facilitating rosuvastatin- and atorvastatin-mediated mitochondrial toxicity. We also studied potential changes in the expression of specific mitochondrial electron transport chain complexes that may be involved in statin-mediated toxicity (**Figure 3.14A**). Although quantitative analysis did not yield an effect of OATP2B1 nor statin/substrate treatment, we observed a

trend of decreased expression of complex III in OATP2B1-overexpressing cells following 100 μ M atorvastatin treatment compared to DMSO (**Figure 3.14B**).

With regards to ATP, an important signaling molecule for of insulin secretion, we observed that 24-hour treatment with 100 μ M rosuvastatin and atorvastatin led to reduced ATP concentration relative to DMSO control in OATP2B1-overexpressing cells, and with atorvastatin, this difference was also significantly lower than Ad-LacZ cells, suggesting a role of OATP2B1 in atorvastatin-induced reduction in ATP level reduction at 100 μ M (**Figure 3.15**). Finally, we observed that 24-hour, 10 μ M atorvastatin led to the greatest increase in the activity of caspase 3/7 and caspase 9 relative to both DMSO and Ad-LacZ control, suggesting an effect of OATP2B1 and atorvastatin treatment on apoptosis activation (**Figure 3.16**). This was rescued when co-treated with FPP and GGPP (**Figure 3.16**). A schematic summarizing the key findings from our study in INS-1 cells is shown below (**Figure 4.1**).

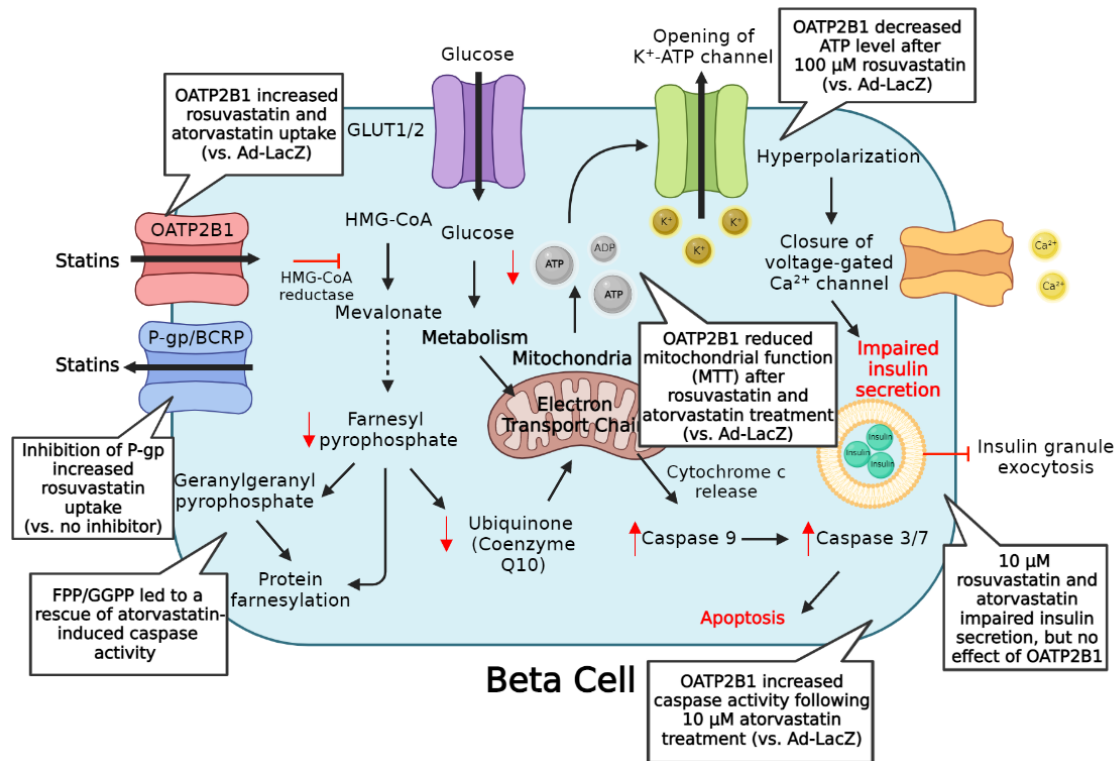


Figure 4.1. A summary of key findings. Figure was created using BioRender.

ATP, adenosine triphosphate; BCRP, breast cancer resistance protein; FPP, farnesyl pyrophosphate; GGPP, geranylgeranyl pyrophosphate; GLUT, glucose transporter; HMG-CoA, 3-hydroxy-3-methylglutaryl coenzyme A; MTT, 3-(4,5-dimethylthiazol-2-yl)-2,5-diphenyltetrazolium bromide; OATP, organic anion transporting polypeptide; P-gp, P-glycoprotein.

4.2 Contribution to Existing Literature

4.2.1. Endogenous expression of statin uptake and efflux transporters in human pancreatic islets and INS-1 cells.

Better understanding the expression of OATPs and ABC efflux transporters of relevance to statin entry into human beta cells can provide additional insights concerning their role in statin accumulation and thus statin-mediated beta cell toxicity. A previous study with over 380 patient samples have reported mRNA expression of OATP1B3 and OATP2B1 in normal human pancreas (Pressler et al., 2011). Remarkably, they reported the mRNA expression of OATP2B1 in the human pancreas to be comparable to that in normal human liver, a tissue known for its high expression of OATP2B1 (Kullak-Ublick et al., 2001). Our lab has recently reported the expression of OATP1B3 and OATP2B1 in normal human islets, and that OATP2B1 is predominantly localized to the beta cells (Kim, 2017). Accordingly, while there is some evidence regarding the expression of statin-transporting OATP2B1 and OATP1B3 in the human islets, data regarding the protein expression of statin efflux transporters in human islets are still quite limited. A previous study assessing gene expression in islets from two human donors using massively parallel signature sequencing analysis reported that P-gp and BCRP are expressed at the mRNA level in the human islets (Kutlu et al., 2009). In addition, preliminary qPCR results from our lab reported an abundant expression of P-gp and BCRP in the human islets (Kim, 2017). Remarkably, the mRNA expression of P-gp and BCRP was over 2000- and 200-fold greater than that in the pancreas, respectively (Kim, 2017). This result suggests that P-gp and BCRP are preferentially expressed in the endocrine islets of the pancreas, which is thought to constitute only 1-5% of the pancreas (Dolenšek et al., 2015). P-gp expression has been previously detected through immunohistochemistry in the islets (Bani et al., 1992; Kloster-Jensen et al., 2015), as well as BCRP expression (Fetsch et al., 2006; Lechner et al., 2002). Here, our study provides novel insights into the protein expression pattern of P-gp and BCRP in both alpha and beta cells, and that BCRP is predominantly localized to the beta cells. Rosuvastatin and atorvastatin are known substrates of human P-gp and BCRP, and our findings suggest

that these ABC transporters may be important determinants of statin accumulation in human beta cells.

Using endogenous INS-1 cells, our qPCR and dual immunofluorescent staining results showed that P-gp and Bcrp are also expressed, confirming a previous report which suggested low, but detectable mRNA expression of P-gp and Bcrp in INS-1 cells (Kutlu et al., 2009). Therefore, our results indicate that INS-1 cells have negligible mRNA expression of rat Oatps that are of relevance for statin transport, similar to what our lab has found previously (Kim, 2017), but do express P-gp and Bcrp in insulin-secreting cells, which may contribute to active statin efflux from cells.

4.2.2. The role of OATP2B1 on cellular statin accumulation with or without known pharmacological inhibitors of statin efflux transporters expressed in INS-1 cells.

We observed that OATP2B1-overexpressing INS-1 cells had a 2.5-fold and 2-fold increase in the cellular uptake of rosuvastatin and atorvastatin, respectively, but did not affect the uptake of pravastatin. This is consistent with the fact that rosuvastatin and atorvastatin are known substrates of OATP2B1, but not pravastatin (Deng et al., 2021). Similar to our results, a previous study using HeLa cells overexpressing OATP2B1 has found a 2-fold increase in the uptake of rosuvastatin and atorvastatin as measured by liquid scintillation spectrometry using ³H-radiolabelled statins (Knauer et al., 2010). While data regarding OATP2B1-mediated transport in INS-1 cells are limited, previous initial data from our lab found that INS-1 cells transduced with Ad-OATP2B1 resulted in a greater cellular uptake of rosuvastatin at 100 MOI (Kim, 2017). Our results at 250 MOI are consistent with this finding, with the difference in rosuvastatin uptake being more pronounced. The dose-dependent reduction in the effect of OATP2B1 on rosuvastatin uptake observed here likely supports OATP2B1 transport saturation. One study using estrone-3-sulfate as the OATP2B1 substrate has found that OATP2B1-mediated transport is indeed saturable, with rate of transport reaching near saturation at 30~100 μ M of estrone sulfate (Sato et al., 2021). Another study investigated rosuvastatin saturation kinetics with OATP2B1, and found a K_m value of 2.4 μ M (Ho et al., 2006). Although we did not specifically test for saturation using a more variety of doses and data on

OATP2B1 saturation kinetics using rosuvastatin are limited, we suspect that a likely saturation kinetic also occurs with rosuvastatin, which may explain the observed decrease in the effect of OATP2B1 as rosuvastatin concentration increased. Lastly, we also showed that the effect of OATP2B1 on rosuvastatin uptake in INS-1 cells is also time-dependent, which may be due to active efflux of rosuvastatin out of the cells.

Accordingly, we showed that, using verapamil, inhibition of statin efflux transporters including P-gp, which is abundant in INS-1 cells, led to the greatest increase in rosuvastatin uptake, suggesting that P-gp may affect cellular rosuvastatin accumulation. Overall, we confirmed OATP2B1-mediated transport of rosuvastatin and atorvastatin, which was both dose- and time-dependent in INS-1 cells. Our findings suggest that the interplay of OATP2B1-mediated uptake and active efflux through ABC transporters like P-gp determines cellular statin accumulation in our cell-based model.

4.2.3. The effect of OATP2B1-mediated statin transport on insulin secretion and beta cell function

In DMSO-treated cells, OATP2B1 overexpression resulted in a significantly increased glucose stimulation relative to Ad-LacZ control. This is potentially due to the mechanism of action of OATP2B1, where substrates like statins are brought into the cell in exchange for the efflux of bicarbonate. One recent study has found that increased bicarbonate concentration in the growth medium stimulates insulin secretion in a beta cell line (Zhang et al., 2022). Furthermore, our study found a dose-dependent reduction in insulin secretion compared to DMSO following rosuvastatin and atorvastatin treatment, but not pravastatin, while no effect of OATP2B1 was observed. Our lab had previously investigated the effect of OATP2B1 on statin-induced beta cell function using a lower MOI of 100 for Ad-OATP2B1 (Section 4.2.2). Specifically, a dose-dependent reduction in glucose-stimulated insulin secretion (GSIS) was observed in INS-1 cells following 24-hour treatment with rosuvastatin and atorvastatin but not pravastatin between 0.1-10 μM compared to DMSO control (Kim, 2017). However, similar to our findings, when represented as stimulation index, no effect of OATP2B1 was observed compared to Ad-LacZ control. Interestingly, co-treatment with an unspecific OATP inhibitor rifampicin did not improve statin-induced impairment in insulin secretion, which may suggest that

OATP-mediated statin transport may not be a major determinant of insulin secretion (Kim, 2017). One previous study using INS-1 cells has shown a similar dose-dependent reduction in insulin secretion, with a ~30% reduction in insulin secretion at 20 μ M rosuvastatin (Salunkhe et al., 2016), a more modest decrease compared to our result at 59% reduction following 10 μ M rosuvastatin treatment. Another study using MIN6 cells, a mouse beta cell line, showed a similar dose-dependent reduction following atorvastatin treatment (Ishikawa et al., 2006). Interestingly, data regarding pravastatin appear to be mixed, with studies suggesting both a positive and negative effect on insulin secretion (Abe et al., 2010; Zhao & Zhao, 2015). Our results are in agreement with these previous findings, but pravastatin data were quite variable and did not have a clear indication. It remains unclear whether uptake transporters such as OATP2B1 actually amplify statin-mediated effects on insulin secretion, since our study was not able to show a significant effect of OATP2B1 for any of the statins or concentrations tested. However, the lack of effect of OATP2B1 could also be partially due to the treatment time being 24 hours, which, as observed from our rosuvastatin uptake study, may involve active statin efflux. The lack of OATP2B1's effect may also be partly explained by variability between experimental days, as well as an unexpected increase in insulin secretion in OATP2B1-overexpressing cells without statin treatment (DMSO control) that may confound the data. Insulin secretion is modulated by numerous environmental factors and its transcription is tightly regulated by many transcription factors and signaling pathways (Melloul et al., 2002). It is possible that there are compensatory mechanisms to regulate the insulin gene transcription that may have masked the effect of OATP2B1-mediated increase in statin accumulation on insulin secretion, or that the concentration ranges or treatment time tested (0.1 to 10 μ M for 24 hours) was not sufficient to cause a notable effect at the level of insulin secretion. The role of OATP2B1 or other OATP-mediated statin transport on insulin secretion still remains elusive and should be studied further.

Importantly, we observed that OATP2B1 facilitated the statin-induced impairment in mitochondrial function, as indicated by a reduced eIC_{50} for formazan formation of rosuvastatin and atorvastatin, but not pravastatin. Although our western blot for mitochondrial electron transport chain complexes I-V did not have a clear indication, we observed a trend of OATP2B1-mediated reduction in complex III expression following

100 μM atorvastatin treatment. Recent studies have suggested that statin-mediated inhibition of complex III may be implicated in decreased mitochondrial function observed in patients with statin-induced myopathy (Allard et al., 2018; Schirris et al., 2015). Complex III is the third enzyme complex in the electron transport chain and serves as an electron carrier which catalyzes the reduction of cytochrome c and the oxidation of ubiquinone, while is involved in the production of reactive oxygen species (Broniarek et al., 2020). By inhibiting the mevalonate pathway, statins reduce the pool of ubiquinone and thus the activity of complex III, and this is thought to attenuate ATP production and induce oxidative stress (Broniarek et al., 2020). As discussed in **Section 1.5**, mitochondrial function is likely a key factor in statin-induced beta cell dysfunction, and these mechanisms overlap considerably with known mechanisms of statin-induced myopathy. Although statin-mediated effects on specific mitochondrial complexes is still relatively new and has only been studied in the context of skeletal muscle and endothelial cell function and viability (Allard et al., 2018; Broniarek et al., 2020; Schirris et al., 2015), its role in statin-induced beta cell dysfunction merits further research.

In INS-1 cells, OATP2B1 was found to accentuate the statin-mediated decrease in ATP level following 100 μM atorvastatin, as well as increase in caspase 3/7/9 activity following 10 μM atorvastatin treatment in INS-1 cells relative to non-OATP2B1-expressing control. However, OATP2B1 did not have an effect on ATP level at up to 10 μM rosuvastatin and atorvastatin treatment. A previous study has confirmed our finding, where they observed no significant effect of statins on ATP level at 10 μM , but atorvastatin leading to a ~70% reduction in ATP level at 100 μM in human skeletal muscle myoblast cells overexpressing OATP2B1 (Knauer et al., 2010). The authors have also suggested that OATP2B1 amplifies statin-induced mitochondrial toxicity as measured by formazan formation following 10 and 100 μM atorvastatin treatment and caspase 3/7 activity was markedly increased in OATP2B1-overexpressing human skeletal muscle myoblast cells (Knauer et al., 2010). We also noted that statin-specific effect on ATP level and caspase activity, with atorvastatin generally having the greatest effect. A previous study has found that 10 μM treatment with rosuvastatin and atorvastatin for 48 hours increased caspase 3/7 and 9 activity by about 1.5-fold relative to Ad-LacZ control in human skeletal muscle myoblasts (Knauer et al., 2010). Our differences in caspase 3/7

activity were more pronounced at about 2-fold, whereas caspase 9 activity was more modest at around 1.3-fold for 10 μ M rosuvastatin and atorvastatin treatment for 24 hours. While these are important initiator (caspase 9) and effector caspases (caspase 3/7), intrinsic, mitochondrion-mediated apoptosis is a complicated chain of events involving the regulation by Bcl-2 family of proteins, mitochondrial outer membrane permeabilization, cytochrome c release and ROS production and is not a complete overview of apoptosis in cells (Seino et al., 2009). Overall, previous studies using human skeletal muscle myoblast cells and preliminary results from our lab suggest that OATP2B1 plays a key role in amplifying statin-induced toxicity at the level of cellular ATP and caspase 3/7/9 activation, particularly at high concentrations, and our results support these findings.

4.3 Limitations of study and future directions

4.3.1. Sample size and methodology

While we report a novel finding that P-gp and BCRP are co-localized to alpha and beta cells, the small sample size (N=3 individuals of different sexes) and the scarcity of pancreatic islets in a given tissue section make it difficult to generalize our findings. Even though expression of proteins is fairly constant in a cell line, protein expression in individuals can vary greatly depending on many factors, including but not limited to ethnicity, age, sex and previous disease history, which we could not accurately gauge due to this limitation. Furthermore, we used a co-localization image processing software/plugin to assess co-localization quantitatively. Although this method is commonly used to provide quantitative results for light or fluorescence microscopy images, other methodologies such as confocal microscopy, combined with greater sample size and increased subject variability, would strengthen our findings.

4.3.2. Limitations on INS-1 cell line and treatments

We used an INS-1 832/13 subclone of INS-1 cell line for our *in vitro* experiments. This cell line has been subcloned to provide a more robust insulin secretion; however, its functionality including insulin secretion and cell marker expression could be affected negatively at >10 passages (Hohmeier et al., 2000). Although we carefully adhered so that this passage number was not exceeded in our GSIS study, it is unclear whether the use of further passages for other experiments would have affected our results. There are other subclones of INS-1 cell line, such as the INS-1E, developed at the University of Geneva. Usage of this cell line has been cited to have a more stable yet similar glucose response and insulin secretion even at passages 70-90 (Špaček et al., 2008).

When assessing cellular statin accumulation, we used verapamil and fumitremorgin C as inhibitors of efflux transporters. However, while fumitremorgin C is a BCRP-specific inhibitor, verapamil is a rather unspecific inhibitor of P-gp and can also affect various Mrps; therefore, we were unable to isolate the effect of P-gp on statin accumulation using verapamil. While the concentrations were selected based on previous studies that showed a sufficient inhibition of the desired transporters, we were also unable to control for the degree of inhibition. We have tried CRISPR-Cas9 knockout strategy in INS-1 cells for various statin efflux transporters (see **Appendix A**), but was unsuccessful in creating a knockout INS-1 cell line. Future studies could therefore use a different knockout strategy to eliminate the respective genes to more accurately assess the effect of various statin transporters of relevance.

In addition, it is important to note that the concentration ranges used in our cell-based studies are much higher than serum statin concentrations following therapeutic statin doses in humans (Björkhem-Bergman et al., 2011). As noted earlier, mean plasma statin concentration in the human serum is about 1-15 nM in patients receiving a therapeutic dose of rosuvastatin, and only a fraction of this concentration is pharmacologically active due to protein binding, which reduces this concentration even further (Björkhem-Bergman et al., 2011). However, in target cells including hepatocytes and also beta cells, statin uptake transporters like OATP1B3 and OATP2B1 facilitate the cellular uptake of statins, making the cellular statin concentration higher than the level observed in the plasma. Still, we had to resort to much higher concentrations in the 1 to 100 μ M range in

our *in vitro* studies as a proof-of-principle approach to delineate our findings; however, it must be emphasized that these concentrations are orders of magnitude higher than physiologically relevant values. Yet, even though our statin doses are much higher, our treatment time was kept at 30 minutes for statin accumulation study or 24 hours for other *in vitro* experiments. Patients taking statins are generally on the medication chronically, which makes their statin exposure much longer in duration than what is feasible in *in vitro* experiments, although repeated, prolonged exposure *in vivo* may result in the accumulation of statins in beta cells. Overall, exploring other cell line options and complementing with *in vivo* studies using mice or *ex vivo* studies using isolated mouse/rat islets with a more variable statin concentration/treatment times to confirm some of our findings in the INS-1 cell line would be an appropriate next step.

4.3.3. Mechanisms of statin-induced toxicity

Our study highlighted several aspects of beta cell toxicity resulting from OATP2B1-mediated statin transport. However, we were unable to demonstrate a significant effect of OATP2B1 on glucose induced insulin secretion in any of our treatment groups. It is possible that the concentration ranges we employed (0.1-10 μM) was not sufficient to elicit a notable change in insulin secretion. For example, a recent finding suggested that 24-hour treatment with various concentrations of atorvastatin did not lead to a significant reduction in insulin secretion until 15 μM using primary mouse islets (Hoffmeister et al., 2020). The lack of effect of FPP/GGPP in rescuing statin-mediated impairment in insulin secretion could also be due to the insufficient impairment in insulin secretion resulting from not using a high enough of statin concentration. Future studies could therefore investigate a higher concentration of statins, utilize a more stable alternate cell line, such as INS-1E, and also explore mechanisms behind how OATP2B1-mediated statin transport causes changes at various steps along the insulin secretion pathway. While we showed that higher atorvastatin concentrations lead to reduction in cellular ATP level, an important signaling molecule for insulin secretion, future studies could investigate other steps along the insulin secretory pathway, including L-type Ca^{2+} channel activity and calcium influx using a patch-clamp electrophysiology or steps in the cAMP pathway, which is crucial in mediating insulin granule exocytosis (Seino et al., 2009). Future

studies could therefore assess these other proteins to more accurately assess which steps along the apoptotic pathway statins may induce a toxic effect.

4.4 Conclusion

In conclusion, we demonstrate abundant expression of statin efflux transporters P-gp and BCRP in the adult human pancreas, that like OATP2B1, are expressed in the insulin-secreting beta cells. Moreover, we demonstrate differences in the distribution pattern of P-gp and BCRP in regard to their co-localization with beta and alpha cells in human islets.

Using a murine beta cell model transiently overexpressing human OATP2B1, our results indicate an important role of OATP2B1 in cellular accumulation of rosuvastatin and atorvastatin, but not pravastatin. After 24-hour statin treatment, we confirmed a dose-dependent reduction in insulin secretion for rosuvastatin and atorvastatin, but not pravastatin; however, OATP2B1 did not have an effect for any statins and different concentrations studied. We also observed rosuvastatin- and atorvastatin-induced impairment in mitochondrial function and apoptosis activation at supraphysiological concentrations, and demonstrated that OATP2B1 amplified some of these effects. In conclusion, our results indicate an association between OATP2B1, which is abundant in human beta cells, and statin-mediated toxicity, but not insulin secretion. While our results support a potential role of efflux transporters P-gp and BCRP in cellular accumulation of rosuvastatin, their effect on statin-mediated beta cell dysfunction requires further study.

References

- Abe, M., Toyohara, T., Ishii, A., Suzuki, T., Noguchi, N., Akiyama, Y., Shiwaku, H. O., Nakagomi-Hagihara, R., Zheng, G., Shibata, E., Souma, T., Shindo, T., Shima, H., Takeuchi, Y., Mishima, E., Tanemoto, M., Terasaki, T., Onogawa, T., Unno, M., ... Abe, T. (2010). The HMG-CoA Reductase Inhibitor Pravastatin Stimulates Insulin Secretion through Organic Anion Transporter Polypeptides. In *Drug Metab. Pharmacokinet* (Vol. 25, Issue 3). <http://www.jstage.jst.go.jp/browse/dmpk>
- Allard, N. A. E., Schirris, T. J. J., Verheggen, R. J., Russel, F. G. M., Rodenburg, R. J., Smeitink, J. A. M., Thompson, P. D., Hopman, M. T. E., & Timmers, S. (2018). Statins affect skeletal muscle performance: Evidence for disturbances in energy metabolism. *Journal of Clinical Endocrinology and Metabolism*, *103*(1), 75–84. <https://doi.org/10.1210/jc.2017-01561>
- Aller, S. G., Yu, J., Ward, A., Weng, Y., Chittaboina, S., Zhuo, R., Harrell, P. M., Trinh, Y. T., Zhang, Q., Urbatsch, I. L., & Chang, G. (2009). Structure of P-glycoprotein reveals a molecular basis for poly-specific drug binding. *Science*, *323*(5922), 1718–1722. <https://doi.org/10.1126/science.1168750>
- Ames, J., Hephherd, S., Obbe, T. M. C., Ord, A. F., Sles, H. G. I., Oss, A. R., Orimer, L., Acfarlane, E. W. M., Illop, H. M. C. K., Hristopher, C., Ackard, J. P., & Bldg, O. (1995). From the Departments of Pathological Biochemistry. In *Number* (Vol. 333).
- Antons, K. A., Williams, C. D., Baker, S. K., & Phillips, P. S. (2006). Clinical Perspectives of Statin-Induced Rhabdomyolysis. *American Journal of Medicine*, *119*(5), 400–409. <https://doi.org/10.1016/j.amjmed.2006.02.007>
- Ballatori, N., Hammond, C. L., Cunningham, J. B., Krance, S. M., & Marchan, R. (2005). Molecular mechanisms of reduced glutathione transport: Role of the MRP/CFTR/ABCC and OATP/SLC21A families of membrane proteins. In *Toxicology and Applied Pharmacology* (Vol. 204, Issue 3, pp. 238–255). Academic Press Inc. <https://doi.org/10.1016/j.taap.2004.09.008>

- Ballian, N., & Brunicardi, F. C. (2007). Islet vasculature as a regulator of endocrine pancreas function. *World Journal of Surgery*, *31*(4), 705–714.
<https://doi.org/10.1007/s00268-006-0719-8>
- Bani, D., Brandi, M. L., Axiotis, C. A., & Bani-Sacchi, T. (1992). Histochemistry Detection of P-glycoprotein on endothelial and endocrine cells of the human pancreatic islets by C 494 monoclonal antibody. In *Histochemistry* (Vol. 98).
- Bellosta, S., Paoletti, R., & Corsini, A. (2004). Safety of statins: Focus on clinical pharmacokinetics and drug interactions. In *Circulation* (Vol. 109, Issue 23 SUPPL.).
<https://doi.org/10.1161/01.CIR.0000131519.15067.1f>
- Berger, C., & Zdzienlo, D. (2020). Glucose transporters in pancreatic islets. *Eur J Physiol*, *472*, 1249–1272. <https://doi.org/10.1007/s00424-020-02383-4/Published>
- Betteridge, D. J., & Carmena, R. (2016). The diabetogenic action of statins-mechanisms and clinical implications. In *Nature Reviews Endocrinology* (Vol. 12, Issue 2, pp. 99–110). Nature Publishing Group. <https://doi.org/10.1038/nrendo.2015.194>
- Bitzur, R., Cohen, H., Kamari, Y., & Harats, D. (2013). Intolerance to statins: Mechanisms and management. *Diabetes Care*, *36*(SUPPL.2).
<https://doi.org/10.2337/dcS13-2038>
- Björkhem-Bergman, L., Lindh, J. D., & Bergman, P. (2011). What is a relevant statin concentration in cell experiments claiming pleiotropic effects? In *British Journal of Clinical Pharmacology* (Vol. 72, Issue 1, pp. 164–165).
<https://doi.org/10.1111/j.1365-2125.2011.03907.x>
- Broniarek, I., Dominiak, K., Galganski, L., & Jarmuszkiewicz, W. (2020). The influence of statins on the aerobic metabolism of endothelial cells. *International Journal of Molecular Sciences*, *21*(4). <https://doi.org/10.3390/ijms21041485>
- Cederberg, H., Stančáková, A., Yaluri, N., Modi, S., Kuusisto, J., & Laakso, M. (2015). Increased risk of diabetes with statin treatment is associated with impaired insulin

- sensitivity and insulin secretion: a 6 year follow-up study of the METSIM cohort. *Diabetologia*, 58(5), 1109–1117. <https://doi.org/10.1007/s00125-015-3528-5>
- Chapman, M. J., & McTaggart, F. (2002). Optimizing the pharmacology of statins: characteristics of rosuvastatin. In *Atherosclerosis Supplements* (Vol. 2). www.elsevier.com/locate/atherosclerosis
- Choudhuri, S., & Klaassen, C. (2006). Structure, function, expression, genomic organization, and single nucleotide polymorphisms of human ABCB1 (MDR1), ABCC (MRP), and ABCG2 (BCRP) efflux transporters. In *International Journal of Toxicology* (Vol. 25, Issue 4, pp. 231–259). <https://doi.org/10.1080/10915810600746023>
- Cordoncardo, C., O'Brien, J. P., Casals, D., Rittman-Grauert, L., Biedler, J. L., Melamed, M. R., & Bertino, J. R. (1989). Multidrug-resistance gene (P-glycoprotein) is expressed by endothelial cells at blood-brain barrier sites (monoclonal antibodies/immunohistochemistry/cancer chemotherapy). In *Proc. Natl. Acad. Sci. USA* (Vol. 86).
- Daneman, D. (2006). Type 1 diabetes. In *www.thelancet.com* (Vol. 367). www.thelancet.com
- Davignon, J. (2004). Beneficial cardiovascular pleiotropic effects of statins. *Circulation*, 109(23 SUPPL.), 39–43. <https://doi.org/10.1161/01.cir.0000131517.20177.5a>
- de Graaf, W., Bennink, R. J., Heger, M., Maas, A., de Bruin, K., & van Gulik, T. M. (2011). Quantitative assessment of hepatic function during liver regeneration in a standardized rat model. *Journal of Nuclear Medicine*, 52(2), 294–302. <https://doi.org/10.2967/jnumed.110.078360>
- Dean, M., & Allikmets, R. (2001). Complete Characterization of the Human ABC Gene Family. In *Journal of Bioenergetics and Biomembranes* (Vol. 33, Issue 6).
- DeGorter, M. K., Tirona, R. G., Schwarz, U. I., Choi, Y. H., Dresser, G. K., Suskin, N., Myers, K., Zou, G. Y., Iwuchukwu, O., Wei, W. Q., Wilke, R. A., Hegele, R. A., &

- Kim, R. B. (2013). Clinical and pharmacogenetic predictors of circulating atorvastatin and rosuvastatin concentrations in routine clinical care. *Circulation: Cardiovascular Genetics*, 6(4), 400–408.
<https://doi.org/10.1161/CIRCGENETICS.113.000099>
- Deichmann, R., Lavie, C., & Andrews, S. (2010). *Coenzyme Q10 and Statin-Induced Mitochondrial Dysfunction*. www.ceri.com/mito.htm.
- Deng, F., Tuomi, S. K., Neuvonen, M., Hirvensälo, P., Kulju, S., Wenzel, C., Oswald, S., Filppulä, A. M., & Niemi, M. (2021). Comparative Hepatic and Intestinal Efflux Transport of Statins. *Drug Metabolism and Disposition*, 49(9), 750–759.
<https://doi.org/10.1124/DMD.121.000430>
- Dirks, A. J., & Jones, K. M. (2006). Statin-induced apoptosis and skeletal myopathy. *American Journal of Physiology - Cell Physiology*, 291(6), 1208–1212.
<https://doi.org/10.1152/ajpcell.00226.2006>
- Dolensek, J., Rupnik, M. S., & Stožer, A. (2015). Structural similarities and differences between the human and the mouse pancreas. In *Islets* (Vol. 7, Issue 1). Taylor and Francis Inc. <https://doi.org/10.1080/19382014.2015.1024405>
- Druet, C., Tubiana-Rufi, N., Chevenne, D., Rigal, O., Polak, M., & Levy-Marchal, C. (2006). Rapid Communication: Characterization of insulin secretion and resistance in type 2 diabetes of adolescents. *Journal of Clinical Endocrinology and Metabolism*, 91(2), 401–404. <https://doi.org/10.1210/jc.2005-1672>
- du Souich, P., Roederer, G., & Dufour, R. (2017). Myotoxicity of statins: Mechanism of action. *Pharmacology and Therapeutics*, 175, 1–16.
<https://doi.org/10.1016/j.pharmthera.2017.02.029>
- Faneyte, I. F., Kristel, P. M. P., & van de Vijver, M. J. (2001). *DETERMINING MDRI/P-GLYCOPROTEIN EXPRESSION IN BREAST CANCER*.
- Fetsch, P. A., Abati, A., Litman, T., Morisaki, K., Honjo, Y., Mittal, K., & Bates, S. E. (2006). Localization of the ABCG2 mitoxantrone resistance-associated protein in

normal tissues. *Cancer Letters*, 235(1), 84–92.

<https://doi.org/10.1016/j.canlet.2005.04.024>

Freeman, D. J., Norrie, J., Sattar, N., Dermot, ; R, Neely, G., Cobbe, S. M., Ford, I., Lorimer, ; A Ross, Macfarlane, P. W., Mckillop, J. H., Packard, C. J., Shepherd, J., & Gaw, A. (2001). *Pravastatin and the Development of Diabetes Mellitus Evidence for a Protective Treatment Effect in the West of Scotland Coronary Prevention Study*. <http://www.circulationaha.org>

Fromm, M. F. (2002). The influence of MDR1 polymorphisms on P-glycoprotein expression and function in humans. In *Advanced Drug Delivery Reviews* (Vol. 54). www.elsevier.com/locate/drugdeliv

Fu, Z., Gilbert, E. R., & Liu, D. (2013). Regulation of Insulin Synthesis and Secretion and Pancreatic Beta-Cell Dysfunction in Diabetes. In *Curr Diabetes Rev* (Vol. 9, Issue 1).

Galicia-Garcia, U., Benito-Vicente, A., Jebari, S., Larrea-Sebal, A., Siddiqi, H., Uribe, K. B., Ostolaza, H., & Martín, C. (2020). Pathophysiology of type 2 diabetes mellitus. In *International Journal of Molecular Sciences* (Vol. 21, Issue 17, pp. 1–34). MDPI AG. <https://doi.org/10.3390/ijms21176275>

Glaeser, H., Mandery, K., Sticht, H., Fromm, M., & König, J. (2010). Relevance of conserved lysine and arginine residues in transmembrane helices for the transport activity of organic anion transporting polypeptide 1B3. *British Journal of Pharmacology*, 159(3), 698–708. <https://doi.org/10.1111/j.1476-5381.2009.00568.x>

Goldstein, J. L., & Brown, M. S. (2009). The LDL receptor. *Arteriosclerosis, Thrombosis, and Vascular Biology*, 29(4), 431–438. <https://doi.org/10.1161/ATVBAHA.108.179564>

Hagenbuch, B., & Meier, P. J. (2003.). *The superfamily of organic anion transporting polypeptides*. <http://www.gene.ucl.ac>

- Hagenbuch, B., & Meier, P. J. (2004). Organic anion transporting polypeptides of the OATP/SLC21 family: Phylogenetic classification as OATP/SLCO super-family, new nomenclature and molecular/functional properties. In *Pflugers Archiv European Journal of Physiology* (Vol. 447, Issue 5, pp. 653–665).
<https://doi.org/10.1007/s00424-003-1168-y>
- Hagenbuch, B., & Stieger, B. (2013). The SLCO (former SLC21) superfamily of transporters. In *Molecular Aspects of Medicine* (Vol. 34, Issues 2–3, pp. 396–412).
<https://doi.org/10.1016/j.mam.2012.10.009>
- Hartz, A. M. S., Zhong, Y., Wolf, A., LeVine, H., Miller, D., & Bauer, B. (2016). A β 40 reduces p-glycoprotein at the blood–brain barrier through the ubiquitin–proteasome pathway. *Journal of Neuroscience*, 36(6), 1930–1941.
<https://doi.org/10.1523/JNEUROSCI.0350-15.2016>
- Hatanaka, T. (2000). Clinical Pharmacokinetics of Pravastatin Mechanisms of Pharmacokinetic Events. *Clinical Pharmacokinetics*, 6, 397–412.
- Hennessy, D. A., Tanuseputro, P., Tuna, M., Bennett, C., Perez, R., Shields, M., Ko, D. T., Tu, J., & Manuel, D. G. (2016). Population health impact of statin treatment in Canada. *Health Reports*, 27(1), 20–28.
- Higgins, C. F., Callaghan, R., Linton, K. J., Rosenberg, M. F., & Ford, R. C. (1997). Structure of the multidrug resistance P-glycoprotein. In *CANCER BIOLOGY* (Vol. 8).
- Ho, R. H., Tirona, R. G., Leake, B. F., Glaeser, H., Lee, W., Lemke, C. J., Wang, Y., & Kim, R. B. (2006). Drug and Bile Acid Transporters in Rosuvastatin Hepatic Uptake: Function, Expression, and Pharmacogenetics. *Gastroenterology*, 130(6), 1793–1806. <https://doi.org/10.1053/j.gastro.2006.02.034>
- Hoang, D. T., Matsunari, H., Nagaya, M., Nagashima, H., Millis, J. M., Witkowski, P., Periwal, V., Hara, M., & Jo, J. (2014). A conserved rule for pancreatic islet organization. *PLoS ONE*, 9(10). <https://doi.org/10.1371/journal.pone.0110384>

- Hoffmeister, T., Kaiser, J., Lüdtke, S., Drews, G., & Düfer, M. (2020). Interactions between Atorvastatin and the Farnesoid X Receptor Impair Insulinotropic Effects of Bile Acids and Modulate Diabetogenic Risk. *Molecular Pharmacology*, 97(3), 202–211. <https://doi.org/10.1124/MOL.119.118083>
- Hohmeier, H. E., Mulder, H., Chen, G., Henkel-Rieger, R., Prentki, M., & Newgard, C. B. (2000). Isolation of INS-1-Derived Cell Lines With Robust ATP-Sensitive K⁺ Channel-Dependent and-Independent Glucose-Stimulated Insulin Secretion. In *424 DIABETES* (Vol. 49). <http://diabetesjournals.org/diabetes/article-pdf/49/3/424/365110/10868964.pdf>
- Ishikawa Mayumi, Okajima Fuminori, Inoue Noriyuki, Motomura Kaori, Kato Toyonori, Takahashi Akimitsu, Oikawa Shinichi, Yamada Nobuhiro, & Shimano Hitoshi. (2006). *Materials and Methods*.
- Jialal, I., Stein, D., Balis, D., Grundy, S. M., Adams-Huet, B., & Devaraj, S. (2001). Effect of hydroxymethyl glutaryl coenzyme a reductase inhibitor therapy on high sensitive C-reactive protein levels. *Circulation*, 103(15), 1933–1935. <https://doi.org/10.1161/01.CIR.103.15.1933>
- Kalliokoski, A., & Niemi, M. (2009). Impact of OATP transporters on pharmacokinetics. In *British Journal of Pharmacology* (Vol. 158, Issue 3, pp. 693–705). <https://doi.org/10.1111/j.1476-5381.2009.00430.x>
- Kharroubi, A. T. (2015). Diabetes mellitus: The epidemic of the century. *World Journal of Diabetes*, 6(6), 850. <https://doi.org/10.4239/wjd.v6.i6.850>
- Kim, M., Deacon, P., Tirona, R. G., Kim, R. B., Pin, C. L., Meyer zu Schwabedissen, H. E., Wang, R., & Schwarz, U. I. (2017a). Characterization of OATP1B3 and OATP2B1 transporter expression in the islet of the adult human pancreas. *Histochemistry and Cell Biology*, 148(4), 345–357. <https://doi.org/10.1007/s00418-017-1580-6>

- Kim, M. S. (2017). The Role of OATP-Mediated Statin Transport in Pancreatic Beta The Role of OATP-Mediated Statin Transport in Pancreatic Beta Cell Function Cell Function. *Electronic Thesis and Dissertation Repository*, 4577. <https://doi.org/10.1007/s00418>
- Kloster-Jensen, K., Vethe, N. T., Bremer, S., Abadpour, S., Korsgren, O., Foss, A., Bergan, S., & Scholz, H. (2015). Intracellular sirolimus concentration is reduced by tacrolimus in human pancreatic islets in vitro. *Transplant International*, 28(10), 1152–1161. <https://doi.org/10.1111/tri.12617>
- Knauer, M. J., Urquhart, B. L., Meyer Zu Schwabedissen, H. E., Schwarz, U. I., Lemke, C. J., Leake, B. F., Kim, R. B., & Tirona, R. G. (2010). Human skeletal muscle drug transporters determine local exposure and toxicity of statins. *Circulation Research*, 106(2), 297–306. <https://doi.org/10.1161/CIRCRESAHA.109.203596>
- Koehn, L. M., Dziegielewska, K. M., Møllgård, K., Saudrais, E., Strazielle, N., Ghersi-Egea, J. F., Saunders, N. R., & Habgood, M. D. (2019). Developmental differences in the expression of ABC transporters at rat brain barrier interfaces following chronic exposure to diallyl sulfide. *Scientific Reports*, 9(1). <https://doi.org/10.1038/s41598-019-42402-8>
- Kullak-Ublick, G. A., Ismail, M. G., Stieger, B., Landmann, L., Huber, R., Pizzagalli, F., Fattinger, K., Meier, P. J., & Hagenbuch, B. (2001). Organic anion-transporting polypeptide B (OATP-B) and its functional comparison with three other OATPs of human liver. *Gastroenterology*, 120(2), 525–533. <https://doi.org/10.1053/gast.2001.21176>
- Kutlu, B., Burdick, D., Baxter, D., Rasschaert, J., Flamez, D., Eizirik, D. L., Welsh, N., Goodman, N., & Hood, L. (2009). Detailed transcriptome atlas of the pancreatic beta cell. *BMC Medical Genomics*, 2. <https://doi.org/10.1186/1755-8794-2-3>
- Lechner, A., Leech, C. A., Abraham, E. J., Nolan, A. L., & Habener, J. F. (2002). Nestin-positive progenitor cells derived from adult human pancreatic islets of Langerhans contain side population (SP) cells defined by expression of the ABCG2 (BCRP1)

ATP-binding cassette transporter. *Biochemical and Biophysical Research Communications*, 293, 670–674. www.academicpress.com

- Lennernäs, H. (2003). Clinical Pharmacokinetics of Atorvastatin. In *Clin Pharmacokinetics* (Vol. 42, Issue 13).
- Livak, K. J., & Schmittgen, T. D. (2001). Analysis of relative gene expression data using real-time quantitative PCR and the 2- $\Delta\Delta$ CT method. *Methods*, 25(4), 402–408. <https://doi.org/10.1006/meth.2001.1262>
- Ma, J., Gao, G., Lu, H., Fang, D., Li, L., Wei, G., Chen, A., Yang, Y., Zhang, H., & Huo, J. (2019). Reversal effect of ginsenoside Rh2 on oxaliplatin-resistant colon cancer cells and its mechanism. *Experimental and Therapeutic Medicine*. <https://doi.org/10.3892/etm.2019.7604>
- Mao, Q., & Unadkat, J. D. (2015). Role of the Breast Cancer Resistance Protein (BCRP/ABCG2) in Drug Transport—an Update. *AAPS Journal*, 17(1), 65–82. <https://doi.org/10.1208/s12248-014-9668-6>
- Martin, P. D., Warwick, M. J., Dane, A. L., Hill, S. J., Giles, P. B., Phillips, P. J., & Lenz, E. (2003). Metabolism, Excretion, and Pharmacokinetics of Rosuvastatin in Healthy Adult Male Volunteers. *Clinical Therapeutics*, 25, 2822–2835.
- Martínez-gonzález, J., Raposo, B., Rodríguez, C., & Badimon, L. (2001). *Downregulation by Atherogenic Levels of Native LDLs Balance Between Transcriptional and Posttranscriptional Regulation*. 804–809.
- Medwid, S., Price, H. R., Taylor, D. P., Mailloux, J., Schwarz, U. I., Kim, R. B., & Tirona, R. G. (2021). Organic Anion Transporting Polypeptide 2B1 (OATP2B1) Genetic Variants: In Vitro Functional Characterization and Association With Circulating Concentrations of Endogenous Substrates. *Frontiers in Pharmacology*, 12. <https://doi.org/10.3389/fphar.2021.713567>
- Melloul, D., Marshak, S., & Cerasi, E. (2002). Regulation of insulin gene transcription. *Diabetologia*, 45, 309–326.

- Mollazadeh, H., Tavana, E., Fanni, G., Bo, S., Banach, M., Pirro, M., von Haehling, S., Jamialahmadi, T., & Sahebkar, A. (2021). Effects of statins on mitochondrial pathways. In *Journal of Cachexia, Sarcopenia and Muscle* (Vol. 12, Issue 2, pp. 237–251). John Wiley and Sons Inc. <https://doi.org/10.1002/jcsm.12654>
- Naud, J., Michaud, J., Boisvert, C., Desbiens, K., Leblond, F. A., Mitchell, A., Jones, C., Bonnardeaux, A., & Pichette, V. (2007). Down-regulation of intestinal drug transporters in chronic renal failure in rats. *Journal of Pharmacology and Experimental Therapeutics*, *320*(3), 978–985. <https://doi.org/10.1124/jpet.106.112631>
- Navarese, E. P., Buffon, A., Andreotti, F., Kozinski, M., Welton, N., Fabiszak, T., Caputo, S., Grzesk, G., Kubica, A., Swiatkiewicz, I., Sukiennik, A., Kelm, M., de Servi, S., & Kubica, J. (2013). Meta-analysis of impact of different types and doses of statins on new-onset diabetes mellitus. *American Journal of Cardiology*, *111*(8), 1123–1130. <https://doi.org/10.1016/j.amjcard.2012.12.037>
- Ni, Z., Bikadi, Z., Rosenberg, M. F., & Mao, Q. (2010). *Structure and Function of the Human Breast Cancer Resistance Protein (BCRP/ABCG2)*.
- Nichols, G. A., & Koro, C. E. (2007). Does Statin Therapy Initiation Increase the Risk for Myopathy? An Observational Study of 32,225 Diabetic and Nondiabetic Patients. *Clinical Therapeutics*, *29*(8), 1761–1770. <https://doi.org/10.1016/j.clinthera.2007.08.022>
- Pasternak, R. C., Smith, S. C., Bairey-Merz, C. N., Grundy, S. M., Cleeman, J. I., & Lenfant, C. (2002). ACC/AHA/NHLBI clinical advisory on the use and safety of statins. *Journal of the American College of Cardiology*, *40*(3), 567–572. [https://doi.org/10.1016/S0735-1097\(02\)02030-2](https://doi.org/10.1016/S0735-1097(02)02030-2)
- Pressler, H., Sissung, T. M., Venzon, D., Price, D. K., & Figg, W. D. (2011). Expression of OATP family members in hormone-related cancers: Potential markers of progression. *PLoS ONE*, *6*(5). <https://doi.org/10.1371/journal.pone.0020372>

- Rappa, G., Lorico, A., Flavell, R. A., & Sartorelli, A. C. (1997). *Evidence That the Multidrug Resistance Protein (MRP) Functions as a Co-Transporter of Glutathione and Natural Product Toxins*. <http://aacrjournals.org/cancerres/article-pdf/57/23/5232/2465343/cr0570235232.pdf>
- Ridker, P. M., Danielson, E., Fonseca, F. A. H., Genest, J., Gotto, A. M., Kastelein, J. J. P., Koenig, W., Libby, P., Lorenzatti, A. J., MacFadyen, J. G., Nordestgaard, B. G., Shepherd, J., Willerson, J. T., & Glynn, R. J. (2008). Rosuvastatin to Prevent Vascular Events in Men and Women with Elevated C-Reactive Protein. *New England Journal of Medicine*, 359(21), 2195–2207. <https://doi.org/10.1056/NEJMoa0807646>
- Robey, R. W., Polgar, O., Deeken, J., To, K. W., & Bates, S. E. (2007). ABCG2: Determining its relevance in clinical drug resistance. In *Cancer and Metastasis Reviews* (Vol. 26, Issue 1, pp. 39–57). <https://doi.org/10.1007/s10555-007-9042-6>
- Rodrigue-Way, A., Caron, V., Bilodeau, S., Keil, S., Hassan, M., Lévy, E., Mitchell, G. A., & Tremblay, A. (2014). Scavenger receptor CD36 mediates inhibition of cholesterol synthesis via activation of the PPAR γ / PGC-1 α pathway and Insig1/2 expression in hepatocytes. *FASEB Journal*, 28(4), 1910–1923. <https://doi.org/10.1096/fj.13-240168>
- Roy, U., Barber, P., Tse-Dinh, Y. C., Batrakova, E. v., Mondal, D., & Nair, M. (2015). Role of MRP transporters in regulating antimicrobial drug inefficacy and oxidative stress-induced pathogenesis during HIV-1 and TB infections. In *Frontiers in Microbiology* (Vol. 6, Issue SEP). Frontiers Media S.A. <https://doi.org/10.3389/fmicb.2015.00948>
- Sacher, J., Weigl, L., Werner, M., Szegedi, C., & Hohenegger, M. (2005). Delineation of myotoxicity induced by 3-hydroxy-3-methylglutaryl CoA reductase inhibitors in human skeletal muscle cells. *Journal of Pharmacology and Experimental Therapeutics*, 314(3), 1032–1041. <https://doi.org/10.1124/jpet.105.086462>

- Sakata, N., Yoshimatsu, G., & Kodama, S. (2019). Development and characteristics of pancreatic epsilon cells. *International Journal of Molecular Sciences*, *20*(8).
<https://doi.org/10.3390/ijms20081867>
- Salunkhe, V. A., Elvstam, O., Eliasson, L., & Wendt, A. (2016a). Rosuvastatin treatment affects both basal and glucose-induced insulin secretion in INS-1 832/13 cells. *PLoS ONE*, *11*(3). <https://doi.org/10.1371/journal.pone.0151592>
- Salunkhe, V. A., Elvstam, O., Eliasson, L., & Wendt, A. (2016b). Rosuvastatin treatment affects both basal and glucose-induced insulin secretion in INS-1 832/13 cells. *PLoS ONE*, *11*(3). <https://doi.org/10.1371/journal.pone.0151592>
- Salunkhe, V. A., Mollet, I. G., Ofori, J. K., Malm, H. A., Esguerra, J. L. S., Reinbothe, T. M., Stenkula, K. G., Wendt, A., Eliasson, L., & Vikman, J. (2016). Dual Effect of Rosuvastatin on Glucose Homeostasis Through Improved Insulin Sensitivity and Reduced Insulin Secretion. *EBioMedicine*, *10*, 185–194.
<https://doi.org/10.1016/j.ebiom.2016.07.007>
- Sathasivam, S. (2012). Statin induced myotoxicity. *European Journal of Internal Medicine*, *23*(4), 317–324. <https://doi.org/10.1016/j.ejim.2012.01.004>
- Sato, R., Akiyoshi, T., Morita, T., Katayama, K., Yajima, K., Kataoka, H., Imaoka, A., & Ohtani, H. (2021). Dual kinetics of OATP2B1: Inhibitory potency and pH-dependence of OATP2B1 inhibitors. *Drug Metabolism and Pharmacokinetics*, *41*.
<https://doi.org/10.1016/j.dmpk.2021.100416>
- Sauna, Z. E., Smith, M. M., Uller, M. M. ", Kerr, K. M., & Ambudkar, S. v. (2001). The Mechanism of Action of Multidrug-Resistance-Linked P-Glycoprotein. In *Journal of Bioenergetics and Biomembranes* (Vol. 33, Issue 6).
- Schindelin, J., Arganda-Carreras, I., Frise, E., Kaynig, V., Longair, M., Pietzsch, T., Preibisch, S., Rueden, C., Saalfeld, S., Schmid, B., Tinevez, J. Y., White, D. J., Hartenstein, V., Eliceiri, K., Tomancak, P., & Cardona, A. (2012). Fiji: An open-

- source platform for biological-image analysis. In *Nature Methods* (Vol. 9, Issue 7, pp. 676–682). <https://doi.org/10.1038/nmeth.2019>
- Schinkel, A. H., & Jonker, J. W. (2012). Mammalian drug efflux transporters of the ATP binding cassette (ABC) family: An overview. In *Advanced Drug Delivery Reviews* (Vol. 64, Issue SUPPL., pp. 138–153). <https://doi.org/10.1016/j.addr.2012.09.027>
- Schirris, T. J. J., Renkema, G. H., Ritschel, T., Voermans, N. C., Bilos, A., van Engelen, B. G. M., Brandt, U., Koopman, W. J. H., Beyrath, J. D., Rodenburg, R. J., Willems, P. H. G. M., Smeitink, J. A. M., & Russel, F. G. M. (2015). Statin-induced myopathy is associated with mitochondrial complex III inhibition. *Cell Metabolism*, 22(3), 399–407. <https://doi.org/10.1016/j.cmet.2015.08.002>
- Schulte, R. R., & Ho, R. H. (2019). Organic anion transporting polypeptides: Emerging roles in cancer pharmacology. In *Molecular Pharmacology* (Vol. 95, Issue 5, pp. 490–506). American Society for Pharmacology and Experimental Therapy. <https://doi.org/10.1124/mol.118.114314>
- Seino, S., Takahashi, H., Fujimoto, W., & Shibasaki, T. (2009). Roles of cAMP signalling in insulin granule exocytosis. In *Diabetes, Obesity and Metabolism* (Vol. 11, Issue SUPPL. 4, pp. 180–188). Blackwell Publishing Ltd. <https://doi.org/10.1111/j.1463-1326.2009.01108.x>
- Shaw, J., & Kirshenbaum, L. A. (2006). HAX-1 represses postmitochondrial caspase-9 activation and cell death during hypoxia-reoxygenation. In *Circulation Research* (Vol. 99, Issue 4, pp. 336–338). <https://doi.org/10.1161/01.RES.0000239408.03169.94>
- Shepherd, J., Cobbe, S. M., Ford, I., Isles, C. G., Lorimer, A. R., MacFarlane, P. W., McKillop, J. H., & Packard, C. J. (2004). Prevention of coronary heart disease with pravastatin in men with hypercholesterolemia. 1995. *Atherosclerosis. Supplements*, 5(3), 91–97. <https://doi.org/10.1016/j.atherosclerosissup.2004.08.029>

- Sirvent, P., Mercier, J., & Lacampagne, A. (2008). New insights into mechanisms of statin-associated myotoxicity. *Current Opinion in Pharmacology*, 8(3), 333–338. <https://doi.org/10.1016/j.coph.2007.12.010>
- Špaček, T., Šantorová, J., Zacharovová, K., Berková, Z., Hlavatá, L., Saudek, F., & Ježek, P. (2008). Glucose-stimulated insulin secretion of insulinoma INS-1E cells is associated with elevation of both respiration and mitochondrial membrane potential. *International Journal of Biochemistry and Cell Biology*, 40(8), 1522–1535. <https://doi.org/10.1016/j.biocel.2007.11.015>
- Stancu, C., & Sima, A. (2001). Statins: Mechanism of action and effects. *Journal of Cellular and Molecular Medicine*, 5(4), 378–387. <https://doi.org/10.1111/j.1582-4934.2001.tb00172.x>
- St-Pierre, M. v, Stallmach, T., Freimoser Grundschober, A., Dufour, J., Serrano, M. A., G Marin, J. J., Sugiyama, Y., & Meier, P. J. (2004). Temporal expression profiles of organic anion transport proteins in placenta and fetal liver of the rat. *Am J Physiol Regul Integr Comp Physiol*, 287, 1505–1516. <https://doi.org/10.1152/ajpregu.00279.2003.-Physiological>
- Tachibana-Iimori, R., Tabara, Y., Kusuhara, H., Kohara, K., Kawamoto, R., Nakura, J., Tokunaga, K., Kondo, I., Sugiyama, Y., & Miki, T. (2004). Effect of genetic polymorphism of OATP-C (SLCO1B1) on lipid-lowering response to HMG-CoA reductase inhibitors. *Drug Metabolism and Pharmacokinetics*, 19(5), 375–380. <https://doi.org/10.2133/dmpk.19.375>
- Taha, D. A., de Moor, C. H., Barrett, D. A., & Gershkovich, P. (2014). Translational insight into statin-induced muscle toxicity: From cell culture to clinical studies. In *Translational Research* (Vol. 164, Issue 2, pp. 85–109). Mosby Inc. <https://doi.org/10.1016/j.trsl.2014.01.013>
- van de Steeg, E., Stránecký, V., Hartmannová, H., Nosková, L., Hřebíček, M., Wagenaar, E., van Esch, A., de Waart, D. R., Oude Elferink, R. P. J., Kenworthy, K. E., Sticová, E., Al-Edreesi, M., Knisely, A. S., Knoch, S., Jirsa, M., & Schinkel, A. H.

- (2012). Complete OATP1B1 and OATP1B3 deficiency causes human Rotor syndrome by interrupting conjugated bilirubin reuptake into the liver. *Journal of Clinical Investigation*, 122(2), 519–528. <https://doi.org/10.1172/JCI59526>
- Veluthakal, R., & Thurmond, D. C. (2021). Emerging roles of small gtpases in islet β -cell function. In *Cells* (Vol. 10, Issue 6). MDPI. <https://doi.org/10.3390/cells10061503>
- Ward, N. C., Watts, G. F., & Eckel, R. H. (2019). Statin Toxicity: Mechanistic Insights and Clinical Implications. In *Circulation Research* (Vol. 124, Issue 2, pp. 328–350). Lippincott Williams and Wilkins. <https://doi.org/10.1161/CIRCRESAHA.118.312782>
- Xiang, Q., Chen, S. qing, Ma, L. yue, Hu, K., Zhang, Z., Mu, G. yan, Xie, Q. fen, Zhang, X. dan, & Cui, Y. min. (2018). Association between SLCO1B1 T521C polymorphism and risk of statin-induced myopathy: a meta-analysis. *Pharmacogenomics Journal*, 18(6), 721–729. <https://doi.org/10.1038/s41397-018-0054-0>
- Xu, D., Li, F., Zhang, M., Zhang, J., Liu, C., Hu, M. Y., Zhong, Z. Y., Jia, L. L., Wang, D. W., Wu, J., Liu, L., & Liu, X. D. (2014). Decreased exposure of simvastatin and simvastatin acid in a rat model of type 2 diabetes. *Acta Pharmacologica Sinica*, 35(9), 1215–1225. <https://doi.org/10.1038/aps.2014.39>
- Yada, T., Nakata, M., Shiraishi, T., & Kakei, M. (1999.). *Inhibition by simvastatin, but not pravastatin, of glucose-induced cytosolic Ca²⁺ signalling and insulin secretion due to blockade of L-type Ca²⁺ channels in rat islet b-cells*. <http://www.stocktonpress.co.uk/bjp>
- Zhang, Y. C., Xiong, F. R., Wang, Y. Y., Shen, H., Zhao, R. X., Li, S., Lu, J., & Yang, J. K. (2022). High bicarbonate concentration increases glucose-induced insulin secretion in pancreatic β -cells. *Biochemical and Biophysical Research Communications*, 589, 165–172. <https://doi.org/10.1016/j.bbrc.2021.12.015>

Zhao, W., & Zhao, S. P. (2015). Different effects of statins on induction of diabetes mellitus: An experimental study. *Drug Design, Development and Therapy*, 9, 6211–6223. <https://doi.org/10.2147/DDDT.S87979>

Appendix A: Exploratory Evaluation of Mrp Expression in INS-1 Cells Compared to Rat Liver and Attempted CRISPR-Mediated Downregulation of P-gp, Mrp1 and Mrp3

Supplementary Background

MRP structure, transport mechanism and expression

In humans, the MRP subfamily consists of 12 members, ABCC1-12, but only 9 of these are transporters (Dean & Allikmets, 2001). The MRPs differ considerably in size and molecular structure; the larger MRPs (MRP1, 2, 3, 6 and 7) contain three membrane-spanning domains made up of 17 transmembrane helices, whereas the smaller MRPs (MRP4, 5, 8 and 9) have two membrane-spanning domains consisting of 12 transmembrane helices, making them structurally similar to P-gp (Ballatori et al., 2005; Choudhuri & Klaassen, 2006). Regardless of size, all MRPs contain two intracellular nucleotide binding domains for ATP binding and hydrolysis (Ballatori et al., 2005). While the exact mechanisms vary, reduced glutathione (GSH) is an important cofactor by acting as a low-affinity substrate for MRP1-5 and mediating the co-transport of target compounds, although GSH itself is not transported across the membrane (Ballatori et al., 2005; Rappa et al., 1997; Roy et al., 2015). A summary of MRPs, tissue expression and major substrate specificities is shown in **Supplementary Table 1**.

Even within a given tissue, MRPs show differential location to either the apical or the basolateral side. Specifically, within the hepatocytes, MRP2 is found in the apical membrane, whereas MRP1, 3, 4, 5 and 6 are located on the sinusoidal membrane (Choudhuri & Klaassen, 2006). Within the proximal tubule, MRP2 and 4 are located in the apical side, whereas MRP1, 3, 5 and 6 are expressed on the basolateral side (Choudhuri & Klaassen, 2006). Within the small intestine, MRP2 is found on the luminal side, and MRP1, 3 and 5 are found on the basolateral membrane (Choudhuri & Klaassen, 2006).

Of these, MRP3 was discovered to transport atorvastatin and pravastatin, along with MRP4, which is known to transport rosuvastatin (Deng et al., 2021).

Supplementary Table 1. MRP expression and substrate specificities in humans.

Adapted from Roy et al., 2015.

MRPs	Expression	Substrate Specificity
Mrp1	Ubiquitous	Organic anions, steroid conjugates
Mrp2	Liver, kidney, small intestines	Organic anions
Mrp3	Liver, pancreas, kidney, small intestines	Organic anions, bile acids
Mrp4	Prostate, lung, muscle, pancreas, ovaries, bladder	Organic anions, cyclic nucleotides, steroid conjugates
Mrp5	Ubiquitous	Organic anion, cyclic nucleotides
Mrp6	Liver, kidney	Lipophilic anions
Mrp7	Heart, liver, skeletal muscle, kidney	Lipophilic anions
Mrp8	Liver	Cyclic nucleotides
Mrp9	Breast, testes	Unknown

Mrp, multidrug resistance-associated protein

Supplementary Materials and Methods

We sought to investigate the mRNA expression of various rodent Mrps in our INS-1 cell model. RT-qPCR was performed as described in **Section 2.5**, with primer sequences shown below (**Supplementary Table 2**).

Supplementary Table 2. Forward and reverse sequences of RT-qPCR primers for rat Mrps in INS-1 cells. Primers were designed using the Eurofin Genomics PCR Primer Design Tool, and all primers were obtained from Eurofin Genomics, Toronto, Ontario, Canada.

Gene (rat)	Forward (5` to 3`)	Reverse (5` to 3`)	Reference
Mrp1	CCTTGGGTCTGGTTTACTT	ACAGGGGAACGACTGACAG	Koehn et al., 2019
Mrp2	CACGGTCATCACCATCGCTCAC	AGTTCTTCAGGACTGCCATACTCG	Koehn et al., 2019
Mrp3	CTCGCCCATCTTCTCCCACTTCTCGG	CCGGTTGGAGGCGATGTAGGATAAG	Koehn et al., 2019
Mrp4	GAACGCTACGAGAAAGTCATC	GCCCGTGCCAAGTTCAC	Koehn et al., 2019
Mrp5	AACAGGAAGGATTCTCAACAGG	TGAATGCTGGACGTGATATGG	Koehn et al., 2019

Mrp, multidrug resistance-associated protein

CRISPR-knockout of efflux transporters in INS-1 cells

To investigate the effect of statin efflux transporters on statin uptake and other functional aspects, we created efflux transporter knockout INS-1 cell lines using the CRISPR-Cas9 system. Lipofectamine® CRISPRMAX® Cas9 Transfection Reagent (ThermoFisher Scientific) was used to create a CRISPR-Cas9 knockout line with INS-1 832/13 cells.

The efflux transporters of interest, P-gp, Mrp1 and Mrp3 were chosen as the target knockout genes, due to their low number of off target effects. The target sequences, PAM sequences and the chromosome location for the gRNAs corresponding to each gene were determined using the Invitrogen TrueDesign Genome Editor (ThermoFisher Scientific) and are listed below (**Supplementary Table 3**).

Supplementary Table 3. CRISPR-Cas9 gRNA sequences used for CRISPR knockout in INS-1 cells. Gene name, target sequence, PAM sequence and genomic location for P-gp, Mrp1 and Mrp3 in creating CRISPR-Cas9 knockout INS-1 cells. The primers were designed using Invitrogen TrueDesign Genome Editor (ThermoFisher Scientific) and were obtained from ThermoFisher Scientific.

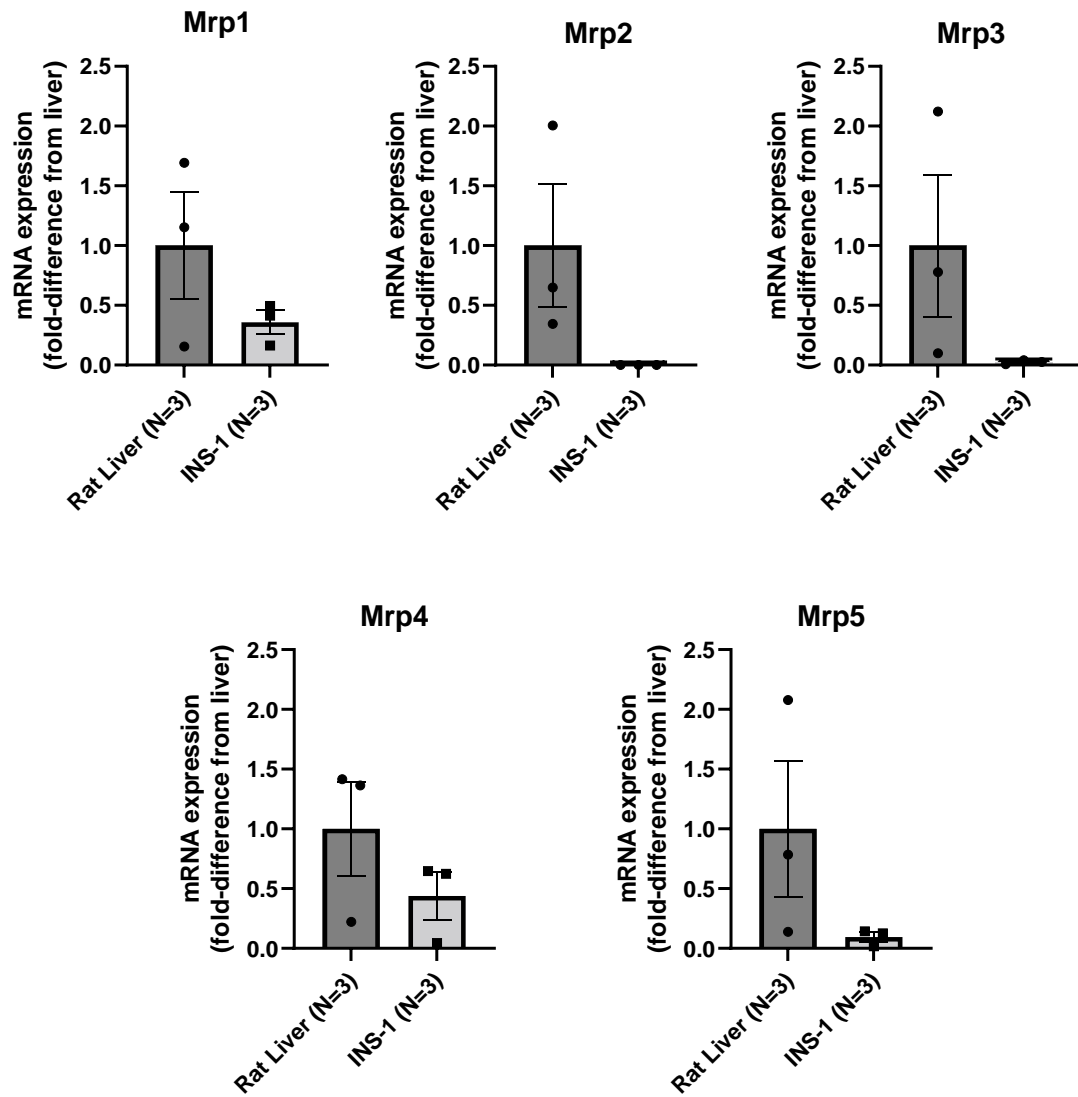
Gene (rat)	Target Sequence (gRNA)	PAM	Genomic Location
P-gp	ACTCTGGCGGCCATTAT CCA	TGG	chr4[22411093]
Mrp1	CTGATGGCTCCGATCCG CTC	TGG	chr10[672171]
Mrp3	ATGGACCGCTTGTGCGG CTC	CGG	chr10[82116621]

CRISPR-Cas9 lipofection was performed according to the manufacturer's protocol and the knockout was assessed 72 hours post-lipofection using RT-qPCR. For each knockout line, a wild-type INS-1 with the same passage served as a control. Following knockout verification, the cell lines were maintained and passaged as previously described (**Section 2.1**).

Supplementary Results

Our results indicate a substantial mRNA expression of Mrp1, Mrp4 and Mrp5 in INS-1 cells, whereas Mrp2 and Mrp3 expression were low (**Supplementary Figure 1**). We show that, along with P-gp and Bcrp, which are expressed in INS-1 cells, Mrp3 and Mrp4 may also contribute to cellular statin accumulation and statin-induced toxicities.

With regards to CRISPR-Cas9 approach, we have tried knockout for P-gp, Mrp1 and Mrp3 in INS-1 cells, but were unable to obtain successful knockout.



Supplementary Figure 1. Mrp expression in INS-1 cells. Rat liver samples (N=3) or INS-1 cells (N=3) were homogenized, and RNA was extracted. RT-qPCR was performed with beta actin as the internal control. Data shown are mean \pm SEM.

References

- Ballatori, N., Hammond, C. L., Cunningham, J. B., Krance, S. M., & Marchan, R. (2005). Molecular mechanisms of reduced glutathione transport: Role of the MRP/CFTR/ABCC and OATP/SLC21A families of membrane proteins. In *Toxicology and Applied Pharmacology* (Vol. 204, Issue 3, pp. 238–255). Academic Press Inc. <https://doi.org/10.1016/j.taap.2004.09.008>
- Choudhuri, S., & Klaassen, C. (2006). Structure, function, expression, genomic organization, and single nucleotide polymorphisms of human ABCB1 (MDR1), ABCC (MRP), and ABCG2 (BCRP) efflux transporters. In *International Journal of Toxicology* (Vol. 25, Issue 4, pp. 231–259). <https://doi.org/10.1080/10915810600746023>
- Dean, M., & Allikmets, R. (2001). Complete Characterization of the Human ABC Gene Family. In *Journal of Bioenergetics and Biomembranes* (Vol. 33, Issue 6).
- Deng, F., Tuomi, S. K., Neuvonen, M., Hirvensälo, P., Kulju, S., Wenzel, C., Oswald, S., Filppulä, A. M., & Niemi, M. (2021). Comparative Hepatic and Intestinal Efflux Transport of Statins. *Drug Metabolism and Disposition*, 49(9), 750–759. <https://doi.org/10.1124/DMD.121.000430>
- Rappa, G., Lorico, A., Flavell, R. A., & Sartorelli, A. C. (1997). Evidence That the Multidrug Resistance Protein (MRP) Functions as a Co-Transporter of Glutathione and Natural Product Toxins'. <http://aacrjournals.org/cancerres/article-pdf/57/23/5232/2465343/cr0570235232.pdf>
- Roy, U., Barber, P., Tse-Dinh, Y. C., Batrakova, E. v., Mondal, D., & Nair, M. (2015). Role of MRP transporters in regulating antimicrobial drug inefficacy and oxidative stress-induced pathogenesis during HIV-1 and TB infections. In *Frontiers in Microbiology* (Vol. 6, Issue SEP). Frontiers Media S.A. <https://doi.org/10.3389/fmicb.2015.00948>

Curriculum Vitae

Name:	Jihoon Kwon
Post-secondary Education and Degrees:	Western University London, Ontario, Canada 2016-2020 BMSc
	Western University London, Ontario, Canada 2020-2022 MSc in Physiology & Pharmacology
Honours and Awards:	Laurene Paterson Estate Scholarship, Western University 2017
	Graduate Research Scholarship, Western University, 2020-2022
	Poster Presentation, Departmental Research Day, Western University, 2021
	Abstract and Poster Presentation, Canadian Society of Pharmacology and Therapeutics Annual Conference, 2022
Related Work Experience	Teaching Assistant, Undergraduate Physiology & Pharmacology Lab, Western University 2020-2021
	Teaching Assistant, Undergraduate Pharmacology Lecture, Western University 2021-2022